Università degli Studi di Cagliari

DOTTORATO DI RICERCA

"Sviluppo e sperimentazione di farmaci antinfettivi"
Ciclo XXVIII

TITOLO TESI

Studi sull'attività sinergica di un cocktail di tre farmaci attivo contro cellule leucemiche e di carcinoma ovarico cisplatino-resistenti

Settore scientifico disciplinare di afferenza
BIO/19 – Microbiologia Generale

Presentata da:	Dott.ssa Elisabetta Pinna
Coordinatore Dottorato:	Prof.ssa Alessandra Pani
Tutor	Prof.ssa Alessandra Pani

Esame finale anno accademico 2014 – 2015

Università degli Studi di Cagliari

RESEARCH DOCTORATE

"Research and Development of Anti-infective Drugs"

XXVIII cycle

THESIS TITLE

Studies on the synergic activity of a three-drug cocktail active against cisplatin-resistant human leukemia and carcinoma cells

Scientific Area

BIO/19 – General Microbiology

Candidate:	Dott.ssa Elisabetta Pinna
Doctorate Coordinator	Prof.ssa Alessandra Pani
Tutor	Prof.ssa Alessandra Pani

Academic Year 2014-2015

Acknowledgements

First of all, I would like to thank prof. Alessandra Pani for leading me through my path of research and for her continuing assistance during the making of my thesis.

I thank all senior and junior colleagues and friends of the lab, Daniela Perra, Giuseppina Sanna, Silvia Madeddu, Rossana Tuveri, Elisa Carta, Roberta Melis, Fabio Contu and Alessandra Serra, for their useful collaboration and for encouraging and cheering me up in hard times.

Special thanks to my colleague and valuable friend Sarah Vascellari, with whom I shared unforgettable experiences, for being always there when I needed her support and for teaching me so much.

I wish to thank also Fabio and Silvia who kindly donated their blood samples needed for my so crucial experiments on ex vivo lymphocytes.

I thank Dr. Tiziana Pivetta and Dr. Elisa Valletta for their professional partnership, and Dr. Eva Fisher for generously providing us human ovarian carcinoma cell lines.

Special thanks to my lovely parents for supporting and helping me during these three years of work.

I thank my friend Claudia for giving me encouragement and believing in me.

I thank Sergio for persuading me to undertake this challenging and fascinating path of study and research.

Last, but definitely not least, I would like to thank my son for having been so patient and not complaining for all the hours I had to spend in the lab. I wish he will have one day the chance to live such a great experience as mine in the field of research. Riccardo, this thesis is dedicated to you!!

ABSTRACT

Objectives. At the light of properties and limits of cisplatin (CDDP) as an anticancer agent, and in view of the potential clinical relevance of the synergic effect of CDDP with the Cu(II)-phen complexes previously reported against T-leukemia cells (Pivetta *et al.*,Talanta, 2013), my research project was aimed at **(1)** extending the studies of CDDP-Cu(II)-phen combinations as such, as well as with the addition of a third drug component; **(2)** determining the potential degree of selectivity of the most synergic drug combinations.

Methods. Most studies were focused on the most potent Cu(II)Phen compound (C0), lead of the cupper-phen complex series. Wild type and CDDP-resistant human T-leukemia CEM cells, wild type and CDDP-resistant human ovarian carcinoma A2780 cells, and *ex vivo* cultures of human peripheral blood lymphocytes from healthy donors, were used as cell models to characterize the cytotoxic activity of both binary and ternary drug combinations. Experimental Design (ED) and Artificial Neural Network (ANN) were used for setting experiments and for evaluation of data.

Results. Binary and ternary drug combinations showed statistically significant synergisms either against the CDDP-sensitive and the CDDP-resistant cancer cell models. The three-drug cocktail was the most potent with a markedly higher cytotoxicity against leukemic lymphocytes than against *ex vivo* healthy proliferating lymphocytes. An ESI-MS study of CDDP-C0 mixed combination showed the formation of copper-platinum adducts which, leading to the release of a phenantroline moiety, may -at least in part- explain the synergism observed in the cell models. In addition, the analysis of phospholipid profiles showed lipid alterations in the CDDP-resistant CEM and A2780 cells with respect to their parental counterparts.

Conclusions. Besides of the need of further studies to unveil the molecular target(s) of the triple-drug cocktail, based on the promising selectivity index (SI = 5) for cancer cells, investigations on its effectiveness in a xenograft mice models of human susceptible and CDDP-resistant ovarian carcinoma are on the way.

TABLE OF CONTENTS

1. INTRODUCTION ……..…..…….. 4

1.1 Cancer ……..……...….……. 4

1.2 Cancers Classification ……..……..……..…… 7

1.3 Cancer Treatments ……...……...… 8

1.3.1 Anticancer Chemotherapy ……..……..……...…. 9

2. RATIONAL OF THE RESEARCH PROJECT……..……..…. 12

2.1 Cisplatin (CDDP) as anticancer agent ……...……. 12

2.1.1 Mechanism(s) of action of cisplatin ……..... 12

2.1.2 CDDP side effects ……..……..… 15

2.1.3 Mechanisms of CDDP resistance ……...…….…… 15

2.2 Glutathione and its involvement in CDDP-resistance …….…….... 17

2.3 Copper physiology and copper complexes as novel anticancer agents …….……. 18

2.4 The research project …… 20

3. RESULTS AND DISCUSSION ……..….. 22

3.1 Selection of CDDP-resistant CEM cells …….…… 22

3.2 Cytotoxic effects of drug combinations against leukemia CEM cells ……....….. 24

3.2.1 Set up of the ED …… 24

3.2.2 Determination of the cytotoxicity of the drugs ……..…..... 26

3.2.3 Training and verification of the artificial neural network ……...….. 26

3.2.4 Prediction of the response (cytotoxicity surfaces) for CEMwt cell line ……..… 27

3.2.5 Calculation of the non-additive effect and of the net multidrug effect index in CEMwt cell line ……..…. 30

3.2.6 Calculation of the non-additive effect and of the net multidrug effect index in CEMres cell line ……..…….……. 33

3.2.7 Test points …….. 35

3.3. Cytotoxic effects of drug combinations against human ovarian carcinoma A2780 cells.……...…… 35

3.3.1 Cytotoxic effects of drug combinations against A2780wt …….……..….. 36

3.3.2 Cytotoxic effects of drug combinations against A2780res. ……..… 38

3.4. Copper-Platinum complexes as a mechanism to explain the synergism of combinations of CDDP with Cu(II) complexes ……..……. 42

Article: Mixed copper-platinum complex formation could explain synergistic antiproliferative effect exhibited by binary mixture of cisplatin and copper-1,10-phenanthroline compounds: an ESI-MS study …….……..… 43

3.5 Analysis of the phospholipid profiles of CDDP-resistant vs. wild type leukemia and carcinoma cell extracts …….. 51

Manuscript: Identification of specific phospholipids to differentiate Cisplatin-resistant and wild type cells in leukemic (CCRF-CEM) and ovarian cancer (A2780) ……...…. 52

3.6 .Study of the selectivity of the ternary drug combination: cytotoxic effect in CEM versus PBLs ……... 82

4. GENERAL CONCLUSIONS ……..…. 90

5. MATERIALS AND METHODS ……..……... 91

5.1 Reagents ……. 91

5.2 Cell lines ……..……... 91

5.3 Selection of the cisplatin-resistant CCRF-CEM subline …….……... 91

5.4 Cytotoxic assays ……. 92

5.5 Peripheral blood Lymphocytes (PBLs) separation and Cytotoxic assays ……..… 93

6. REFERENCES (*Alphabetical order*)……..…….. 94

1. INTRODUCTION

1.1 Cancer

The transformation of a normal cell into a cancer cell involves the progressive accumulation of genetic, functional and morphological abnormalities**.**

It is a slow process that, in most cases, is successfully fought by mechanisms of repair and by the immune system. When these control mechanisms fail, the abnormal cells multiply and differ further, from the viewpoint of the differentiation and function from the origin cells. Greater are the genetic abnormalities accumulated, more the cancer cells deviate from the original and the malignancy will be undifferentiated and invasive leading to uncontrolled proliferation to the detriment of body tissues.

Cellular masses and aggregates can thus generate and interfere with the physiology of the organ in which they develop, possibly migrating to distant organs, i.e. metastatic cancer, thus threatening the life of the subject. As a synonym of the cancer, in the sense of malignant proliferation, the term neoplasia is also used.

The benign cancer is characterized by an expanding type of growth and it is separated from the healthy tissue by a capsule, which is not due to the proliferation of the connective tissue, but to the fact that the cancer mass, while growing compress the surrounding connective; however, unlike the malignant cancer, it does not spread and if surgically removed it does not relapse.

It is well known now that the causes of cancer are a combination of several internal and external factors. Internal factors are inherent to the body's cells themselves, as gene mutations, hormones, misfunction of the immune system and, generally, they cannot be changed. External factors, instead, are related both to the living and working environment (infectious agents, chemicals, ionizing and non-ionizing radiations, etc.) and the subject’s lifestyle (diet, physical activity, smoking). These can be modified through specific prevention interventions whose effectiveness are amply demonstrated (AIRTUM Associazione italiana dei registri tumori)

As mentioned above, cancer cell often results from mutations of oncogenes or of cancer suppressor genes and/or alterations of signalling pathways. Among many gene products, p53 plays a key role in the prevention of cancer growth. In fact, it does not function or it works incorrectly in most human cancers. p53 network in normal, non-activated conditions is not

functional, but it is activated in the cell in response to various signals that occur in the process of carcinogenesis (Vogelstein *et al*., Nature, 2000). The main function of p53 is the inhibition of abnormal cell growth (Sionov & Haupt, Oncogene, 1999) and the triggering of programmed cell death (Heinrichs & Deppert, Oncogene, 2003). Because these processes ensure genomic integrity, or destroy the damaged cell, p53 has been called the "guardian of the genome" (Lane, Nature, 1992). Later on, other important functions, such as DNA repair (Albrechtsen, Oncogene, 1999) and inhibition of angiogenesis (Vogelstein *et al*., Nature, 2000), were demonstrated.

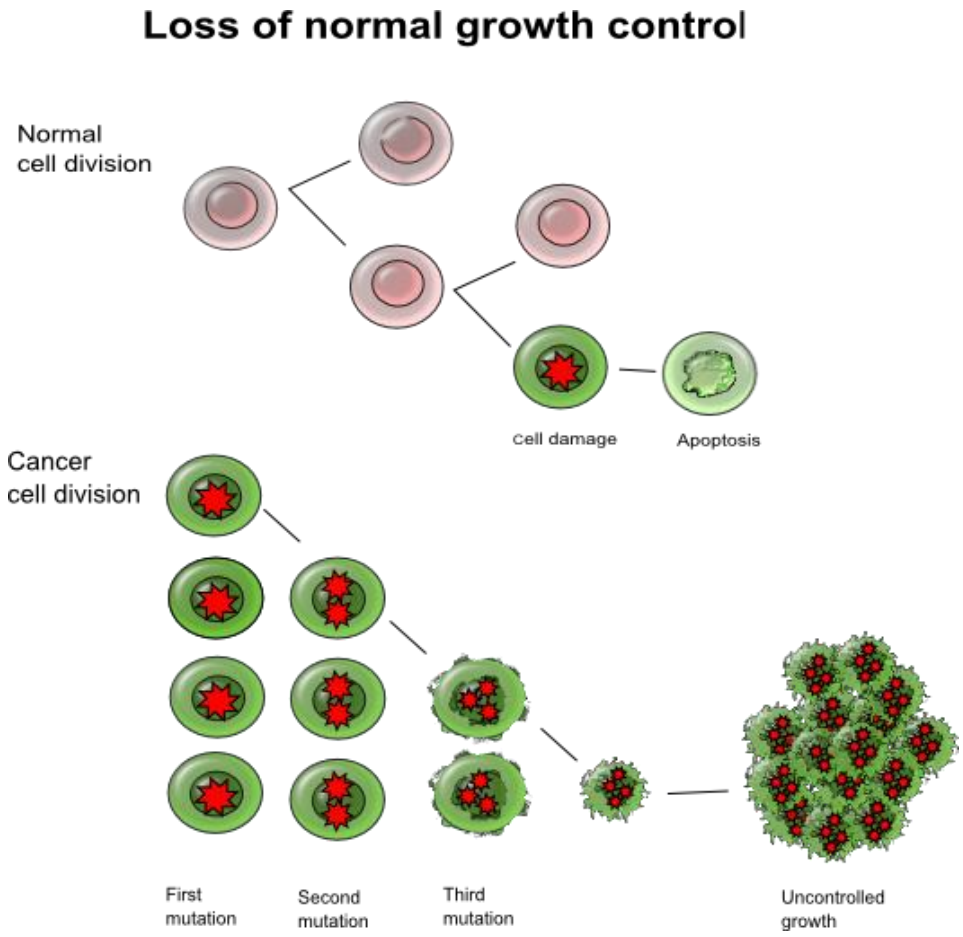

Figure 1. Cancer progression

Cancer metastasis is a multistage process, during which the malignant cells detach from the original tissue and spread via the hematic or lymphatic systems to other organs where they reproduce and generate new cancers. Metastasis is a sequence of interconnected steps, each of them can be limiting because the failure of any stage may stop the process. The result of the process depends on the intrinsic properties of cancer cells and of the host response. For the metastasis development, it is needed the generation of a vascular network and the escaping to the immune response.

Moreover, organ-specific factors can influence the metastasis growth. The entry of cancer cells into the circulation is common but they are rapidly eliminated. The development of metastasis is a rare event and it does not exceed 0.01%. Only a few cells in a primary cancer are able to give metastasis. Therefore, the formation of clinically relevant metastases represents the survival and growth of selected subpopulations of cells that preexist in primary tumours (Talmadge and Fidler, Cancer Res., 2010).

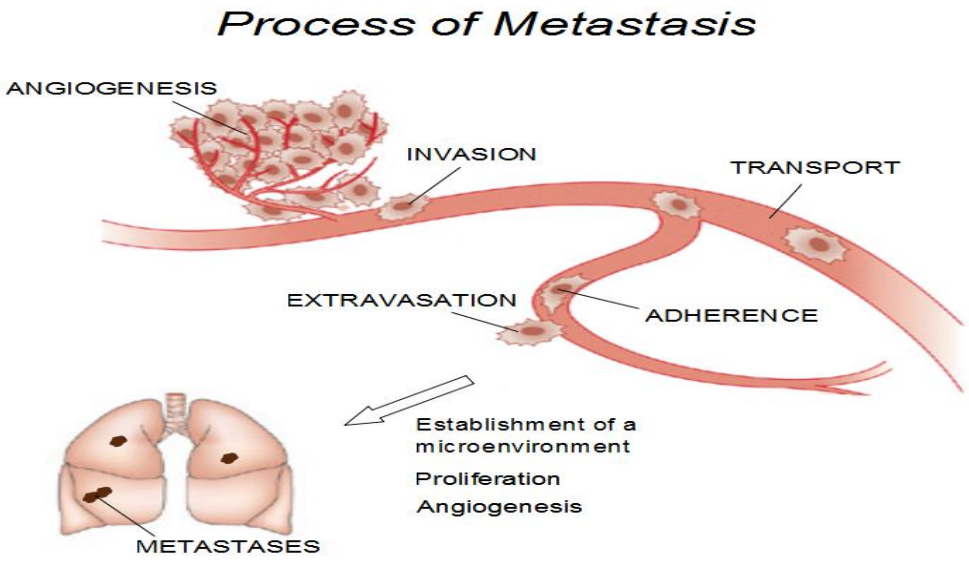

Figure 2. The process of cancer metastasis

1.2 Cancers Classification

The international classification system of the stage of a cancer (staging) is based on the criteria stated by American Joint Committe on Cancer (AJCC) which considers the following three parameters:

- size of the primary cancer (T)
- involvement of regional lymphnodes adjacent to the cancer (N)
- metastases (M)

Each category, in turn, is divided into subgroups, depending on the progressively growing size of the cancer, the number of involved lymph nodes, and the presence or absence of distant metastases.

Depending on the size stand five degrees, from T0 to T4.

As regards the lymph nodes, N0 is defined a condition where the regional lymph nodes are not affected, and with an acronym growing N1 to N3 the progressive involvement of a greater number of nodal stations. The presence of metastasis is characterized by an indication M1, while M0 indicates their absence.

Cancer staging is crucial to determine the most effective treatment plan. The main categories of cancer are:

- Carcinoma: cancer that begins in the skin or in tissues that line or cover internal organs.

- Sarcoma: cancer that begins in 'bone, cartilage, fat, muscle, blood vessels, or other connective or supportive tissue

- Leukemia: cancer that originates in hematopoietic tissues, such as bone marrow

- Lymphoma and Myeloma: cancers that arise from cells of the immune system.

- Cancers of the central nervous system: cancers that originate in the CNS.

1.3 Cancer Treatments

Cancer is one of the most important health problems in different countries of the world.

The data of the National Institute of Statistics (ISTAT), report about 175,000 deaths due to cancer out of about 580,000 deaths that occurred in Italy in 2011. Cancer is the second leading cause of death (30% of all deaths), following those due to cardio-circulatory diseases (38%).

As a general rule, aim of cancer treatments is to destroy cancer cells causing the least possible damage to normal tissues. The type of the clinical intervention depends on different individual factors, i.e. cancer localization, health status of the patient, characteristics and properties of the cancer cells (Luqmani, Med Princ Pract, 2005).

In the last decades, great advances in the field of cancer therapy have produced a marked improvement in the successful control of many types of cancer. Surgical excision, radiotherapy and cytotoxic drugs administration are the tools available for the treatment of cancer. Often **surgery** is the main option in the majority of solid cancers and it may be a decisive cure when there is early diagnosis. **Radiotherapy** uses radiations to destroy the cancerous cells. Over the past century, radiotherapy has been the main intervention for the treatment of malignant cancers. It can be used prior to surgery to reduce the size of a solid cancer or during surgery, intraoperating radiation therapy, or sometimes as the only therapy if the cancer is very sensitive to radiations. Technological developments in physics, computing capabilities, and imaging have improved greatly the use of this type of therapy (Ahamad and Jhingran, Int. J.Gynecol Cancer, 2004).

Drug therapy is based on the administration of four categories of drugs: cytotoxic drugs (chemotherapy), hormones and antihormones (endocrine therapy), immunotherapeutic agents (immunotherapy) and molecular target agents (targeted therapy).

C*hemotherapy* employs a wide group of drugs that have cytotoxic effects and preferentially, but not exclusively, target the rapidly dividing cancer cells. *Endocrinetherapy* is a more specific form of treatment, used for example in breast cancer, prostate cancer and endometrial cancer. It prevents the proliferation of cancer cells that overexpress the receptor for the hormone that stimulates proliferation. For example, in breast cancer, the drug controls growth in cells overexpressing the oestrogen receptor. This can be effective in 60-70% of breast cancer patients.

Immunotherapy acts on the immune system with immunotherapeutic agents capable of stimulating and amplifying the specific immune response and activating it to attack and fight

cancer cells. *Targeted therapies* have been employed exploiting the overexpression of protein in many cancer cells.

Metabolic inhibitors intervene on specific proteins and pathways involved especially in cancer cell growth and associated with cell cycle regulation. However, these drugs are at an experimental stage of development, but represent a very promising approach for future strategies (Luqmani, Med Princ.Pract., 2005).

1.3.1 Anticancer Chemotherapy

Chemotherapy is a procedure that consists in the administration of cytotoxic drugs in order to destroy the cancer cells. It is the therapeutic modality more used to cure cancer. The treatment includes the administration of several drugs selected from a range of about 50 commercially available products. The decision as to which is the best treatment depends on many factors, such as the type and stage of the cancer and the clinical conditions of the patient. Chemotherapy may be implemented after surgery or radiotherapy in order to destroy any remaining cancer cells, grouped in masses too small to be detected by the diagnostic tools and so it can reduce the chances of recurrence or, in certain types of cancer, can lead to healing.

Unfortunately, a relevant problem in cancer chemotherapy is the low selectivity of the antineoplastic drugs. Often, toxic effects are superimposed to the therapeutic effects, as drugs also affect healthy cells. The action of the common anticancer agents is not, in fact, determined by specific biological differences between normal cells and cancer cells, but rather only by the speed at which the later multiply. The conventional chemotherapy is mostly based on the evidence that proliferating cells are more sensitive to anticancer agents than non-dividing cells. This is the main reason why these compounds are not cancer specific and their selectivity is generally in favour of rapidly growing cells (haematopoietic or intestine. i.e.) rather than discriminating against any fundamental biological difference between normal and cancer cells (Marchini *et al.*, Curr. Med. Chem. Anticancer Agents, 2004).The sensitivity of the healthy organs to the various chemotherapy drugs causes the appearance of a multitude of side effects that vary in part depending on the type of drugs used. The toxicity of chemotherapy occurs mainly in tissues with high proliferative index: bone marrow (leucopenia, thrombocytopenia, anemia, immunosuppression, infections), gastrointestinal mucosa (stomatitis, enteritis, mucus-

membranous colitis, diarrhea), skin and skin appendages (hair loss), gonads (amenorrhea, azoospermia)

Moreover, the real effectiveness of anticancer drugs is hampered by the mechanism(s) of **chemoresistance** that emerges in the population of cancer cells during chemocycles. To overcome drug resistance, the best therapeutic strategy is to associate more drugs with different mechanisms of action in multidrug cocktails. Actually, **combinatory chemotherapy** (polychemotherapy) is successfully used in the clinical practice as, by combining different drugs simultaneously addressing different cell targets, the frequency of drug-resistant mutants is strongly reduced.

Many anticancer agents are natural compounds extracted from plants, while others are of synthetic origin. On the basis of mode and site of action, they can be divided into three major groups: **antimetabolites**, **genotoxic agents** and **mitotic spindle inhibitors.**

Antimetabolites are drugs capable of interfering with the synthesis or use of a cellular metabolite. Examples are folate, pyrimidine and purine antagonists.

Folate Antagonists or Antifolates are inhibitors of dihydrofolate reductase (DHFR). Among Folate Antagonists there is Methotrexate that is used for the treatment of a variety of cancer including acute lymphocytic leukaemia, large cell lymphoma, high grade lymphoma, choriocarcinoma and cancer of the breast, bladder, head and neck and bone as well as many inflammatory diseases. *Pyrimidine Antagonists* may block pyrimidine nucleotide formation or may be incorporated into newly synthesized DNA, causing its premature termination. Among Pyrimidine Antagonists there is 5-FU. It is used in the treatment of breast, colon, stomach, rectum and pancreas cancers.

Purine Antagonists inhibit synthesis of adenine and guanine. The main examples are Acyclovir, 6-Mercaptopurine and 6-Thioguanine. They are used to cure acute lymphocytic or myelocytic leukaemia, lymphoblastic leukaemia and acute myelogenous and myelomonocytic leukaemia.

Genotoxic Agents bind to DNA or blocking the enzymes involved in replication, leading the cell to apoptosis. This class of drugs can be divided into several groups.

1*) alkylating agents* that modify the bases of DNA, interfering with replication and transcription. Examples include Cyclophosphamide, Melphalan, Mitomycin C and Temozolomide. *2) Intercalating Agents* that bind in the grooves of the DNA, interfering with the

activity of the polymerase during replication / transcription. Examples include Cisplatin, Epirubicin and Doxorubicin. 3) *Enzyme Inhibitors* that block replication by inhibiting enzymes such as topoisomerase. The mutagenic properties of these drugs make them carcinogenic, and so their use involves additional risk of secondary cancers, such as leukemia. Examples of these are Etoposide, Topotecan and Irinotecan.

Mitotic Spindle Inhibitors interrupt mitosis by preventing the polymerization of tubulin monomers, indispensable for the formation of the microtubules that form the spindle needed for chromosome alignment. Examples are the alkaloids of vegetable and synthetic origin paclitaxel and docetaxel (Luqmani, Med. Princ. Pract., 2005).

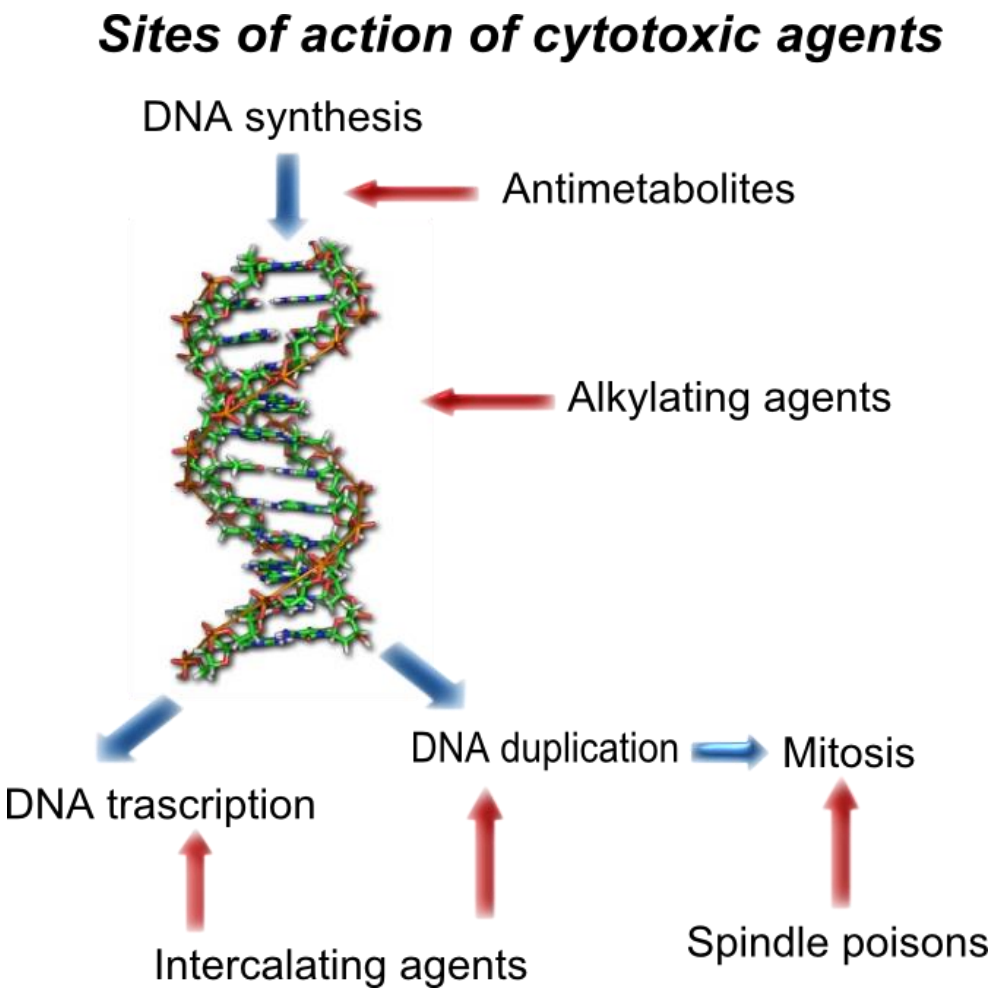

Figure 3. Sites of action of cytotoxic agents.

2. RATIONAL OF THE RESEARCH PROJECT

2.1 Cisplatin (CDDP) as anticancer agent

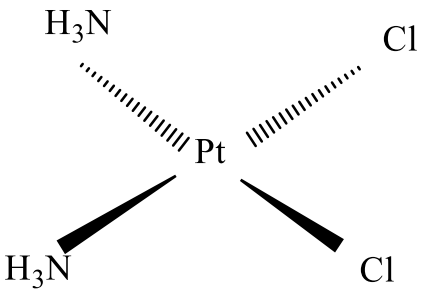

CDDP, **[Pt(NH3)2Cl2]***cis*-diammineplatinum(II) dichloride, is a small planar molecule with a central platinum ion surrounded by four ligands, two chloride ions and two molecules of ammonia arranged in the *cis* position (Goodsell, Stem Cells, 2006). In 1845, it was synthetized for the first time and in 1893 Alfred Werner deduced its structure (Desoize and Madoulet, Crit. Rev. Oncol. Hematol. 2002). Later Rosenberg tested the effects of several platinum complexes on rat sarcomas (Rosenberg, B., Spiro, T.G., Ed., Wiley & Sons, Inc., NY, USA, 1980).

In 1971, for the first time, was administered to a cancer patient (Lebwohl and Canetta, Eur. J. Cancer, 1998). In 1978, it became available for clinical practice as Platinol® (Bristol-Myers Squibb).

The discovery of CDDP as an anti-cancer drug gave away to new era in cancer treatment. In fact, it is widely used in clinical therapy of several solid cancers as ovarian, testicular, breast, head and neck and small cell lung cancer (Kelland, Nat. Rev. Cancer, 2007).

2.1.1 Mechanism(s) of action of cisplatin

Cisplatin enters the cells *via* passive diffusion and with protein-mediated transport systems such as human organic cation transporter hOCT2 and copper transporter Ctr1(Ishida *et al*., Proc. Natl. Acad. Sci. USA, 2002; Song, *et al*., Mol. Cancer Ther., 2004; Burger *et al*., Br. J. Pharmacol., 2010).

Cisplatin applies its biological activity, through hydrolysis, by interaction with DNA. When it is inside the cell, one of the chloride ligand of the complex is displaced by a water molecule to form the aqua-complex [Pt(NH3)2(H2O)Cl]+.This species binds DNA, losing the water molecule, and forming the mono-functional adduct [PtCl(DNA)(NH3)2]+. Then the second chloride of this species is displaced by a water molecule, forming another aqua-complex [Pt(H2O)(DNA)(NH3)2]2+. This species interacts with DNA to form the bi-functional adduct [Pt(DNA)(NH3)2]2+ (Alderden *et al*., J. Chem. Educ., 2006; Trzaska, Chem. Eng. News, 2005; Jamieson and Lippard, Chem. Rev., 1999; Toddand Lippard, Metallomics, 2009**).**

The damage caused by the binding of CDDP to gDNA can interfere with the normal mechanism of replication and transcription of DNA and it can lead to death of the cancer cell. It is also known that CDDP form a high amount of adducts in mitochondrial DNA (mtDNA) (Jamieson and Lippard, Chem. Rev., 1999) and furthermore, the mitochondria are unable to carry out the nucleotide excision repair (NER), an important route for the removal CDDP-DNA adducts (Perez, Eur. J. Cancer, 1998), it can be an important pharmacological target of cisplatin.

The most accessible and reactive nucleophilic sites for platinum binding to DNA are the N7 atoms of the imidazole rings of guanine and adenine located in the major groove of the double helix (Yang and Wang, Pharm. and Therap.,1999). The CDDP forms with the DNA various types of adducts. At first monofunctional adducts are formed but most of them further react to produce inter-strand or intra-strand cross-links, which block replication and prevent transcription (Payet *et al*., Nucleic Acid Res., 1993).

The principal bifunctional adduct with DNA is the 1,2-intra-strand cross-linking with two adjacent guanines, which is supposed to be responsible for the cytotoxic activity of the drug (Toddand Lippard, Metallomics, 2009).

If the cell is not able to repair CDDP-induced DNA damage, apoptosis is triggered. In some cell lines CDDP causes necrosis, which is considered a mode of cell death due to general cell machinery failure. In the same population of CDDP-treated cells necrotic and apoptotic cell death may take place together. It is also known that in the cell only 5-10% of cisplatin is bound to DNA, while 75-85% of the drug binds to proteins through the sulphur atoms of cysteine and / or methionine residues and to the nitrogen atoms of istidina residues. The consequence is that the toxicity of the CDDP is also due to functional protein damage.

In addition, before CDDP accumulates in the cell, it may bind to phospholipids and phosphotidylserine of the cell membrane. In the cytoplasm many cellular constituents that have

soft nucleophilic sites such as cytoskeletal microfilaments, thiol-containing peptides, proteins and RNA react with CDDP. (Fuertes *et al*., Chemical Review, 2003)

CDDP also induces reactive oxygen species (ROS) that can break normal biological functions and carry out cell death. The formation of ROS depends on the duration of exposure to CDDP and its concentration (Brozovic *et al*., Crit. Rev. Toxicol., 2010).

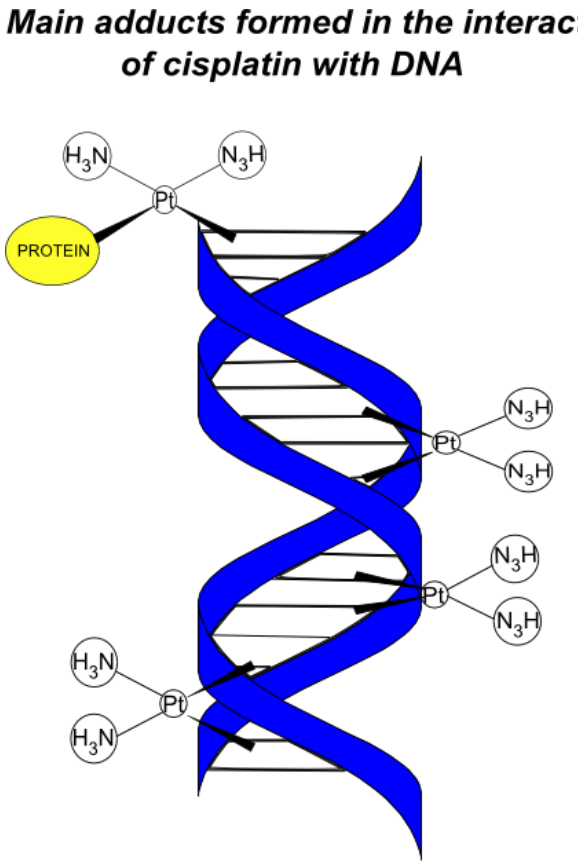

Figure 4. Main adducts formed in the interaction of cisplatin with DNA

2.1.2 CDDP side effects

CDDP shows a high toxicity for normal tissues and this is a restriction for the dose which can be administered. Side effects are nausea and vomiting, decreased blood cell and platelet production in bone marrow (myelosuppresion) and decreased response to infection (immunosuppression). More specific side effects include damage to the kidney (nephrotoxicity), damage of neurons (neurotoxicity) and hearing loss. (Desoize and Madoulet, Crit. Rev. Oncol. Hematol., 2002; Tsang *et al*., Drug Saf., 2009).

Management and strategies are renoprotection and enhance elimination of the drug by intravenous hydration with the possibility of using an osmotic diuretic.

Earing loss occurs mainly at high frequencies and is more pronounced when cisplatin is given once every second week (Rademaker-Lakhai, J. Clin. Oncol., 2006). It is necessary to use otoprotective agents to avoid compromising cancer treatment (Drottar *et al.*, Laryngoscope 2006). Cardio toxicity has also been associated to CDDP treatment.

2.1.3 Mechanisms of CDDP resistance

The effectiveness of CDDP is limited by the emergence of drug resistant cells in the population of susceptible cancer cells. As said, drug resistance acquired in the course of therapy is a major obstacle in the successful treatment of many cancers. A promising initial response of the cancer to chemotherapy by shrinking of the cancer volume is frequently observed, followed by appearance of chemoresistance, so that cancer cells do not respond to treatment with the drug (Duhem *et al*., The Oncologist, 1996).

CDDP-resistant cells often show several resistance mechanisms acting simultaneously (Eckstein N., Journal of Experimental and Clinical Cancer Research 2011), which include:

- increased drug efflux / diminished drug accumulation
- reduced uptake
- increased drug inactivation
- increased DNA repair / elevated DNA damage tolerance
- inhibition of apoptosis
- inactivation of the p53 pathway

One of the best studied mechanisms of chemoresistance is the increased drug efflux. The drug efflux reduces intracellular drug concentration and it is partially mediated by cell surface glycoproteins, which belong to the family of ATP-binding cassette (ABC) of multidrug transporters (Gottesman, Annu. Rev. Med., 2002). ABC transporters – such as MDR1 and MRP1– are highly expressed in many human cancers (Haber *et al*., European Journal of Cancer, 1997; Norris *et al*., Pharm. Res., 1997; Blanc *et al*., American Journal of Pathology, 2003; Munoz *et al*., IUBMB Life, 2007), and they are associated with the resistance of these cancers to chemotherapeutic drugs (Haber *et al.*, 1997; *Norris et al*., Pharm. Res.1997; Gottesman *et al*., Annu. Rev. Med., 2002).

Alternatively, CDDP-resistance emerges in mutant cells with an increased ability to repair or tolerate damaged DNA (Andrews *et al*., Cancer Cells 2, 1990; *et al*., Anticancer Res., 1989) or in cancer cells able to increase the intracellular levels of GSH (reduced glutathione) (Florea *et al*., Cancers, 2011), which binds to and inactivate CDDP. Altered sensitivity to CDDP may also be due to modified expression of regulatory proteins involved in signal transduction pathways that controls the apoptotic pathways and alterations in the expression of oncogenes (such as *c-fos*, *c-myc*, *H-ras*, *c-jun*, and *c-abl*) and cancer suppressor genes (such as *p53*) have also been implicated in the cellular resistance to CDDP (Kartalou *et al*., Mutat. Res., 2001).

It also has been suggested that Copper transporter 1 (CTR1) can play an important role in CDDP uptake and resistance. High expression of CTR1 in patients with ovarian carcinoma was associated with good therapeutic response, while low levels of the protein lead to poor therapeutic outcome so the transporter appears to be clinically relevant (Lee Y.Y. *et al*., Gynecol. Oncol. 2011). Deletion of CTR1 was reported to decrease cisplatin accumulation and to increase resistance in vitro and in vivo (Ishida *et al*., Proc. Natl. Acad. Sci. U.S.A. 2002; Lin *et al*., Mol. Pharmacol., 2002).

Whatever is the underlying mechanism of resistance, and despite of CDDP is part of several effective polychemotherapeutic protocols for the treatment of various types of cancer, its real effectiveness is yet limited by the emergence of drug resistant cell populations. Efforts to overcome the CDDP resistance have long been made (DeVita *et al*., Cancer, 1975); for example, CDDP has been tested in combination with other antineoplastic drugs, such as Fluvastatin (Taylor-Harding *et al*., Gynecol. Oncol., 2012), 5-Fluorouracil, Vincristine (Tang *et al*.,W. J. of Gastroent., 1998) and Taxol (Huang *et al*., Jpn J. Clin. Oncol., 2004) leading to promising results. Although some of these drug combinations have further progressed to Phase I and II *in vivo* trials,

due to inefficacy or intolerable toxicity, none of them reached a standard use in the clinic (Rodriguez-Enriquez *et al*., Mol. Nutr. Food Res., 2009)

2.2 Glutathione and its involvement in CDDP-resistance

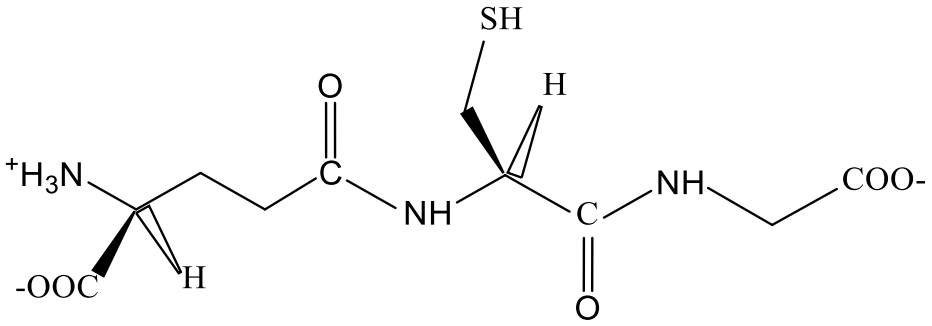

GSH is a thiol-containing tri-peptide (Glu-Cys-Gly), constituting 1-10mM in mammalian cells. De novo biosynthesis of GSH is controlled by the rate-limiting enzyme, glutamate-cysteine ligase (GCL, also known as γ-glutamylcysteinesynthetase, γ-GCS) which consists of a catalytic (heavy) (γ-GCSh) and a regulatory (light) subunit (γ-GCSl).

γ-GCS carries out the initial ligating reaction of glutamine (Glu) and cysteine (Cys). Production of GSH is accomplished by the subsequent reaction involving glycine (Gly) by GSH synthetase.GSH has different physiological functions, first of all the protection of the cell against oxidative damage. It can reduce metal ions and oxidant species such as reactive oxygen species (ROS). The oxidized form of glutathione (GSSG) is formed by two glutathione molecules bound with a disulfide bridge between the cysteine residuals. GSH is oxidized to GSSG by GSH peroxidase, whereas GSSG can be reduced back to GSH by GSSG reductase using NADPH as a cofactor.In physiological conditions the intracellular concentration of GSSG is 1/10 of that of GSH. When the normal ratio GSH / GSSG decreases, glutathione depletion derives.

This problem is correlated with pathologic conditions including cancer. In fact, it has been shown that the level of GSH in cancer cells is lower with respect to that in normal ones (Chen and Kuo, Metal-Based Drugs, 2010) and increased cellular GSH levels have been correlated with resistance to CDDP (Godwin *et al*., PNAS, 1992).

To explain the role of glutathione (GSH) in regulation of cisplatin resistance several mechanisms have been proposed: (1) GSH may serve as a cofactor of multidrug resistance

protein 2 (MRP2) that mediates CDDP efflux in mammalian cells; (2) GSH can serve as a cytoprotective through detoxification, based on the observations that many CDDP-resistant cells overexpress γ- glutamylcysteine (γ-GCS), the rate-limiting enzyme for GSH biosynthesis (Chen and Kuo, Metal-Based Drugs, 2010); (3) Platinum (II) shows high affinity versus the thiolic group. Indeed Pt(II) is a soft ion and it has more affinity towards a soft donor such as the sulfur atom of GSH than toward a hard one such as nitrogen of DNA bases. If CDDP reacts and forms adducts with GSH, is no longer able to interact with DNA, resulting deactivated as a drug (Kasherman *et al.*, J. Med. Chem., 2009). Actually, the formation of this kind of adduct is controversial in literature. In fact, according to some authors there is the displacement of both the amine ligands of CDDP to form with GSH the bis-(glutathionato)-platinum [Pt(GS)2]. (Ishikawaand Ali-OsmanJ. Biol Chem.,1993). Other authors propose that direct binding of CDDP with GSH is not the most important cellular interaction that leads to the inactivation of the cellular cisplatin (Kasherman *et al*., J. Med. Chem., 2009). Since the increasing of GSH concentration is not associated to a decreasing in Pt(II)-DNA adducts in the tumor cell, it has been supposed that GSH plays a role in apoptotic regulatory pathways (Siddik, Oncogene, 2003).

GSH may also function as a copper (Cu) chelator. Elevated GSH expression depletes the cellular bioavailable Cu pool, resulting in upregulation of the high-affinity Cu transporter (hCtr1), which is also a CDDP transporter. Copper transporter 1 (CTR1) is the major plasma-membrane transporter involved in intracellular Cu homeostasis, and it has been found to play a substantial role in the active transport of the CDDP. According to some authors, the increase of the GSH levels inside the cells could enhance the sensibility of cancer cells to CDDP by increasing the number of copper transporter and thus the drug uptake within the cell (Chen *et al*., Mol. Pharm., 2008).

2.3 Copper physiology and copper complexes as novel anticancer agents

Copper is a ubiquitous essential metal ion and it is a catalytic enzymatic co-factor in several biological pathways, as energy metabolism, respiration and DNA synthesis (Marzano *et al*., Anti-Cancer Agents in Med. Chem., 2011).Copper produces reactive oxygen species (ROS) and so, in large quantities, it is toxic to organisms (Halliwelland Gutteridge, Methods Enzymol., 1990)

To control copper levels there is a fine mechanism of homeostasis, based on proteins that contain cysteine, methionine or histidine-rich domains, that bind free copper (Marzano *et al*., Anti-Cancer Agents in Med. Chem., 2011). In human serum, copper is bound to ceruloplasmin,

an enzyme containing six copper atoms that are present both as Cu(I) and as Cu(II), or to albumin or amino acids (Laussac and Sarker, Biochemistry, 1984).

The Cu(II) can reach the cell where it is reduced to Cu(I) by a hypothetical membrane bound metalloreductase and absorbed by membrane transporters, basically CTR1 (Marzano *et al*., Anti-Cancer Agents in Med. Chem., 2011). Inside the cell the copper is complexed by a large variety of ligands, preventing the interaction of free copper with DNA and keeping its concentration lower than 10^{-18} M, (Safaei *et al*., J. Inorg. Biochem., 2004). The cytoplasmatic copper(I) is complexed mainly by GSH (Freedman *et al*., J. Biol. Chem., 1989) that can provide the metal ion to different intracellular proteins, such as metallothioneins and copper chaperones (Ferreira *et al*., Biochem., J. 1993). Being copper an essential element, Cu-complexes might be less toxic than those of non-essential metal ions, like platinum. As a consequence, in the last years many copper complexes have been prepared and tested as potential antitumoral agents. Copper(II) complexes are supposed to act against cancer cells in different ways with respect to cisplatin (Santini *et al*., Chem. Rev., 2014). In most studies, cell apoptosis and enzyme inhibition (proteasome, topoisomerase I and II, tyrosin protein kinase) were involved (Tripathi *et al*., Indian J. Cancer 2007; Nelson and Cox, Lehninger Principles of Biochemistry, 5th ed., 2008), whereas DNA appears to be the target of copper complexes containing nitrogen chelators, such as phen (Sigman *et al*., J. Biol. Chem., 1979).

Copper-phen complexes possess antiproliferative activity towards several tumor cell lines, since they are able to act as chemical nucleases, cleaving DNA and leading the cancer cells to death (Chakravarty *et al*., Proc.Indian Acad. Sci., 2002); some of them have shown anticancer effects *in vitro* and *in vivo* studies (Carvallo-Chaigneau *et al*., Biometals, 2008).

In a previous work made in my lab, an interesting *in vitro* antiproliferative activity towards several tumor cell lines, i.e. murine neuroblastoma , human prostate and lung carcinoma cell lines, T and B leukemia derived cells, has been shown by a novel class of copper complexes(II) with1,10-phenantroline (phen) (Pivetta *et al*., J. Inorg. Biochem., 2011 and 2012). In a further study, it was also shown that three Cu(II)-phen complexes of the series, i.e. Cu(phen)(OH2)2 (OClO3)2 [1], [Cu(phen)2(OH2)](ClO4)2 C0 and [Cu(phen)2(imidazolidine-2-thione)](ClO4)2 [C1], synergistically interact with CDDP in cells derived from a human T-lymphoblastic leukemia, CCRF-CEM (Pivetta T. *et al*., Talanta, 2013).

The cytotoxic effects of CDDP in combination with the above Cu(II)-phen complexes were evaluated by using the Experimental Design (ED) - Artificial Neural Network (ANN), a new and

more reliable methodological approach to determine types of effect and extent of multiple drug treatments

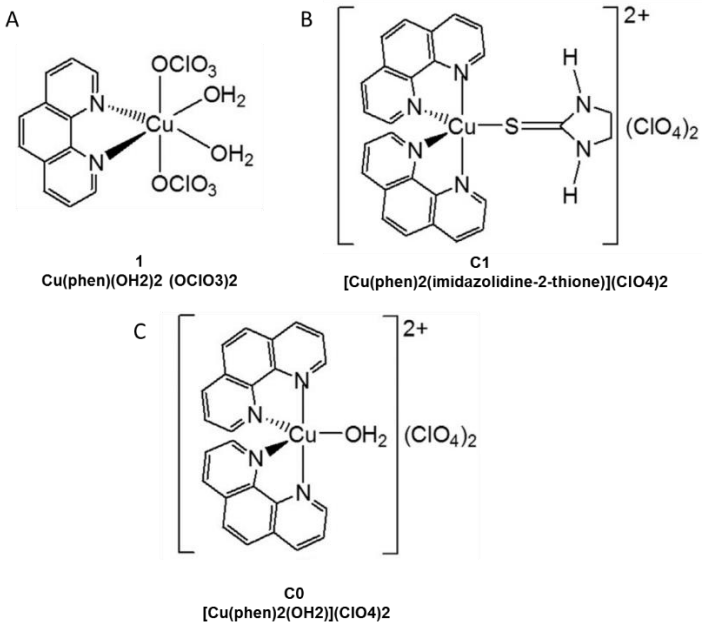

Figure 5 (A-C). Chemical structure of the compounds [1], C1and.C0

2.4 The research project

In the light of the large amount of information available in the literature on the properties and limits of CDDP as anticancer agent, including mechanisms of drug-resistance and in view of the potential clinical relevance of the synergic effect of CDDP with the Cu(II)-phen complexes, previously reported in T-leukemia cells (Pivetta *et al*., Talanta, 2013), my research project was aimed at extending the studies on the efficacy of CDDP - Cu(II)Phens combinations in:

a) cells derived from a human type of carcinoma usually treated with CDDP (i.e ovarian cancer);

b) CCDP-resistant cancer cell populations of hematologic and carcinoma origin;

c) human peripheral blood lymphocytes from healthy donors, in order to assess the potential degree of selectivity of the most synergic drug combinations.

Most studies were focused on the most potent compound C0 (fig.5B), the lead of our new Cu(II)-phen series. As experimental cell models, CDDP-resistant CEM cells (CEMres) selected from the parental T-leukemia CEM cells (CEMwt; reference cell line), and human ovarian

carcinoma A2780 cells, either wild type (A2780wt) and CDDP-resistant (A2780res), were used. The CEMres subline was purposely selected by myself in order to verify whether the synergistic effect of C0 and CDDP in CEM cells was maintained in a CDDP-resistant counterpart. The A2780 cells were chosen because they are derived from ovarian cancer for which CDDP yet remains one of the drugs of choice, and because this type of carcinoma is very sensitive to cisplatin at first, but it becomes resistant to the drug during the chemotherapy cycles, or in recurrences (Eckstein N., J. Exp. Clin. Cancer Res, 2011).

In regard to the role of GSH in the CDDP-resistance (Florea and Busselberg, Cancers 2011), worth mentioning is that GSH can reduce free Cu(II) to Cu(I), with the subsequent oxidation of GSH to GSSG, but not Cu(II) to Cu(I) in the C0 complex, due to the stabilization effect of phen ligand towards the bivalent form of the metal ion. Recent data from my lab showed in fact the formation of two complexes, with one or two molecules of GSH per metal ion (Pivetta *et al*., J. Inorg. Biochem., 2012).

Finally, based on the notion that neoplastic cells generally display altered lipid composition and distribution (Lladó *et al*., Biochim. Biophys. Acta, 2014; Szachowicz-Petelska *et al*., J. Environ. Biol., 2010; Riboni *et al.*, Glia, 2002), the phospholipid profiles of CDDP-resistant vs. those of wild type leukemia and carcinoma cell lines were also investigated.

All studies implying drug combinations were performed using the Experimental Design (ED), for the choice of the mixtures, and the Artificial Neural Network (ANN), for the evaluation of experimental results in terms of type and degree of drugs' interactions.

3. RESULTS AND DISCUSSION

3.1 Selection of CDDP-resistant CEM cells

As said above, a synergic cytotoxic effect was previously observed (Pivetta *et al.*,Talanta, 2013) in T-leukemia CEM cells by combinatory cell treatments of CDDP with the Cu(II)-phen complexes **[1]**, [**C1],** and, especially,**C0,** by using the Experimental Design (ED) - Artificial Neural Network (ANN), the novel methodological approach that allows to determine type and extent of drug interactions in multiple drug treatments.

Given the potential relevance of this finding for the clinic of cancer, it was of primary importance to investigate the effect of such drug combinations in sub-populations of the same cell line that showed a phenotype of resistance to CDDP (CEMres). To this end, a parallel culture of CEM cells was serially passaged in the presence of increasing concentrations of CDDP. The selection of a CEM subline with a stable phenotype of CDDP resistance was a long procedure that took about 7 months as cell cultivation in the presence of increasing drug doses had to be alternate with several passages at a constant concentration in order to avoid total cell death.

At first, cells were grown in the presence of a concentration of CDDP equal to 1/2 of the CC_{50}, i.e. 0.5 μM. This CDDP concentration was initially increased by 0.25 μM doses at each passage, but once the concentration of1.50 μM was reached, it was necessary to dwell for five consecutive passages at the same concentration. If further increased, in fact, the cells started growing with difficulty, the percentage of viability dropped, and the few viable cells showed the tendency to form clusters, an unusual feature for this type of cells. After that, the CDDP concentration could be increased to1.75μM for 2 passages, to 2 μM for 12 passages, then to 2.50 μM for 14 passages, and finally to 5 μM, the maximum drug concentration at which cells seemed able to multiply; in my hands, in fact, CEM cells were not able to adapt to CDDP concentrations higher than 5 μM. The latter cell population was stabilized at 5 μM CDDP by further 15 passages, then amplified, grown for one passage in the absence of the drug. Aliquots were stored in liquid nitrogen for experimental use.

At different times during the selection procedure, the sensitivity of cells to CDDP was determined and compared to that of the wild type-CEM cells by the MTT method. As can be seen (Table 1A, B, C), only after 52 passages in the presence of CDDP it was possible to obtain a stable CEM-CDDPres subline showing a Resistance Index (RI) of about 6 (Table 1C).

It is worth mentioning that cell populations growing in the presence of CDDP, as well as the final one resistant to CDDP, never showed at any extent cross-resistance to the Cu(II)Phen complex C0, indicating a different mechanism(s) of resistance of the two drugs, and thus also different molecular targets and modes of action. No modification in the cell sensitivity to the reference compound doxorubicin was ever observed (Table 1 A-C).

Table 1 (A-C). Citotoxicity of CDDPand C0 against CEMwtand CEMres

A

	CDDP	**C0**	**Doxorubicin**
CEMwt	1.12 µM	1 µM	0.02 µM
CEMres	2.6 µM	0.8 µM	0.02 µM
R.I.= 2.32 (14^{th} passage)			

B

	CDDP	**C0**	**Doxorubicin**
CEMwt	1.12 µM	1.1 µM	0.02 µM
CEMres	2.52 µM	0.8 µM	0.02 µM
R.I.= 2.25 (26^{th} passage)			

C

	CDDP	**C0**	**Doxorubicin**
CEMwt	1.12 µM	1 µM	0.02 µM
CEMres	6.98 µM	0.74 µM	0.02 µM
R.I.= 6.23 (52^{th} passage)			

Because cell resistance to CDDP has been reported to be multifactorial, i.e. reduced drug accumulation, increased drug inactivation, enhanced DNA-repair and increased DNA-damage tolerance, we deemed appropriate to obtain mechanistically homogenous cell clones from the mixed CDDP-resistant cell population in order to study them separately. However, despite of the several efforts made to grow cell clones by single-cell dilutions, an otherwise successful procedure to obtain cloned cell populations, in no case single-celI cultures were able to survive and multiply. Failed the separation of CDDP-resistant cells into different cloned populations, all studies implying CDDP-resistant CEM cells had to be performed on the cell subline stabilized at 5 µM CDDP (Table 1C).

3.2 Cytotoxic effects of drug combinations against leukemia CEM cells

3.2.1 Set up of the ED

For the study of drug combinations, the concentrations of the drugs should be chosen in the range within 0 and twice the CC_{50} (concentration of compound that reduce the viable cell by 50% with respect to untreated cells). Then the knowledge of a simple estimation of CC_{50} is needed. To model the dose response curve of each drug and the cytotoxicity response surface an adequate number of experiments is required. A non-symmetrical experimental design has been used.

The C0 and CDDP compounds were studied in the range of concentration of 0-2 μM while GSH in the interval 0-1000 μM.

We prepared for CEMwt i) 6 combinations of GSH and C0; ii) 6 combinations of GSH and CDDP; iii) 7 combinations of C0 and CDDP; iv) 52 combinations of GSH, C0 and CDDP; v) 10 solutions of CDDP alone, vi) 9 solutions of GSH alone and vii) 11 solutions of C0 alone; for CEM-res i) 9 combinations of GSH and C0; ii) 9 combinations of GSH and CDDP; iii) 9 combinations of C0 and CDDP; iv) 27 combinations of GSH, C0 and CDDP; v) 3 solutions of CDDP alone, vi) 3 solutions of GSH alone and vii) 3 solutions of C0 alone.

Following the Experimental Design reported in Figures 6-7, solutions as i), vi) and vii) were used to study the binary system GSH-C0 (Figures 6A,7A); solutions as ii), v) and vi) were used to study the binary system GSH-CDDP (Figures 6B, 7B); solutions as iii), v) and vii) were used to study the binary system CDDP-C0 (Figures 6C, 7C); solutions as iv), v), vi) and vii) were used to study the ternary system CDDP-GSH-C0 (Figures 6D, 7D).

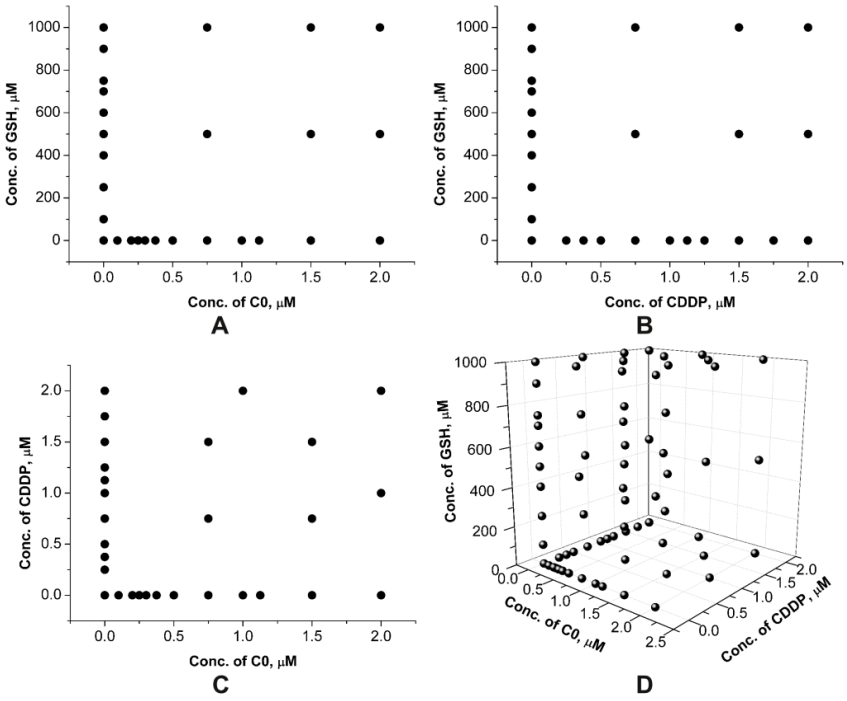

Figure 6. Concentration of combinations of (A) GSH and C0, (B) GSH and CDDP, (C) CDDP and C0, (D) GSH, C0 and CDDP for CEMwt cell line.

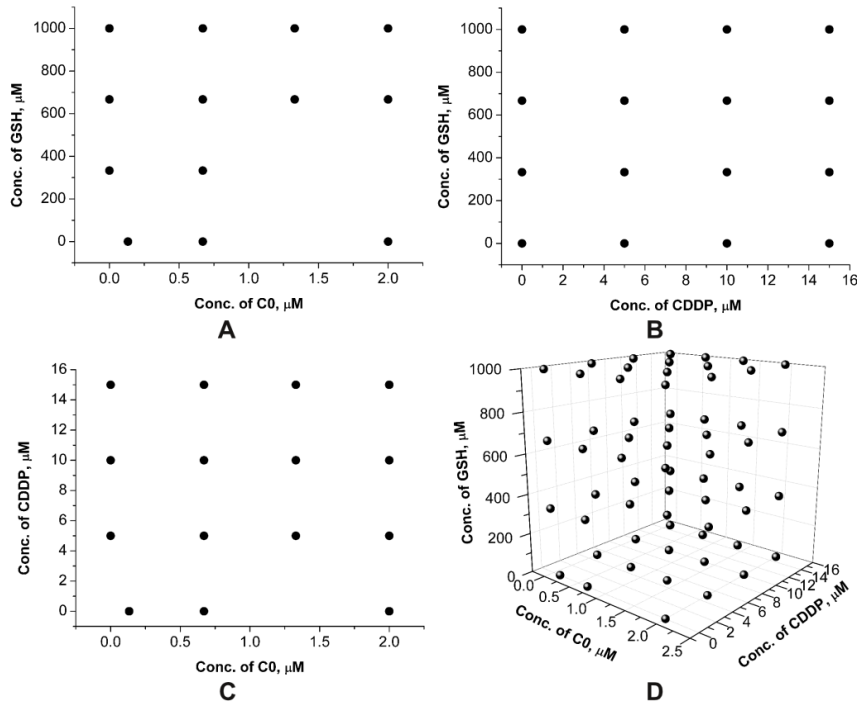

Figure 7. Concentration of combinations of (A) GSH and C0, (B) GSH and CDDP, (C) CDDP and C0, (D) GSH, C0 and CDDP for CEMres cell line.

3.2.2 Determination of the cytotoxicity of the drugs

The experiments were carried out in three replicates. The vitality (% of living cells) after the treatment with the drugs was measured for each solution with respect to the control (untreated cells) and converted, for calculation purpose, into mortality (as 100% minus vitality).

3.2.3 Training and verification of the artificial neural network

The concentrations of drugs and the related mortality values were used to form the data matrix. Concentrations of drugs were used as input data and the experimental mortality as output ones. The standard back-propagation was used as training algorithm. The optimal neural network architecture was searched for using the criteria of lowest RMSE and it was found that a three layers structure with 4 (binary systems) and 5 (ternary system) neurons in the hidden layer was sufficient. The architecture of the network for the ternary system is shown in Figure 8.

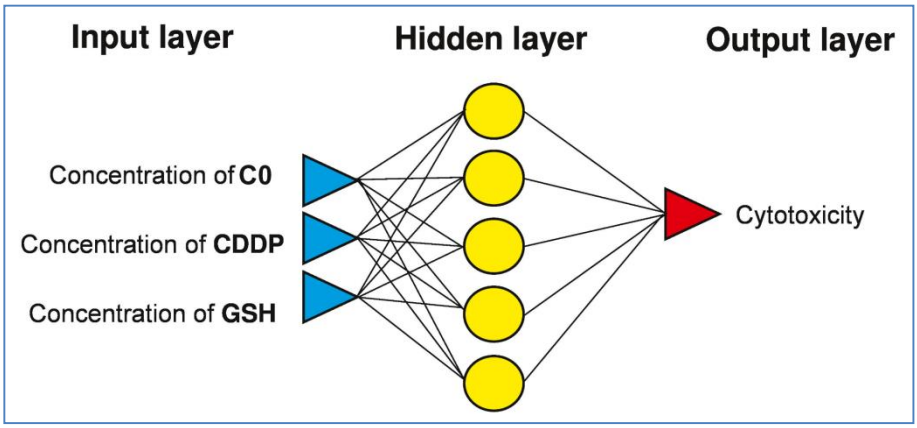

Figure 8. Architecture of the network used for the study of C0-CDDP-GSH ternary system.

The network was trained and verified using the training and validation sets. All points lying on the borders of the experimental design were included in the training set. Validation points were chosen randomly on the working space. Among the prepared 101 solutions for CEMwt, 80 were used as training set, 9 as validation set and 12 as test set, among the prepared 63 solutions for CEMres, 40 were used as training set, 11 as validation set and 12 as test set.

The generalization ability of the network was used to predict the cytotoxicity on the whole working space according to a bi-dimensional grid with 40 points per side for the binary systems and according to a cube with 20 points per side for the ternary system. At first, the data of binary

systems were processed individually. Then, data of binary and ternary systems were processed together. The results for the binary systems obtained in the two processes were strictly comparable, proving the robustness and the reliability of the method. The agreement between calculated and experimental values for all the data for CEMwt cell line is shown in Figure 9 as example.

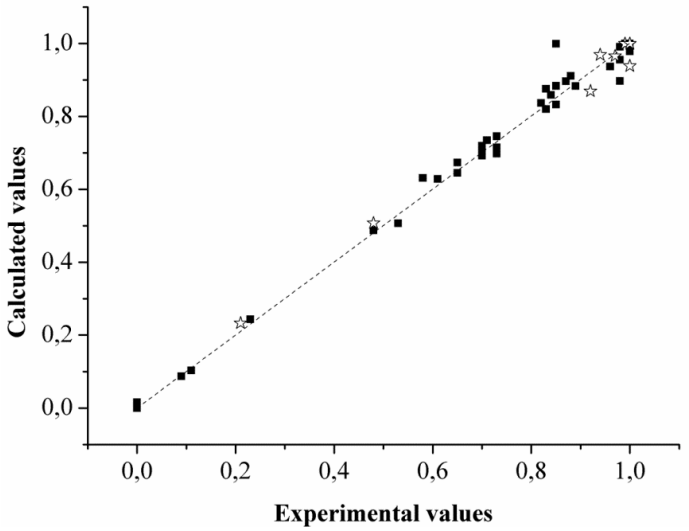

Figure 9. Comparison between experimental and calculated mortality values (■ training set, ☆ validation set) for the ternary systems C0-CDDP-GSH for CEMwt cell line (linear fitting parameters for the equation $y = mx+q$ are m = 0.9951, q = 0.007 with r = 0.9974 for training set, m = 0.9536, q = 0.0038 with r = 0.9947 for validation set, m = 0.9912, q = 0.0092 with r = 0.9974 for all the data).

3.2.4 Prediction of the response (cytotoxicity surfaces) for CEMwt cell line

The cytotoxicity of the mixtures and that of the drugs alone for the whole working space, were calculated by using the network. The dose-response curves for each compound and the cytotoxicity surface were then obtained.

The calculated dose-response curves together with the experimental points for CDDP, GSH and C0 for CEMwt cell line are reported in Figure 10 A,B,C, respectively.

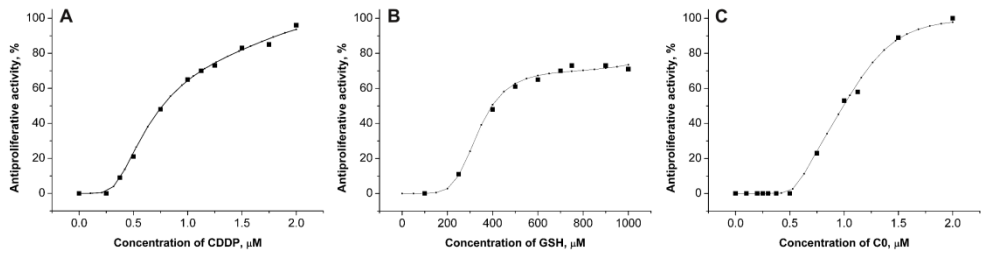

Figure 10. Calculated dose-response curve (-•-) and experimental points (■) for (A) CDDP, (B) GSH and (C) C0, for CEMwt cell line.

The different trends of the curves may suggest a different action mechanism inside the cells. The threshold doses (the minimum dose at which the drug presents an effect) for the three compounds are: 0.25 µM for CDDP, 150 µM for GSH and 0.5 µM for C0. The CC_{50} values are in the order CDDP (0.78 µM) <C0(1.05 µM) << GSH (332.1 µM).

The cytotoxicity of C0 and CDDP are comparable. Also GSH presents a cytotoxic activity towards cancer cells.

Binary mixtures

The response surfaces calculated by the network (together with the experimental points) and the related contour plots for C0-CDDP, CDDP-GSH, and C0-GSH systems are shown in Figure 11 A,B,C. The calculated values are in good agreement with the experimental ones. The mortality increases with the concentrations of the two drugs, having similar trend to that one of the dose-response curve.

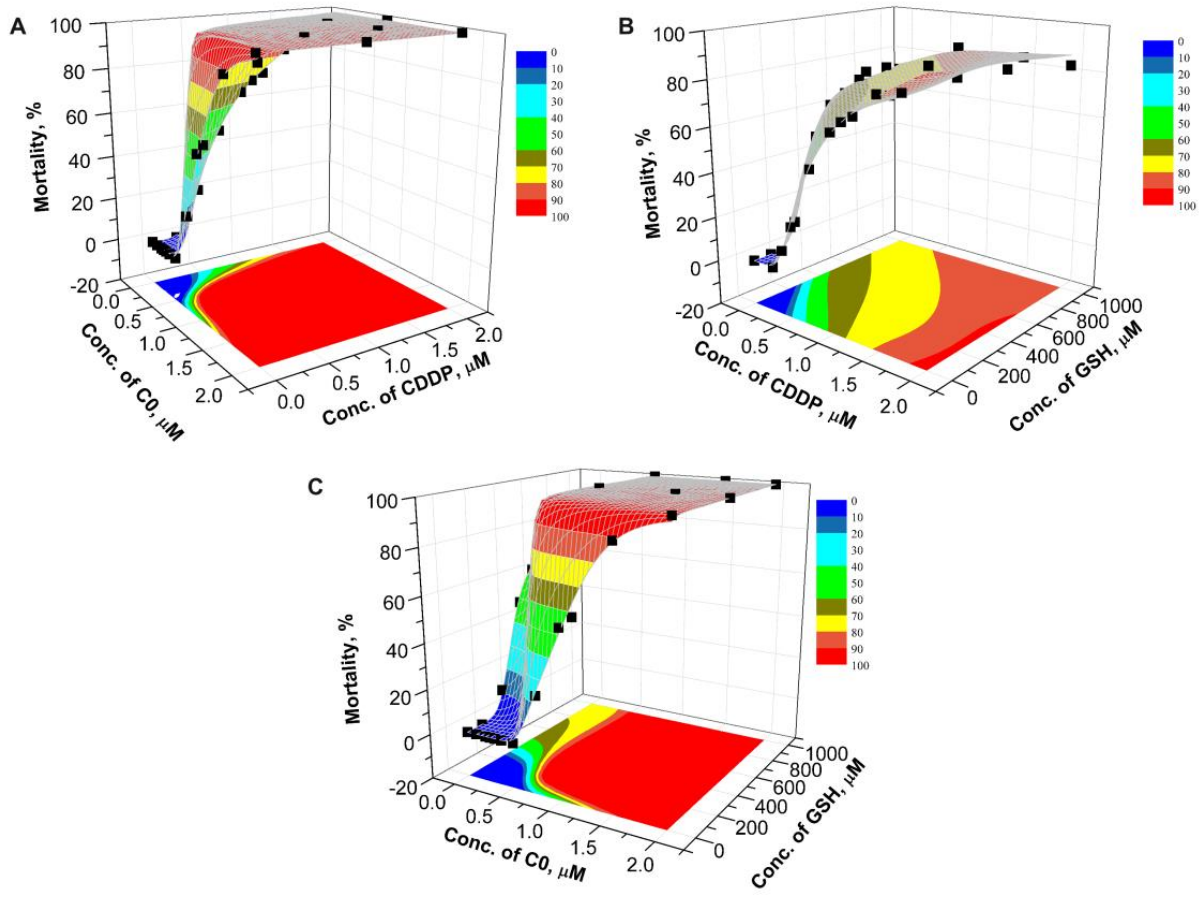

Figure11. Calculated response surface and contour plot of cytotoxicity iso-values for the systems (A) C0-CDDP, (B) CDDP-GSH and (C) C0-GSH for CEMwt cell line; experimental points (■) are superimposed.

The areas of cytotoxicity iso-values of the contour plot for the binary mixtures can be explored to discover the combination with desired cytotoxicity and the related dose of both drugs. For example, if a toxicity of 50% is searched for, instead of choosing C0 alone at a concentration of 0.99 μM or CDDP alone at a concentration of 0.77 μM or GSH alone at a concentration of 403 μM, selected combination may be choosen, as:

- C0 at 0.26 μM and CDDP at 0.40 μM (Figure 11A);
- CDDP at 0.32 μM and GSH at 200 μM (Figure 11B);
- C0 at 0.42 μM and GSH at 200 μM (Figure 11C).

For a toxicity of 70%, instead of choosing C0 alone at a concentration of 1.20 μM or CDDP alone at a concentration of 1.13 μM or GSH alone at a concentration of 769 μM, selected combination may be choosen, as:

- C0 at 0.32 μM and CDDP at 0.40 μM (Figure 11A);
- CDDP at 0.63 μM and GSH at 240 μM (Figure 11B);
- C0 at 0.47 μM and GSH at 200 μM (Figure 11C).

The possibility to reach the same effect but with lower doses of the drugs gives the chance to minimize the side effects related to the doses.

Ternary mixtures

The mortality surfaces calculated by the network for the ternary system CDDP-GSH-C0 is shown in Figure 12 A (colour is proportional to the cytotoxic activity of the mixtures). To simplify the interpretation of the graph and to appreciate the trend of the cytotoxicity also in the core of the cube, only seven planes along the z axis have been reported in Figure 12 B.

As can be seen from the graph, a low value of cytotoxicity appears for low concentrations of all the compounds, while for concentration higher than 1 μM for C0 or CDDP the activity reaches quickly the highest value of 100%. Several combinations with a cytotoxic activity of 50% or 70% may be chosen, as for example:

- C0 at 0.11 μM, CDDP at 0.21 μM and GSH at 250 μM (mortality values of 50%)
- C0 at 0.32 μM, CDDP at 0.11 μM and GSH at 200 μM (mortality values of 50%)
- C0 at 0.11 μM, CDDP at 0.63 μM and GSH at 200 μM (mortality values of 70%)
- C0 at 0.11 μM, CDDP at 0.11 μM and GSH at 650 μM (mortality values of 70%)
- C0 at 0.11 μM, CDDP at 0.42 μM and GSH at 400 μM (mortality values of 70%)

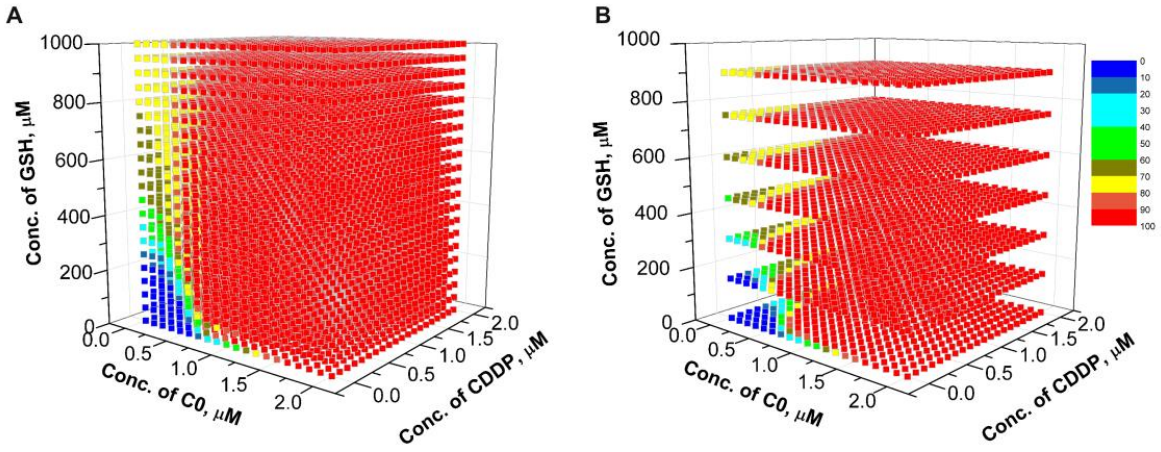

Figure 12. Full calculated response surface for the ternary systems CDDP-GSH-C0 for CCRF-CEMwt cell line (A), some selected planes are reported for clarity (B); the colour of the point is proportional to the cytotoxic activity.

3.2.5 Calculation of the non-additive effect and of the net multidrug effect index in CEMwt cell line

The non-algebraic additive effect (NAEE) of the combined drugs was calculated according to the equation already presented (Pivetta *et al.* Talanta, 2013). The synergistic/antagonistic effect was evaluated calculating the net multi drug effect index (NMDEI) (Pivetta *et al.* Talanta, 2013) for all the points of the used grid. The calculated surfaces show (Figure 13 for the binary systems and Figure 14 for the ternary system) the possible interactions occurring between two or among three drugs, allowing to determine if there is a synergistic or an antagonistic effect.

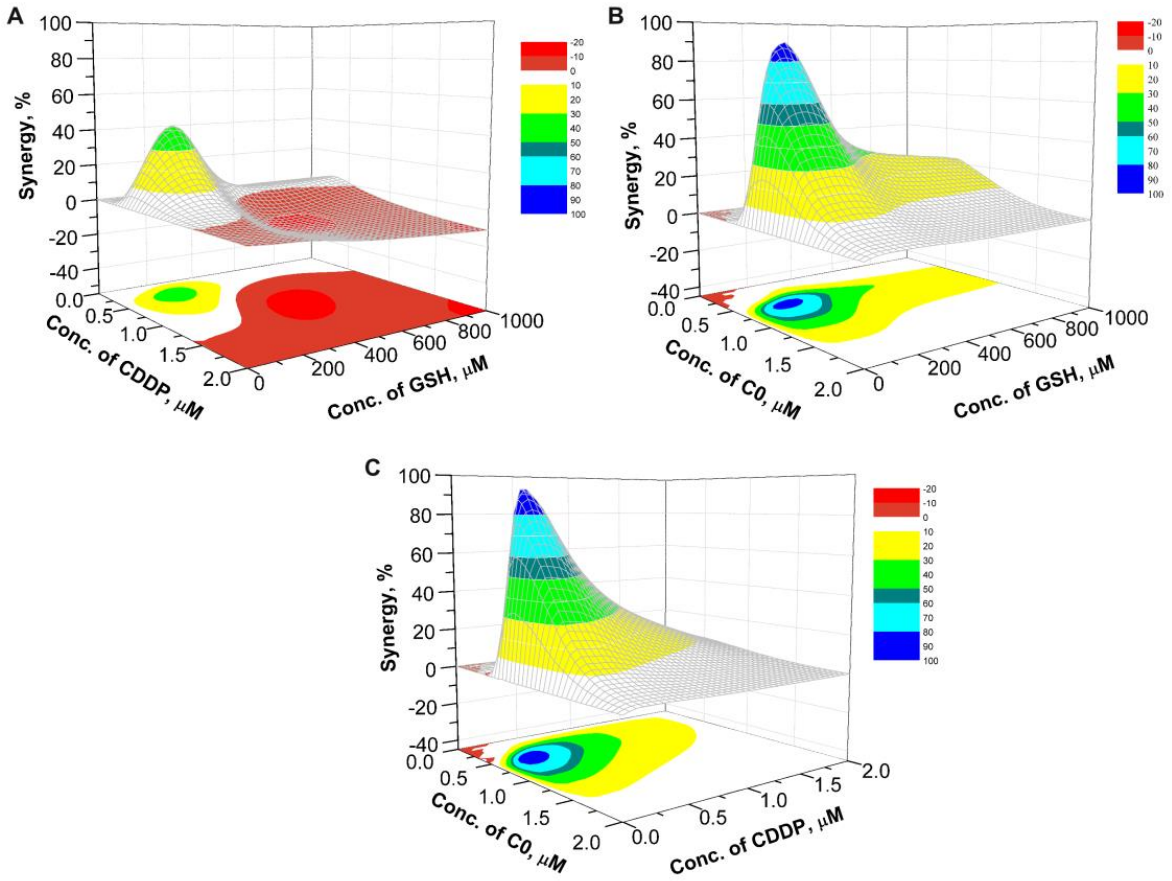

Figure 13. Synergistic surfaces for the binary systems of (A) CDDP and GSH, (B) C0 and GSH, (C) C0 and CDDP for CEMwt cell line.

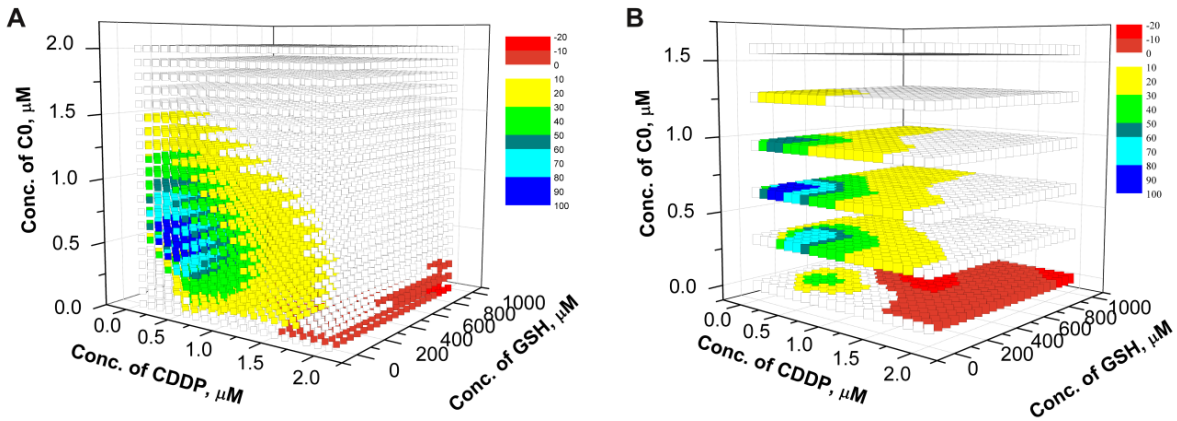

Figure 14. Synergistic surfaces for the ternary systems CDDP-GSH-C0 for CEMwt cell line (A), some selected planes are reported for clarity (B); the color of the points is proportional to the synergistic effect.

Binary mixtures of CDDP and GSH

In the plot of the NMDEI as a function of CDDP and GSH concentrations (Figure 12A) a maximum (value is 42.0) is present for a concentration of CDDP 0.39 µM and of GSH 247 µM. At these concentrations both the two drugs, taken individually, present a mortality value of 10%, while their combination present a mortality value of 53.9% (Figure 11B). A synergistic effect is evident.

In the plot there is a wide area of negative values, in particular in the region where 0.76 µM ≤ CDDP ≤ 1.48 µM and 384 µM ≤ GSH ≤ 684 µM, with a minimum (value is -12.4) at CDDP 1.14 µM and GSH 533 µM. This combination presents a cytotoxicity value of 75.7% (Figure 11B), while the two drugs alone show at the same concentrations, a cytotoxicity of 69.6% and 65.0%, respectively. In this case an antagonistic effect is present.

Binary mixtures of C0 and CDDP

In Figure 13C is showed the plot of NMDEI as a function of the concentration of C0 and CDDP. There is a wide positive area that indicates a synergistic effect between the two drugs. A maximum of NMDEI (value is 91.9) appears for CDDP 0.34 µM and C0 0.54 µM. This combination shows a cytotoxicity of 96.7% (Figure 11A) while the two compounds alone show at the same concentration of the combination, a cytotoxicity values of 3% and 6%, respectively. The synergistic effect between C0 and CDDP is in agreement with previous findings (Pivetta T. *et al.*, Talanta, 2013)

Binary mixtures of C0 and GSH

In Figure 13B is reported the plot of the NMDEI as a function of C0 and GSH concentrations. A maximum (value is 89.2) is present for C0 at 0.60 µM and GSH at 220 µM. At these concentrations the two drugs, taken individually, present a mortality value of 8% and 6% respectively, while their combination present a mortality value of 95.7% (Figure 11C). A clear synergistic effect is evident.

Ternary mixtures of CDDP, GSH and C0

For the evaluation of the three-drug system, cubic surface has been build up, representing the NMDEI value with the colour of the points (Figure 14A). For clarity, only 6 planes were

represented in Figure 14B. It shows the influence of the concentration of C0 to the cytotoxicity of the mixtures. In absence of C0 (first plane from the bottom)**,** for high concentrations of GSH, there is antagonism between CDDP and GSH. In presence of concentrations of C0 higher than 0.5 μM the antagonism between CDDP and GSH disappears. There is synergism between C0 and CDDP only at low concentration of GSH (for [C0]=[CDDP]= about 0.75 μM) (this could be explained by the formation of an adduct Pt-C0 and high concentration of GSH interfere with this reaction).

Summarizing it is possible to see that:

- at low concentrations of C0, there is antagonism between GSH and CDDP**;**
- at low concentrations of GSH, there is a good synergy between C0 and CDDP, for a combination in molar ration of about 1:1.

3.2.6 Calculation of the non-additive effect and of the net multidrug effect index in CEMres cell line

The cytotoxicity of mixtures and drugs alone, together with the response surfaces, were calculated by using the network, for the case CEM-res, following the same procedure adopted for the CEM-wt. The calculated surfaces for the binary systems and that for the ternary system are reported in Figure 15 and Figure 16, respectively.

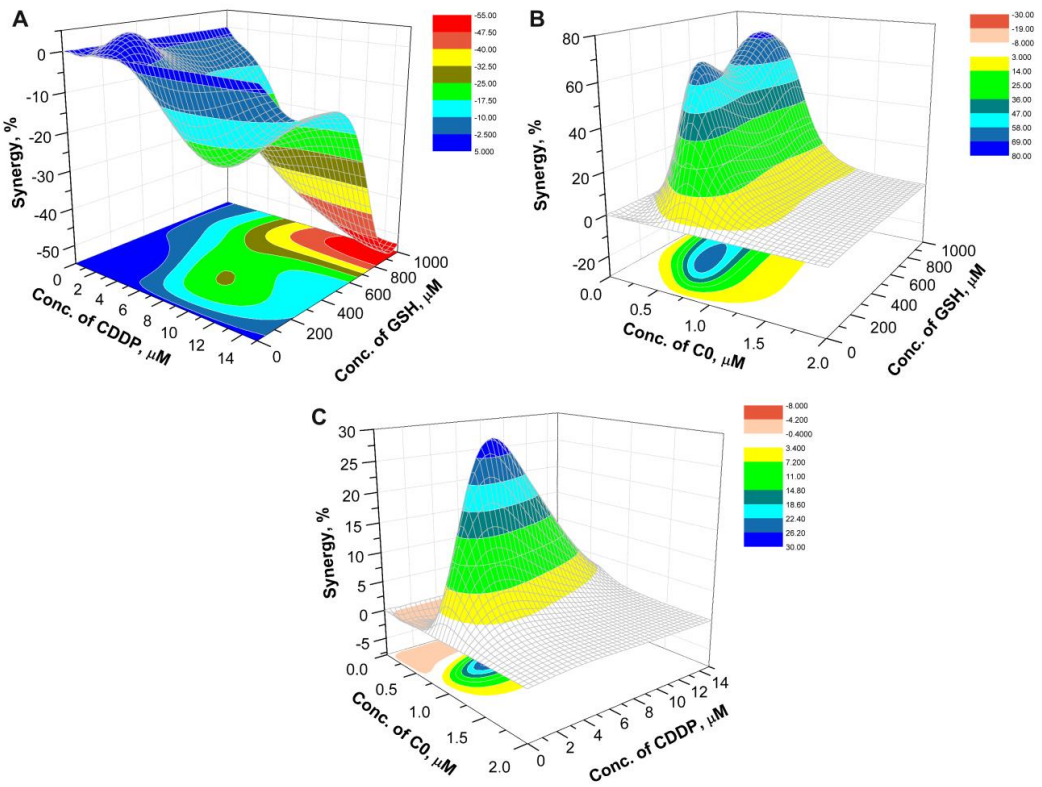

Figure 15. Synergistic surfaces for the binary systems of (A) CDDP and GSH, (B) C0 and GSH, (C) C0 and CDDP for CEM-res cell line.

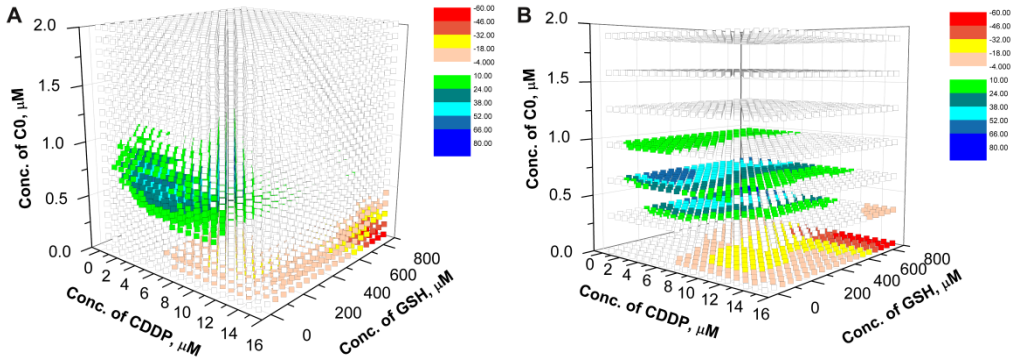

Figure 16. Synergistic surfaces for the ternary system CDDP-GSH-C0 for CEM-res cell line (A), some selected planes are reported for clarity (B); the color of the points is proportional to the synergistic effect.

Binary mixtures

In the plot of the NMDEI as a function of CDDP and GSH concentrations (Figure 15A), there is a wide negative area that indicates an antagonistic effect between the two drugs. A minimum of NMDEI (value is -53.8) appears for CDDP 15 µM and GSH 950 µM. This combination shows a cytotoxicity of 42 %, while the two drugs alone show at the same concentrations, a cytotoxicity of 94.4 % and 24.9 %, respectively. In the plot, there is a limited positive area, in particular in

the region where 0.79 µM <CDDP< 3.95 µM and 50 µM < GSH < 300 µM, with a maximum of 4.1.

In Figure 15B, is reported the plot of NMDEI as a function of the concentration of C0 and GSH. In all the studied region, a synergistic effect is evident. Two maximums (values are 70.9 and 65.4) appear for C0 0.42 µM and GSH 900 µM, and for C0 0.53 µM and GSH 350 µM. The second combination presents a cytotoxicity value of 95.6 %, while the two drugs alone show at the same concentrations, a cytotoxicity of 10.8 % and 21.8 %, respectively.

In Figure 15C, is showed the plot of the NMDEI as a function of C0 and CDDP concentrations. The wide positive area indicates a synergistic effect between the two drugs. A maximum of NMDEI (value is 28.3) appears for C0 0.74 µM and CDDP 4.74 µM. This combination shows a cytotoxicity of 87.8 %, while the two compounds alone show at the same concentrations of the combination, a cytotoxicity values of 45.5 % and 25.7 %, respectively. In the plot there is a limited negative area, in particular in the region where 0.11 µM <C0< 0.52 µM and 0.78 µM <CDDP< 8.68 µM, with a minimum of -2.9.

Ternary mixtures of CDDP, GSH and C0

In Figure 16, the plots show the influence of the concentration of C0 to the cytotoxicity of the mixtures CDDP-GSH. As for CEMwt, in absence of C0 there is antagonism between CDDP and GSH. In presence of concentrations of C0 higher than 0.4 µM the antagonism between CDDP and GSH disappears.

3.2.7 Test points

The most relevant combinations of drugs were chosen as test point and the mixture were prepared and the corresponding cytotoxicity measured, to compare the experimental values with the ones calculated by the network. The mortality values calculated with the network are in good agreement with the experimental ones, confirming the predicting abilities of the network.

3.3 Cytotoxic effects of drug combinations against ovarian carcinoma A2780 cells

It was interesting to investigate if the drugs in binary and ternary combinations one with another were also active against human ovarian carcinoma cell lines, wild type (A2780wt) and CDDP-resistant (A2780res). As said above, in fact, CDDP yet remains one of the drugs of choice

in the treatment of ovarian cancer. This type of carcinoma is very sensitive to cisplatin at first, but it becomes resistant to the drug during the chemotherapy cycles or in recurrences.

3.3.1 Cytotoxic effects of drug combinations against A2780wt

Cytotoxicity of C0, CDDP and GSH, alone, in binary, and ternary combinations was evaluated against A2780wt cells after 96 hours of treatment. The numbers of viable cells, as determined by trypan blue exclusion method, were reported as percentage of untreated controls and converted in percentage of mortality. Dose-response curves for each compound were determined (not shown); CC_{50} values were 0,11µM for C0 and 0,22µM for CDDP. GSH displayed a biphasic curve, but the mortality of GSH-treated cells was below 50% at any concentration (range 1mM-300µM) tested. With the ED/ANN experimental approach, we prepared for A2780wt cells: i) 9 combinations of GSH and C0;ii) 9 combinations of GSH and CDDP; iii) 9 combinations of CDDP and C0;iv) 27 combinations of CDDP, GSH and C0; v) 3 solutions of CDDP alone; vi) 3 solutions of GSH alone; vii) 3 solutions of C0 alone.

The non-algebraic addictive effect (NAEE) of the combined drugs was calculated according to the equation already reported (Pivetta *et al.*, Talanta, 2013).

The synergistic/antagonistic effect was determined by calculating the net multidrug effect index (NMDEI) (Pivetta *et al.*, Talanta, 2013) for all the combinations.

In tables 2 and 3 are reported some of the results with the binary and ternary combinations. In A2780wt cells, single drug treatment with 0,5 µM, 1 µM and 1,5 µM CDDP showed a cell mortality values of 66,5%, 68,52 % and 73,91%, respectively. In agreement with the detoxifying role of GSH into the cells (Godwin *et al*., Proc. Nat. Ac. Sc. U.S.A., 1992), when CDDP was in binary combinations with 333 µM, 666 µM and 1000 µM GSH, the mortality was reduced to only 8%, clearly indicating an antagonistic effect in these range of GSH concentrations. On the contrary, when CDDP was tested in binary combinations with C0, a strong synergism was obtained with a percentage of cell mortality of 93%. A synergistic effect was also observed with the combinations of C0 - GSH: the highest index of synergism (SI $\geq$ 26) was obtained with 0,075µM C0 and 1000µM GSH.

As already seen in T-leukemia (CEM) cells, also in the A2780wt, when C0 was added to the antagonistic combinations of CDDP+GSH , mortality values reached 100%, thus clearly showing that C0 was not only able to annul the antagonism of GSH on the cytotoxicity of CDDP, but even to increase further the anti-cellular effect of CDDP-C0 combinations.

Table 2. Antiproliferative activity (%) against A2780wt of C0, CDDP, GSH, alone and in binary combinations

	Cell mortality (%)					
Compound concentrations	C0	CDDP	GSH	Binary combinations	Effect	Index (%)
C0 0,075 µM CDDP 1 µM	18,62811	68,527236		76,66443	synergism	2,274408
C0 0,155 µM CDDP 1,5 µM	63,68527	73,907196		93,36247	synergism	2,838006
C0 0,075 µM GSH 333 µM	18,62811		19,4351	47,34364	synergism	12,90082
CDDP 0,5 µM GSH 333 µM		66,509751	19,4351	37,12172	antagonism	-35,8969
C0 0,25 µM GSH 666 µM	86,0121		36,11298	98,4768	synergism	7,413248
CDDP 0,5 µM GSH 666 µM		66,509751	36,11298	35,44048	antagonism	-43,1636
CDDP 1 µM GSH 666 µM		68,527236	36,11298	49,96638	antagonism	-29,9266
C0 0,075 µM GSH 1000 µM	18,62811		8,809684	51,91661	synergism	26,11989
CDDP 0,5 µM GSH 1000 µM		66,509751	8,809684	30,93477	antagonism	-38,5254
CDDP 1 µM GSH 1000 µM		68,527236	8,809684	45,52791	antagonism	-25,772

Table 3. .Antiproliferative activity (%) against A2780wt of C0, CDDP, GSH, alone and in ternary combinations.

	Cell mortality (%)					
Compound concentrations	C0	CDDP	GSH	Ternary combinations	Effect	Index (%)
C0 0,155 µM CDDP 0,5 µM GSH 666 µM	63,68527	66,50975	36,11298	97,26967	synergism	5,039541
C0 0,155 µM CDDP 1 µM GSH 666 µM	63,68527	68,52724	36,11298	95,76328	synergism	3,065088
C0 0,155 µM CDDP 0,5 µM GSH 1000 µM	63,68527	66,50975	8,809684	97,56557	synergism	8,656037
C0 0,155 µM CDDP 1 µM GSH 1000 µM	63,68527	68,52724	8,809684	100	synergism	10,42237

3.3.2 Cytotoxic effects of drug combinations against A2780res

Cytotoxicity of C0, CDDP and GSH, alone, in binary and ternary combinations was also evaluated against A2780res cells under the same experimental conditions. Dose-response curves for each compound were determined (not shown). CC50 values were 0,38 µM for C0 and 5.7µM for CDDP. Again, GSH displayed a biphasic curve, but in the A2780res it did not show any cytotoxicity at any of the concentrations used (i.e. 1mM-300 µM).

We then prepared: i) 9 combinations of GSH and C0;ii) 9 combinations of GSH and CDDP; iii) 9 combinations of CDDP and C0; iv) 27 combinations of CDDP, GSH and C0; v) 3 solutions of CDDP alone; vi) 3 solutions of GSH alone; vii) 3 solutions of C0 alone (Figure 17). The non-algebraic addictive effect (NAEE) and the synergistic/antagonistic effect was calculated as above.

In tables 4 and 5 are reported some of the results with binary and ternary combinations. Similar effects to those showed in wild type cell line, were observed in the resistant cells. Single drug treatment with 4 µM, 8 µM and 13µM CCDP showed a cell mortality values of respectively 38%, 70% and 87%. When CDDP was in binary combinations with 333 µM, 666 µM and 1000 µM GSH, its toxic effect decreased, while using the highest GSH concentration it became no toxic demonstrating a strong antagonism effect. When CDDP was tested in binary combinations with C0 a synergic effect was detected, and the percentage of mortality increased until 94% with a index of synergy of 7%. A synergistic effect was also observed when cells were treated with the combinations of C0 and GSH; 0,2 µM C0 with GSH 333µM showing the highest index of synergy of 87% (table 4).

When C0 was added to binary combinations of CDDP+GSH, the antagonism disappeared and all the ternary combinations resulted synergistic. CCDP 4 µM in single-drug treatment had a cytotoxic effect (38% of cell mortality) whereas with GSH and 0,2 µM C0 cytotoxicity increased leading to up to a 98% of cell mortality with a index of synergy of 60 % (table 5). The calculated surfaces (Figure 18) show the possible interactions occurring between the three drugs.

Table 4. Antiproliferative activity (%) against A2780res of C0, CDDP, GSH, alone and in binary combinations.

	Cell mortality (%)					
	C0	CDDP	GSH	Binary combinations	Effect	Index (%)
C0 0,2 µM CDDP 4 µM	0	38		52	synergism	14
C0 0,4 µM CDDP 4 µM	53	38		86	synergism	15,14
C0 0,4 µM CDDP 8 µM	53	70		92,4	synergism	6,5
C0 0,2 µM CDDP 13 µM	0	87		94,1	synergism	7,1
C0 0,1 µM GSH 333 µM	0		0	81	synergism	81
C0 0,2 µM GSH 333 µM	0		0	87	synergism	87
C0 0,4 µM GSH 333 µM	53		0	99	synergism	46
CDDP 8 µM GSH 333 µM		70	0	30	antagonism	-40
C0 0,1 µM GSH 666 µM	0		0	64	synergism	64
C0 0,2 µM GSH 666 µM	0		0	85	synergism	85
C0 0,4 µM GSH 666 µM	53		0	96,3	synergism	43,3
CDDP 4 µM GSH 666 µM		38	0	7	antagonism	-31
CDDP 8 µM GSH 666 µM		70	0	59,6	antagonism	-10,4
CDDP 13 µM GSH 666 µM		87	0	69,2	antagonism	-17,8
C0 0,2 µM GSH 1000 µM	0		0	84,8	synergism	84,8
C0 0,4 µM GSH 1000 µM	53		0	90,3	synergism	37,3
CDDP 4 µM GSH 1000 µM		38	0	0	antagonism	-38
CDDP 8 µM GSH 1000 µM		70	0	0	antagonism	-70
CDDP 13 µM GSH 1000 µM		87	0	0	antagonism	-87

Table 5. Antiproliferative activity (%) against A2780res of C0, CDDP, GSH, alone and in ternary combinations.

	Cell mortality (%)					
	C0	CDDP	GSH	Ternary combinations	Effect	Index (%)
C0 0,1 µM CDDP 4 µM GSH 333 µM	0	38	0	81	38	43
C0 0,2 µM CDDP 4 µM GSH 333 µM	0	38	0	98	38	60
C0 0,2 µM CDDP 8 µM GSH 333 µM	0	70	0	98,6	70	28,6
C0 0,1 µM CDDP 4 µM GSH 666 µM	0	38	0	63	38	25
C0 0,2 µM CDDP 4 µM GSH 666 µM	0	38	0	85	38	47
C0 0,2 µM CDDP 8 µM GSH 666 µM	0	70	0	93,4	70	23,4
C0 0,2 µM CDDP 4 µM GSH 1000 µM	0	38	0	85	38	47

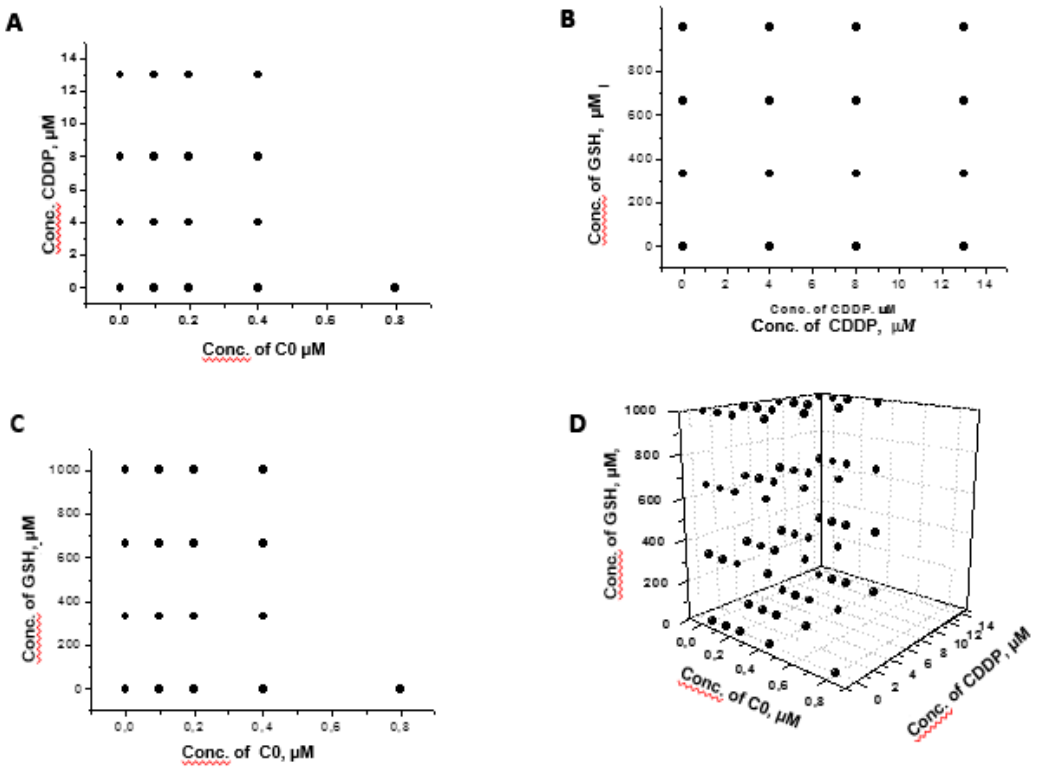

Figure 17. Concentrations of combinations of (A) CDDP and C0, (B) GSH and CDDP, (C)GSH and C0 (D) GSH, C0 and CDDP for A2780res cell line.

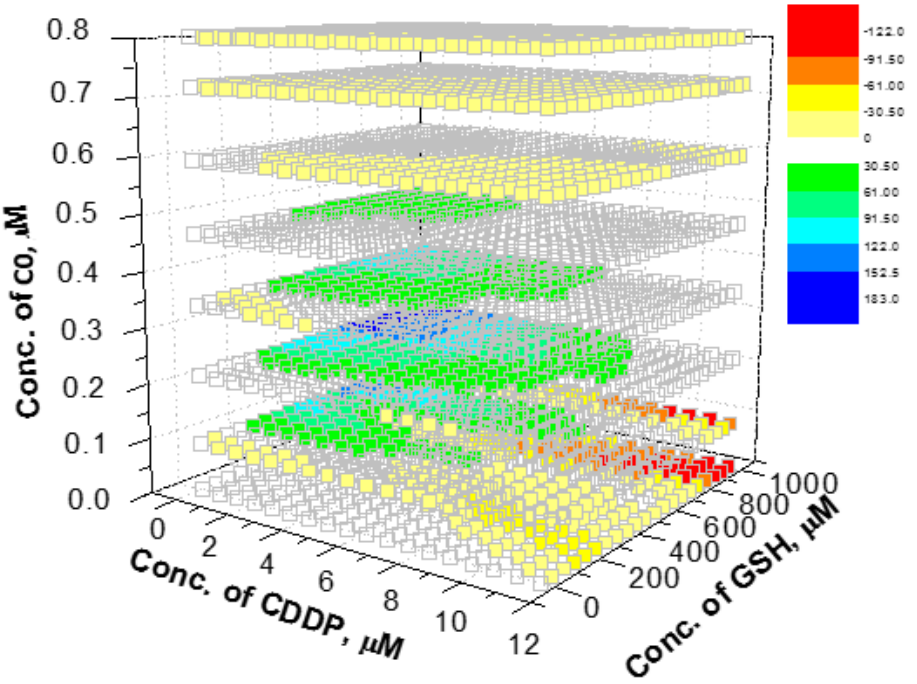

Figure 18. Some selected planes of the synergistic surfaces for the ternary system CDDP-GSH-C0 for A2780res cells; the color of the points is proportional to the synergistic effect.

3.4 Copper-Platinum complexes as a mechanism to explain the synergism of combinations of CDDP with Cu(II)complexes

The results of the effects of the some binary combinations CDDP+C0 against CEMres and A2780res have altready been published in the Journal of Inorganic biochemistryin 2015 (see below).

The combinations showed a synergistic cytotoxic effect in both resistant cell lines, and have proved able to suppress the drug-resistance This synergistic effect could be due to the simultaneous involvement of the same or different targets (DNA, proteins, enzymes, biomolecules), or by the formation of adducts, containing copper and platinum. To verify the presence of these adducts, mass spectra of solutions containing CDDP and Cu(II)-phen complexes, have been measured, using the atmospheric pressure Electrospray Ionisation at atmospheric pressure Mass Spectroscopy (ESI-MS). This method was more useful than others, because the processes of fragmentation are greatly reduced, allowing the detection of even weak complexes, which cannot be put in evidence with the other systems of ionization stronger which detected only the signals of the individual complexes. The stoichiometry of the complex observed with this method was then evaluated based on the models and the results of isotopic fragmentation spectroscopy tandem MS-MS. Although the same method was used to verify the presence of adducts between CDDP and the other two complexes of Cu (II)phen,[1] and C1, but they have not been tested in the resistant cell lines. In all cases, regardless of the copper complex used, the formation of a mixed complex was detected. In the adducts the copper and platinum ions were connected by a bridge of two chlorine atoms, with stoichiometry [CuPt(1,10-phenathroline)(NH3)(H2O)Cl]+. In reactions of C0, or C1, with CDDP it is also released a phenanthroline, that being itself cytotoxic, could explain the higher antiproliferative activity shown by the mixtures containing these two complexes, rather than the one containing C1. The formation of the mixed compound detected with this method, may be a possible mechanism of the synergistic effect observed. Since the synergistic effect was observed against CDDP-resistant cell lines, it could also be involved in one or more of the mechanisms that lead to the CDDP resistance. Worth mentioning, in the published article, complex C0 was named [2], while throughout my thesis the term C0 was preferred.

Link at the published article: http://dx.doi.org/10.1016/j.jinorgbio.2015.05.004

Journal of Inorganic Biochemistry 151 (2015) 107–114

Contents lists available at ScienceDirect

Journal of Inorganic Biochemistry

journal homepage: www.elsevier.com/locate/jinorgbio

Mixed copper–platinum complex formation could explain synergistic antiproliferative effect exhibited by binary mixtures of cisplatin and copper-1,10-phenanthroline compounds: An ESI–MS study

Tiziana Pivetta [a,*], Viola Lallai [a], Elisa Valletta [a], Federica Trudu [a], Francesco Isaia [a], Daniela Perra [b], Elisabetta Pinna [b], Alessandra Pani [b]

[a] Dipartimento di Scienze Chimiche e Geologiche, University of Cagliari, Cittadella Universitaria, 09042 Monserrato, Cagliari, Italy
[b] Dipartimento di Scienze Biomediche, University of Cagliari, Cittadella Universitaria, 09042 Monserrato, Cagliari, Italy

ARTICLE INFO

Article history:
Received 26 January 2015
Received in revised form 5 May 2015
Accepted 6 May 2015
Available online 14 May 2015

Keywords:
Synergistic effect
Antiproliferative activity
ESI–MS
Cisplatin
Copper complexes
Cisplatin-resistant cells

ABSTRACT

Cisplatin, *cis*-diammineplatinum(II) dichloride, is a metal complex used in clinical practice for the treatment of cancer. Despite its great efficacy, it causes adverse reactions and most patients develop a resistance to cisplatin. To overcome these issues, a multi-drug therapy was introduced as a modern approach to exploit the drug synergy. A synergistic effect had been previously found when testing binary combinations of cisplatin and three copper complexes *in vitro*, namely, $Cu(phen)(OH_2)_2(OClO_3)_2$, $[Cu(phen)_2(OH_2)](ClO_4)_2$ and $[Cu(phen)_2(H_2dit)](ClO_4)_2$,(phen = 1,10-phenanthroline, H_2dit = imidazolidine-2-thione), against the human acute T-lymphoblastic leukaemia cell line (CCRF-CEM). In this work $[Cu(phen)_2(OH_2)](ClO_4)_2$ was also tested in combination with cisplatin against cisplatin-resistant sublines of CCRF-CEM (CCRF-CEM-res) and ovarian (A2780-res) cancer cell lines. The tested combinations show a synergistic effect against both the types of resistant cells. The possibility that this effect was caused by the formation of new adducts was considered and mass spectra of solutions containing cisplatin and one of the three copper complexes at a time were measured using electrospray ionisation at atmospheric-pressure mass spectrometry (ESI–MS). A mixed complex was detected and its stoichiometry was assessed on the basis of the isotopic pattern and the results of tandem mass spectrometry experiments. The formed complex was found to be $[Cu(phen)(OH)\mu\text{-}(Cl)_2Pt(NH_3)(H_2O)]^+$.

1. Introduction

Cisplatin, *cis*-diammineplatinum(II) dichloride, is a metal complex widely used in clinical practice for the treatment of cancer. Cisplatin is able to enter the cells through passive diffusion and with protein-mediated transport systems such as human organic cation transporter T2 and copper transporter Ctr1 [1–3]. Cisplatin exerts its biological activity by interacting with DNA through hydrolysis. In fact, once inside the cell, one chloride ligand of the complex is displaced by a water molecule to form the aquo-complex $[Pt(NH_3)_2(H_2O)Cl]^+$. This species binds DNA, losing the water molecule, and forming the mono-functional adduct $[PtCl(DNA)(NH_3)_2]^+$. The second chloride of this species is now displaced by a water molecule, forming another aquo-complex $[Pt(H_2O)(DNA)(NH_3)_2]^{2+}$. This species interacts with DNA to form the bi-functional adduct $[Pt(DNA)(NH_3)_2]^{2+}$ [4–7]. The principal bi-functional adduct with DNA is the 1,2-intra-strand cross-linking with two adjacent guanines, which is supposed to be responsible for the cytotoxic activity of the drug [7]. Despite its great efficacy against deadly types of tumour, such as breast, ovarian, prostate, testes, and non-small cell lung cancers [8–11], it causes adverse reactions with dose-dependent side effects. Furthermore, after some treatment, most patients develop resistance to cisplatin [12], and, in order to reach the same therapeutic efficacy, higher doses of the drug are required with a higher incidence of side effects related to the dose. Cisplatin resistance could be caused by several mechanisms, such as a decreased influx inside the cell, an increased deactivation by biomolecules present in the cytosol, an increased capacity of DNA repair and an increased efflux outside the cell [13,14]. To defeat the drug resistance and reduce the side effects, a multi-drug (MD) therapy was introduced as a modern approach. Under the MD regimen, two or more drugs are administered simultaneously to exploit their synergism, achieving several advantages [15]. Synergism arises when the mixture of drugs shows a cytotoxic activity higher than the pure additive effect of the single drugs. In synergistic drug combinations, lower doses of each drug can be administered, achieving equal or higher therapeutic effects while reducing side effects and lowering resistance development. With this purpose, cisplatin has often been proposed in combinatorial therapies with other drugs or with natural products [16–22]. We tested, in a

* Corresponding author. Tel.: +39 0706754473; fax: +39 070 584597.
E-mail address: tpivetta@unica.it (T. Pivetta).

http://dx.doi.org/10.1016/j.jinorgbio.2015.05.004
0162-0134/

previous study, several binary combinations of cisplatin with $[Cu(phen)(OH_2)_2(OClO_3)_2]$ (**1**), $[Cu(phen)_2(OH_2)](ClO_4)_2$ (**2**) and $[Cu(phen)_2(H_2dit)](ClO_4)_2$ (**C1**) (phen = 1,10-phenanthroline, H_2dit = imidazolidine-2-thione) *in vitro* against the wild type human acute T-lymphoblastic leukaemia cell line (CCRF-CEM-wt), finding a synergistic effect. Especially, the maximum of synergistic effect was observed for particular combinations of copper complexes and cisplatin, i.e. 5:1 for **1** and cisplatin, 1:1 for **2** and cisplatin and 1:2 for **C1** and cisplatin [15]. In this work, we extended the study of the cytotoxic activity of the most promising copper complex **2** as a leader compound, on cisplatin-resistant sublines of leukemic (CCRF-CEM-res) and ovarian (A2780-res) cancer cell lines. The CCRF-CEM-res cells were purposely selected in order to verify whether the synergistic effect shown by **2** and cisplatin in the CCRF-CEM-wt cell line [15] was maintained in a cisplatin-resistant counterpart, even if cisplatin is not used in the chemotherapic treatment of leukaemia. The A2780-res cells were selected since they are derived from the ovarian cancer for which cisplatin is still now one of the chemotherapic agent of choice. This kind of cancer is actually sensitive to cisplatin but becomes resistant to this drug during chemotherapy cycles or in recurrences [23].

Copper(II) complexes are supposed to act against cancer cells in different ways with respect to cisplatin, but the real mechanisms are not completely clarified to date [24]. Furthermore, as both copper(I) and copper(II) are involved in several biological functions, it is not universally accepted that the cytotoxic properties of copper complexes are related to a specific oxidation state of the metal ion. In most studies, cell apoptosis and enzyme inhibition (proteasome, topoisomerase I and II, tyrosin protein kinase) are involved [25,26], whereas DNA appears to be the target of copper complexes containing nitrogen chelators, such as phen [27]. The synergistic effect shown by cisplatin and our copper complexes containing one or two phen molecules may then arise from several mechanisms, that is, simultaneous involvement of the same or different targets, such as DNA, proteins, enzymes, biomolecules, but also through the formation of new adducts. According to the Pearson acid–base concept [28], platinum(II) and copper(I) are both soft ions, whereas copper(II) has a hard–soft intermediate character. These ions present an affinity for the same ligands, which may lead to the formation of polynuclear complexes containing both platinum and copper. Starting from the above considerations, we decided to verify the formation of mixed complexes, acquiring mass spectra of solutions containing cisplatin and copper complexes, using electrospray ionisation in atmospheric-pressure mass (ESI–MS). This ionisation system limits fragmentation processes, allowing the additional detection of complexes that fragment readily. The ESI–MS technique is, in fact, suitable for the study of various complexes [29] and was successfully applied for the study of copper and platinum complexes [30–36]. Preliminary measurements made using stronger ionisation systems, such as laser desorption ionisation (LDI) or matrix-assisted laser desorption ionisation (MALDI), only showed evidence of signals deriving from the platinum ion and from copper–phen complexes [15]. Instead, using ESI–MS, polynuclear complexes containing copper and platinum were found, and their stoichiometry was assessed on the basis of isotopic patterns and fragmentation results of tandem mass spectrometry (MS–MS). The molecules studied in this work are reported in Fig. 1.

2. Experimental section

2.1. Reagents and apparatus

Methanol (CH_3OH), propanol ($CH_3(CH_2)_2OH$), isopropanol ($(CH_3)_2CHOH$), CH_3CN, DMSO, H_2dit, phen and trifluoroacetic acid (HTFA) were purchased from Sigma-Aldrich. *Cis*-diammineplatinum(II) dichloride (cisplatin) was purchased from Alfa-Aesar. The commercial reagents were used as received, without any further purification. Ultrapure water obtained with MilliQ Millipore was used for all experiments. Mass spectra in positive-ion mode were obtained on a triple quadruple

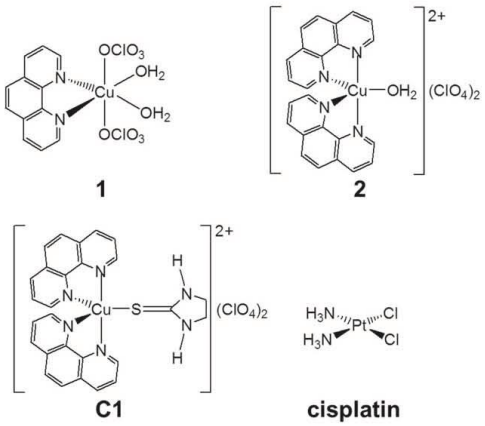

Fig. 1. Formulas and acronyms of the molecules studied in this work. Complex **1** is $Cu(phen)(OH_2)_2(OClO_3)_2$, **2** is $[Cu(phen)_2(OH_2)](ClO_4)_2$, **C1** is $[Cu(phen)_2(H_2dit)](ClO_4)_2$ and cisplatin is *cis*-diammineplatinum(II) dichloride (phen = 1,10-phenanthroline, H_2dit = the imidazolidine-2-thione).

QqQ Varian 310-MS mass spectrometer using the atmospheric-pressure ESI technique. The sample solutions were infused directly into the ESI source using a programmable syringe pump at a flow rate of 1.50 ml/h. A dwell time of 14 s was used and the spectra were accumulated for at least 10 min in order to increase the signal-to-noise ratio. Tandem MS–MS experiments were performed with argon as the collision gas (1.8 PSI) using a needle voltage of 6000 V, shield voltage of 800 V, housing temperature of 60 °C, drying gas temperature of 120 °C, nebuliser gas pressure of 40 PSI, drying gas pressure of 20 PSI and a detector voltage of 2000 V. The collision energy was varied from 2 to 45 V. The isotopic patterns of the measured peaks in the mass spectra were analysed using mMass 5.5.0 software package [37–39]. The assignments were based on the copper-63 and platinum-195 isotopes.

2.2. Preparation of *1*, *2* and *C1*

The synthesis methods for **1**, **2** and **C1** have previously been reported [40,41]. However, in this work, we report new synthetic routes with less-toxic solvents and/or with higher yields.

$[Cu(phen)(OH_2)_2(OClO_3)_2]$ **(1):** The basic carbonate of copper(II) $Cu_2(CO_3)(OH)_2$ (1.0 g, 4.54 mmol) was suspended in isopropanol (50 ml), and the suspension was warmed to boiling point. Concentrated perchloric acid was slowly added to the suspension, whilst stirring, until a clear-blue solution was obtained. The solution was boiled for 10 min to remove all carbon dioxide that was formed, and then it was cooled to room temperature. An isopropanolic solution of phen (0.4 g, 2.22 mmol) was slowly added drop-wise whilst stirring. In presence of opalescence, the addition of phen was interrupted and the solution was left stirring until the precipitate disappeared, and phen addition was then resumed. The entire process required 3 h. The resulting blue solution was filtered, concentrated under vacuum (10 ml) and left to crystallise. Blue crystals were obtained after 12 h. The percentage yield was 95% (calculated on the basis of the amount of phen). The product was re-crystallised from CH_3CN. The final yield was 98%. Anal. Calcd. for $Cu(phen)(OH_2)_2(ClO_4)_2$: C 30.11, H 2.53, N 5.85, found: C 30.87, H 2.66, N 5.79.

$[Cu(phen)_2(OH_2)](ClO_4)_2$ **(2)**: The basic carbonate of copper(II) $Cu_2(CO_3)(OH)_2$ (1.0 g, 2.22 mmol) was suspended in isopropanol (50 ml) and the suspension was warmed to boiling point. Concentrated perchloric acid was slowly added to the suspension, whilst stirring, until a clear-blue solution was obtained. The solution was boiled for 10 min to

remove all carbon dioxide that was formed, and then it was cooled to room temperature and an isopropanolic solution of phen (1.64 g, 4.44 mmol) was slowly added. The resulting turquoise precipitate was filtered off under vacuum, washed with isopropanol and dried at room temperature. The percentage yield was 88%. The product was re-crystallised from CH_3CN. The final yield was 99%. Anal. Calcd. for $Cu(phen)_2(OH_2)(ClO_4)_2$: C 44.98, H 2.84, N 8.74, found: C 44.30, H 2.96, N 8.91.

$[Cu(phen)_2(H_2dit)](ClO_4)_2$ **(C1)**: A portion of **2** (0.30 g, 0.41 mmol) and H_2dit (0.048 g, colourless) were suspended in distilled water (50 ml). The suspension was stirred for 12 h at room temperature, after which a green powder was recovered by filtration under vacuum. The product was washed with water and dried at room temperature. Yield: 80%. The product was re-crystallised from CH_3CN. The final yield was 97%. Anal. Calcd. for $Cu(phen)_2(H_2dit)(ClO_4)_2$: C 44.73, H 3.06, N 11.59, found: C 45.01, H 2.98, N 11.30.

2.3. ESI–MS measurements

2.3.1. Copper complexes

A solution of **1** was prepared by dissolving an appropriate amount of the compound in water containing 0.05% of HTFA (v/v). Solutions of **2** and **C1**, which are both insoluble in water, were prepared by dissolving an appropriate amount of the compounds in DMSO (100 μl) and diluting to 50 ml with water containing 0.05% of HTFA (v/v). The stability of the compounds in DMSO or in DMSO/water/HTFA solutions was checked by measuring the UV–visible (UV–Vis) absorbance of the resulting solutions during the time. No changes in the UV–Vis absorbance were evidenced in 14 days.

All sample solutions were mixed with methanol in 1:1 H_2O/CH_3OH volume ratio immediately before the mass measurements in order to improve the quality of the spectra. Mass spectra of **1**, **2** and **C1** were recorded in the *m/z* range 100–1000 at a final concentration of 0.5 mM. The same experimental conditions were used for the three compounds (needle voltage 4500 V, shield voltage 600 V, housing temperature 60 °C, drying gas temperature 120 °C, nebuliser gas pressure 40 PSI, drying gas pressure 20 PSI, and detector voltage 1450 V).

2.3.2. Cisplatin

A solution of cisplatin was prepared by dissolving an appropriate amount of the compound in water containing 0.05% of HTFA (v/v). The solution was mixed with methanol in 1:1 H_2O/CH_3OH volume ratio immediately before the mass measurements in order to improve the quality of the spectra. The mass spectrum of cisplatin was recorded in the *m/z* range 100–1000 at a final concentration of 0.5 mM. The experimental conditions were: needle voltage 6000 V, shield voltage 600 V, housing temperature 60 °C, drying gas temperature 120 °C, nebuliser gas pressure 40 PSI, drying gas pressure 20 PSI, and detector voltage 2000 V.

2.3.3. Binary combinations

Solutions containing a copper complex and cisplatin in 10:1, 5:1 and 1:1 Pt/Cu molar ratios were prepared, keeping the cisplatin concentration constant (1.0 mM). Sample solutions were mixed with methanol in 1:1 H_2O/CH_3OH volume ratio in order to improve the quality of the spectra. So as not to alter the complex formation equilibria, methanol was added immediately before the mass spectra were recorded. Solutions containing cisplatin and the copper complex were analysed at 4500, 600 and 1500 V as needle, shield and detector voltages, respectively, for studying masses in the *m/z* range 100–450, and at 6000, 800 and 2000 V as needle, shield and detector voltages, respectively, for studying masses in the *m/z* range 450–1000. All other parameters were kept constant during the experiments (housing temperature 60 °C, drying gas temperature 120 °C, nebuliser gas pressure 40 PSI, and drying gas pressure 20 PSI).

2.4. Biological assays

2.4.1. Cell lines

The cisplatin-resistant subline of human acute T-lymphoblastic leukaemia (CCRF-CEM-res) and cisplatin-resistant subline of human ovarian carcinoma (A2780-res) were used in the study. The CCRF-CEM-res subline was obtained by us (see Section 2.4.2); the cell line was maintained in culture between 1×10^5 cells/ml and 1×10^6 cells/ml in RPMI medium 10% foetal bovine serum (FBS) with 1% kanamycin (growth medium). To the growth medium for CCRF-CEM-res cell cultures, we also added cisplatin (5 μM). A2780-res cells were a generous gift by Dr. Eva Fischer (Tumor Biology Laboratory, The Ion Chiricuta Oncology Institute, Cluj-Napoca, Romania) and were grown in RPMI medium with 2 mM glutamine and 10% FBS. Cell monolayers were sub-cultivated when they reached 70% confluency (every 3–4 days) by a 1:3 ratio. In order to keep the cisplatin resistance, A2780-res were cultured in the presence of 1 μM cisplatin every two to three passages. All cell lines were periodically checked for micoplasma contamination. For the experiments, each cell line was replaced every 3 months with freshly-towed cells from the cell stores in liquid nitrogen.

2.4.2. Selection of the cisplatin-resistant CCRF-CEM subline

A CCRF-CEM subline able to grow at the same extent in the absence and in the presence of 5 μM cisplatin (CCRF-CEM-res) was obtained by serial passages of wild-type cells in the presence of increasing cisplatin concentrations, starting from a sub-inhibitory concentration (0.5 μM). At each cell passage (every 3–4 days), the number of viable cells of cisplatin-treated cultures was compared to that of duplicate untreated cultures. The cisplatin concentration was increased at each cell passage up to 1.50 μM; from then on, cisplatin-treated cultures grew poorly and much slower than their untreated counterparts and had to be kept (5–10 passages) at the same cisplatin concentration until the cell population had regained original growth timing and viability. At intervals during the selection process, the level of cisplatin resistance was checked by the 3-(4,5-dimethylthiazol-2-yl)-2,5-diphenyl-tetrazolium bromide (MTT) method in cells that had grown without the drug for one passage; doxorubicin was used as a reference compound to evaluate the cisplatin-resistance specificity. Given that cell cultures never survived at concentrations over 5 μM, the cell population was stabilised by 15 further passages at 5 μM cisplatin, and then grown without the drug for one passage, checked for the level of resistance as described above, and finally stored in aliquots in liquid nitrogen for further use.

2.4.3. Cytotoxic assays

Stock solutions of the copper complexes were prepared in DMSO (1 mM) and stored at 4 °C in the dark. The biological stability of these solutions was checked verifying the cytotoxic activity measured by using the same solutions over more than 6 months. The tested compounds maintained the same IC50 (concentration required to inhibit cell proliferation by 50% with respect to untreated cells) in all the performed experiments. The DMSO solutions of cisplatin (1000× of the highest concentration to be used on the cell culture), being stable only for few hours and showing a decreasing of the cytotoxic potency during the time, were prepared in DMSO and diluted to the necessary concentration each time immediately before the experiments.

Dilutions of the drug stocks for biologic investigations were made in RPMI medium at 2× the final concentration for single drug evaluations, or at 4× the final concentration for evaluation of dual drug combinations. The concentration of DMSO in the cells was never higher than 0.1%. The effects of the drugs and drug combinations were evaluated in cultures of exponentially growing cells; for experiments in cisplatin-resistant cell cultures, both CCRF-CEM-res and A2780-res cells were allowed to grow in the absence of the drug for 1 passage. CCRF-CEM-res cells were seeded at a density of 1×10^5 cells/ml of growth medium in flat-bottomed 96-well plates and simultaneously exposed to the drugs or drug combinations. A2780-res cells were seeded

at 5×10^3 cells/well of flat-bottomed 96-well plates and allowed to adhere overnight before of the addition of the drugs or the drug combinations. Cell growth in the absence and presence of drugs was determined after 96 h of incubation at 37 °C and 5% CO_2 (corresponding to three to four duplication rounds of untreated cells), through both the viable cell counting, with the trypan blue exclusion method, and the MTT method [42,43]. Values obtained in drug-treated samples were expressed as percentages of those of their respective controls. Dose–response curves for each drug were determined and the IC50s of single drugs and drug combinations were calculated.

3. Results and discussion

3.1. Synthesis

The synthesised compounds were characterised, in addition to elemental analysis, by infrared (IR) and UV–Vis spectroscopy, finding results in agreement with the previously reported data [40,41]. The new synthesis method of **1** led to a crystalline product with a higher purity (≥95%) and yield. The obtained compound, which must be stored under vacuum, is hygroscopic and deliquescent. It is stable for a number of months at room temperature in a desiccator, but if warmed, its colour changes from blue to turquoise. The turquoise product was characterised by elemental analysis and IR spectroscopy and it resulted to be **2**. In the synthesis method of **C1**, the previously used solvent CH_3CN was changed to H_2O.

3.2. Cytotoxicity measurements

The cytotoxic activities of **2** and cisplatin, both alone and in dual drug combinations, were evaluated against CCFR-CEM-res and A2780-res human cell lines. Dose–response curves for **2** and cisplatin were obtained, and the IC50 values were determined. Copper complex **2** showed IC50 values of 0.75 and 0.24 μM in CCFR-CEM-res and A2780-res cells, respectively. Cisplatin showed IC50 values of 6.98 and 5.3 μM for CCFR-CEM-res and A2780-res cells, respectively. Dose–response curves of **2** and cisplatin in cisplatin-resistant cell lines are reported in the Supplementary Information (Fig. S1). The effects of single drugs and dual drug combinations on the tested cell lines are reported in Table 1 as a percentage of the untreated controls. In all cases, combinatorial treatment gave rise to a synergistic interaction between cisplatin and the studied copper complex. In particular, it is worth mentioning the synergistic effect shown by combinatorial treatments against cisplatin-resistant cell lines, which has evident potential in the clinic of cisplatin-resistant cancers.

Table 1
Antiproliferative activity (%) against cisplatin-resistant leukemic cancer cells (CCRF-CEM-res), cisplatin-resistant ovarian cancer cells (A2780-res) exhibited by copper complex **2**, cisplatin and their binary combinations.

2 (μM)	Cisplatin (μM)	Antiproliferative activity (%)	Cell line	Effect	Index of synergy*
0.67		40.0	CCRF-CEM-res		
	5.0	28.2			
0.67	5.0	88.0		synergism	31%
0.60		24.0			
	4.0	17.5			
0.60	4.0	59.5		synergism	22%
0.20		32.7	A2780-res		
	4.0	6.0			
0.20	4.0	58.4		synergism	22%
0.10		6.0			
0.10	4.0	20.0		synergism	8%

* Calculated as in Ref. [15].

3.3. ESI–MS results

3.3.1. Copper complexes

In the mass spectra of **1**, **2** and **C1**, only mono-charged species containing copper(II) or copper(I) were evidenced. Reduction of Cu(II) to Cu(I) is commonly observed in the ESI phase for solutions of Cu(II) salts [44]. Characteristic isotopic peaks for copper- and copper–chlorine-containing ions were clearly seen, and the isotopic patterns of these peaks confirmed the elemental composition of the observed ions. The most relevant peaks are assigned in the shown spectra (Fig. 2), whereas calculated and experimental isotopic patterns for selected peaks are reported in the Supplementary Information (Fig. S2). In the spectrum of **1** (Fig. 2A), the most important signals correspond to $[Cu^{(II)}(phen)(ClO_4)]^+$ (*m/z* 342), $[Cu^{(II)}(phen)Cl]^+$ (*m/z* 278) and $[Cu^{(I)}(phen)]^+$ (*m/z* 243) species. The last two species derive from fragmentation–recombination reactions occurring during the MS–MS of the parent compound $[Cu^{(II)}(phen)(ClO_4)]^+$. In the insert the peaks falling in the *m/z* range 340–350 are reported. Also other complexes were recognised, but they were identified as adducts with TFA or as the products of exchange reactions with fluorine carried out by the TFA. These complexes were $[Cu^{(II)}(phen)(TFA)]^+$ (*m/z* 356), $[Cu^{(II)}(phen)F]^+$ (*m/z* 262), and $[Cu^{(II)}(phen)_2(TFA)]^+$ (*m/z* 536). In the spectrum of **2** (Fig. 2B), some species observed in the spectrum of **1** are present ($[Cu^{(II)}(phen)Cl]^+$ (*m/z* 278), $[Cu^{(II)}(phen)(TFA)]^+$ (*m/z* 356), $[Cu^{(II)}(phen)_2(TFA)]^+$ (*m/z* 536)) together with $[phen+H]^+$ (*m/z* 181), $[Cu^{(I)}(phen)_2]^+$ (*m/z* 423), $[Cu^{(II)}(phen)_2Cl]^+$ (*m/z* 458), and $[Cu^{(II)}(phen)_2(ClO_4)]^+$ (*m/z* 522). The species $[phen+H]^+$, $[Cu^{(I)}(phen)_2]^+$ and $[Cu^{(II)}(phen)_2Cl]^+$ are fragmentation products of the parent compound $[Cu^{(II)}(phen)_2(ClO_4)]^+$. In the spectrum of **C1** (Fig. 2C), some species observed in the spectrum of **1** and **2** are

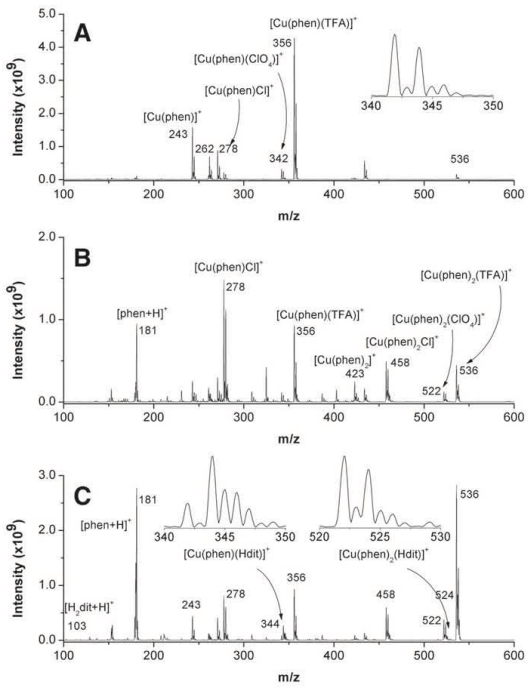

Fig. 2. ESI mass spectra (+) of **1** (A), **2** (B) and **C1** (C); 0.5 mM, 50:50 methanol/water with 0.05% of trifluroacetic acid (phen = 1,10-phenanthroline, H_2dit = the imidazolidine-2-thione, TFA = trifluroacetate ion).

present ($[phen+H]^+$ (*m/z* 181), $[Cu^{(I)}(phen)]^+$ (*m/z* 243), $[Cu^{(II)}(phen)Cl]^+$ (*m/z* 278), $[Cu^{(II)}(phen)(TFA)]^+$ (*m/z* 356), $[Cu^{(II)}(phen)_2Cl]^+$ (*m/z* 458), $[Cu^{(II)}(phen)_2(ClO_4)]^+$ (*m/z* 522), $[Cu^{(II)}(phen)_2(TFA)]^+$ (*m/z* 536)) together with species containing the thionic ligand H_2dit, that is, $[Cu^{(II)}(phen)_2(Hdit)]^+$ (*m/z* 524), $[Cu^{(II)}(phen)(Hdit)]^+$ (*m/z* 344), and $[H_2dit+H]^+$ (*m/z* 103). In the inserts are reported the peaks falling in the *m/z* ranges 340–350 and 520–530. The presence of the $[phen+H]^+$ signal in the spectra of **2** and **C1**, is due to the fragmentation of the Cu–phen complexes. The species $[Cu^{(I)}(phen)]^+$, $[Cu^{(II)}(phen)Cl]^+$, $[Cu^{(II)}(phen)(TFA)]^+$, $[Cu^{(II)}(phen)_2(TFA)]^+$ are detectable in all the spectra, as fragmentation products of the parent compounds. The species $[Cu^{(II)}(phen)(Hdit)]^+$ and $[H_2dit+H]^+$ are fragmentation products of the parent compound $[Cu^{(II)}(phen)_2(Hdit)]^+$. The occurrence of $[Cu(phen)_2(TFA)]^+$ also in the spectrum of **1**, is due to a reaction in ESI phase between the monochelate complex Cu–phen and the freed phen (the intensity of the related signal at *m/z* 536, lowers directly with the needle potential). All the fragmentation processes were studied by tandem MS-MS. The assignments are tabulated with calculated *m/z* values in Table 2 (rows 1–18).

It is interesting to remark that, although the copper complexes have been measured at the same molar concentration, their mass spectra presented different intensities, from 4.5×10^9 (for **1**) to 1.75×10^9 a.u. (for **2**).

3.3.2. Cisplatin

The ESI–MS spectrum of cisplatin is reported from *m/z* 200 to 315 in Fig. 3 and from 300 to 600 in Fig. S3. Due to the number of the isotopic peaks of the metal ion and to the limited resolving power of the instrument, the peaks in the spectrum appear broad. The signal related to the protonated cisplatin, $[Pt(NH_3)_2Cl_2+H]^+$, appears at *m/z* 300. Other signals related to $[Pt(NH_3)_2Cl]^+$, $[Pt(NH_3)Cl]^+$ and $[Pt(NH_2)]^+$ are present at *m/z* 264, 247, and 211, respectively. A signal interpreted as a mixture of $[Pt(NH_3)_3(H_2O)_2Cl]^+$ (78%) and $[Pt(NH_3)_2(H_2O)_3Cl]^+$ (22%) is present at *m/z* 317–318. At *m/z* 546 and 563, signals of the di-nuclear complexes $[Pt_2(NH_3)_3Cl_3]^+$ and $[Pt_2(NH_3)_4Cl_3]^+$ can be seen. Calculated and experimental isotopic patterns for selected peaks are reported in the Supplementary Information (Fig. S4). In the species containing platinum and NH_2^-, a double bond between platinum and nitrogen ion is present, which has already been reported [36,45]. It is important to remark that the mass-spectral profile of cisplatin solutions begins to change 1 h after preparation, as the compound undergoes hydrolysis. In fact, the signals at *m/z* 300, 264 and 247 decrease in intensity and adducts with water and methanol are formed. The assignments are tabulated with calculated *m/z* values in Table 2 (rows 19–26).

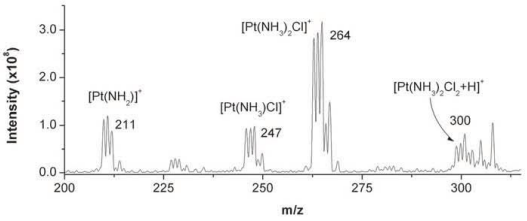

Fig. 3. ESI–MS (+) spectrum of cisplatin in the *m/z* 200–315 range; 0.5 mM, 50:50 methanol/water with 0.05% of trifluroacetic acid.

3.3.3. Binary combinations

Several binary mixtures of cisplatin and copper complexes were prepared and their mass spectra were acquired in order to verify the formation of a mixed complex.

3.3.3.1. Cisplatin and copper complexes. The number and the aspect of the signals present in the spectra are strongly dependent on the chosen experimental conditions of needle, shield and detector voltages. Generally, increasing the voltage of the needle, shield and detectors causes the fragmentation processes to increase. The fragmentations are helpful, as they are characteristic of the molecule and provide structural information. However, as the fragments themselves can undergo to a further fragmentation, the resulting spectra could become difficult to understand. On the other hand, a voltage that is too low determines a fall in the overall ion current, leading to a reduction in the ionisation efficiency. These issues could determine non-reliable signals [46].

The mass spectra of the binary combinations were collected by varying the voltage values in order to find the optimal conditions. In all the experiments, signals with isotopic pattern characteristic of species containing both copper and platinum were observed. However, at needle, shield, and detector voltages of 4500, 600, and 1500 V, respectively, the signals with reliable intensities (10^9 magnitude) were characteristic of species containing only copper as the metal ion. In particular, signals of the species $[Cu^{(II)}(phen)(TFA)]^+$ (*m/z* 356), $[Cu^{(I)}(phen)(H_2O)]^+$ (*m/z* 261), and $[Cu^{(I)}(phen)]^+$ (*m/z* 243) were present. To observe signals of the other ions with sufficient intensity, needle, shield, and detector voltages of 6000, 800, and 2000 V, respectively, were used. The binary combinations were tested at 1:1, 5:1 and 10:1 platinum/copper molar ratios. In the spectra of the equimolar mixtures, the signals originating from the copper complexes were more intense than those originating from cisplatin. The measured mass spectra of the solutions containing cisplatin and **2** at the three different molar ratios are reported as an example in Fig. S5. The signals of the mixed complexes containing both copper and platinum appeared at all molar ratios for all of the studied systems; however, at 1:1 platinum/copper, the more intense signals (marked with "*" in Fig. S5) were attributed to mono- and polynuclear copper complexes. The stoichiometry of these complexes were identified from the *m/z* value and from the isotopic pattern as $[Cu^{(II)}_2(phen)_2(TFA)Cl_2]^+$ (*m/z* 669), $[Cu^{(I)}_3(phen)_2(TFA)(OH)(H_2O)_2]^+$

Table 2
Species identified from the ESI–MS studies.

Row	Ion	Composition	Exp. *m/z**	Calc. *m/z**
1	$[Cu_2(phen)_2(TFA)_2(ClO_4)]^+$	$C_{28}H_{16}ClCu_2F_6N_4O_8$	810.94	810.91
2	$[Cu_2(phen)_2(TFA)_2Cl]^+$	$C_{28}H_{16}ClCu_2F_6N_4O_4$	746.90	746.94
3	$[Cu_3(phen)_2(TFA)(OH)(H_2O)_2]^+$	$C_{26}H_{21}Cu_3F_3N_4O_5$	714.86	714.93
4	$[Cu_2(phen)_2(TFA)Cl_2]^+$	$C_{26}H_{16}Cl_2Cu_2F_3N_4O_2$	668.87	668.92
5	$[Cu(phen)_2(TFA)]^+$	$C_{26}H_{16}CuF_3N_4O_2$	536.11	536.05
6	$[Cu(phen)_2(Hdit)]^+$	$C_{27}H_{21}CuN_6S$	522.02	524.08
7	$[Cu(phen)_2(ClO_4)]^+$	$C_{24}H_{16}ClCuN_4O_4$	521.95	522.01
8	$[Cu(phen)_2Cl]^+$	$C_{24}H_{16}ClCuN_4$	458.03	458.04
9	$[Cu(phen)_2]^+$	$C_{24}H_{16}CuN_4$	423.05	423.07
10	$[Cu(phen)(TFA)]^+$	$C_{14}H_8CuF_3N_2O_2$	355.94	355.98
11	$[Cu(phen)(Hdit)]^+$	$C_{15}H_{13}CuN_4S$	343.99	344.02
12	$[Cu(phen)(ClO_4)]^+$	$C_{12}H_8ClCuN_2O_4$	341.88	341.95
13	$[Cu(phen)Cl]^+$	$C_{12}H_8ClCuN_2$	277.92	277.97
14	$[Cu(phen)F]^+$	$C_{12}H_8CuFN_2$	261.95	262.00
15	$[Cu(phen)(H_2O)]^+$	$C_{12}H_{10}CuN_2O$	260.94	261.01
16	$[Cu(phen)]^+$	$C_{12}H_8CuN_2$	242.96	243.00
17	$[phen+H]^+$	$C_{12}H_9N_2$	181.05	181.08
18	$[H_2dit+H]^+$	$C_3H_7N_2S$	102.99	103.03
19	$[Pt_2(NH_3)_4Cl_3]^+$	$H_{12}Cl_3N_4Pt_2$	562.79	562.94
20	$[Pt_2(NH_3)_3Cl_3]^+$	$H_9Cl_3N_3Pt_2$	545.80	545.92
21	$[Pt(NH_3)_2(H_2O)_3Cl]^+$	$H_{12}ClN_2O_3Pt$	318.88	318.02
22	$[Pt(NH_3)_3(H_2O)_2Cl]^+$	$H_{13}ClN_3O_2Pt$	317.84	317.03
23	$[Pt(NH_3)_2Cl_2+H]^+$	$H_7Cl_2N_2Pt$	300.84	299.96
24	$[Pt(NH_3)_2Cl]^+$	H_6ClN_2Pt	263.88	263.99
25	$[Pt(NH_3)Cl]^+$	H_3ClNPt	246.85	246.96
26	$[Pt(NH_2)]^+$	H_2NPt	210.88	210.98
27	$[CuPt(phen)(H_2O)_2(OH)Cl_2]^+$	$C_{12}H_{13}Cl_2CuN_2O_3Pt$	560.90	560.92
28	$[CuPt(phen)(H_2O)(NH_3)(OH)Cl_2]^+$	$C_{12}H_{14}Cl_2CuN_3O_2Pt$	559.90	559.94
29	$[CuPt(phen)(H_2O)_2Cl_2]^+$	$C_{12}H_{12}Cl_2CuN_2O_2Pt$	543.95	543.92

* The experimental and calculated *m/z* values refer to the peak representative of the monoisotopic mass.

(m/z 715), $[Cu^{(II)}_2(phen)_2(TFA)_2Cl]^+$ (m/z 747) and $[Cu^{(II)}_2(phen)_2(TFA)_2(ClO_4)]^+$ (m/z 811).

At 10:1 platinum/copper molar ratio, together with signals of copper and mixed copper–platinum complexes, signals of poly-nuclear complexes containing two or more platinum ions and a variable number of chlorine, ammonia and water molecules, were present in the m/z range 800–1000. The lack of a good pattern resolution prevented the determination of their exact stoichiometry. From these results, it followed that the combination at 5:1 platinum/copper molar ratio was the best one to study mixed platinum–copper complexes.

In Fig. 4, the mass spectra of solutions containing cisplatin and **1**, cisplatin and **2** as well as cisplatin and **C1**, at 5:1 platinum/copper molar ratio, are reported (signals from the copper complexes are marked with "*"). As can be seen, the mass spectra of all systems present a similar profile, even if they have different intensities, indicating that the same mixed complexes were formed. In particular, the signals with the isotopic pattern typical of mixed platinum–copper complexes fall in the m/z range 540–660. As for the copper complexes, the stoichiometry of these mixed complexes was identified from the m/z value and from the isotopic pattern. In many cases, convoluted signals were observed, owing to the simultaneous presence of complexes with similar masses. In this case, the experimental pattern was attributed to a weighted combination of the isotopic pattern of the different molecules. The weights, that is, the percentage in which each molecule was present, were obtained by multivariate regression analysis of the experimental data. An example of this treatment is reported in Fig. S6, in which the experimental pattern can be compared to the theoretical one, calculated as a contribution of four molecules.

From the analysis of the spectra, we identified three principal complexes, all mono-charged with the following stoichiometries: **I**) $[CuPt(phen)(H_2O)_2(OH)Cl_2]^+$ (m/z 561), **II**) $[CuPt(phen)(H_2O)(NH_3)(OH)Cl_2]^+$ (m/z 560), and **III**) $[CuPt(phen)(H_2O)_2Cl_2]^+$ (m/z 544). Together with **I–III**, nine other complexes were identified, but they turned out to be adducts with TFA or products of exchange reactions with the fluorine carried out by the TFA. These nine complexes could be thought as by-products (the complete list of these complexes is reported in the Supplementary, Table S1). The assignments are tabulated with calculated m/z values in Table 2 (rows 27–29).

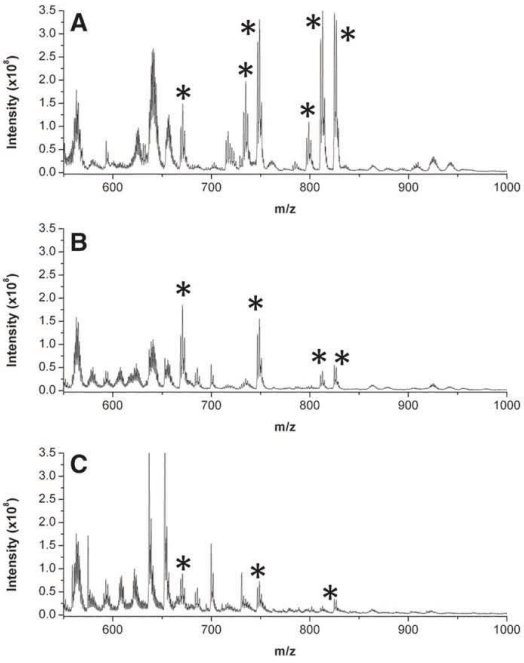

Fig. 4. ESI mass (+) spectra of cisplatin and **1** (A), cisplatin and **2** (B), cisplatin and **C1** (C) (cisplatin 0.5 mM, copper complex 0.1 mM, 50:50 methanol/water with 0.05% of trifluroacetic acid). In the spectra, copper complexes are marked with "*".

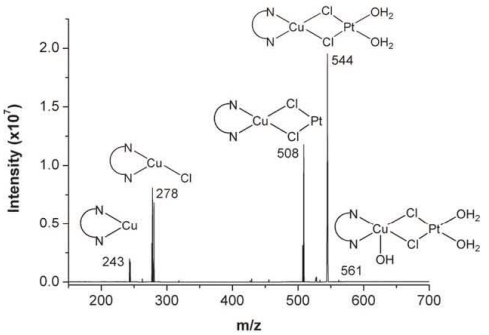

Fig. 5. Tandem MS–MS spectrum of the signals at m/z 561. The isotopic pattern was partially lost for the low signal intensity and for the little range of m/z isolated (collision energy 20 V, charges are omitted for clarity, the two nitrogen connected by a curved line represent the phen molecule).

3.3.3.2. Tandem MS–MS. Tandem mass spectrometry was essential to confirm the proposed stoichiometry and to hypothesise the structure of the formed complexes. A brief description of this technique is reported in the caption of the Fig. S7.

The fragmentation profiles obtained for compounds **I–III** are reported in Figs. 5–7. As can be seen in Fig. 5 for **I**, species with stoichiometries $[Cu(phen)]^+$ (m/z 243), $[Cu(phen)Cl]^+$ (m/z 278), and $[CuPt(phen)Cl_2]^+$ (m/z 508) were visible as fragments of the parent compound $[CuPt(phen)(H_2O)_2(OH)Cl_2]^+$ (m/z 561). The structures of the $[Cu(phen)]^+$, $[Cu(phen)Cl]^+$ and $[CuPt(phen)Cl_2]^+$ ions were easily proposed, as shown in the figure. To define the structure of the fragment at m/z 544, it was convenient to consider it as (m/z 508 + m/z 2 × 18). Three possibilities were considered as two water molecules linked to the copper (case *i*) or to the platinum (case *ii*) or one water molecule linked to the copper and one to the platinum (case *iii*). If one or two water molecules were linked to the copper, the resulting

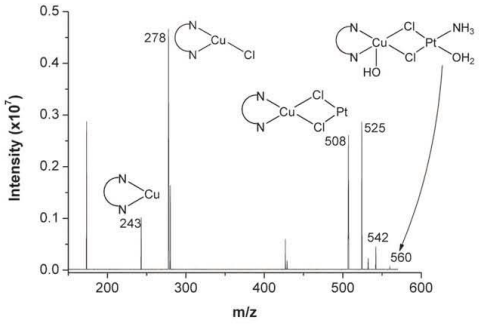

Fig. 6. Tandem MS–MS spectrum of the signals at m/z 560. The isotopic pattern was partially lost for the low signal intensity and for the little range of m/z isolated (collision energy 20 V, charges are omitted for clarity, the two nitrogen connected by a curved line represent the phen molecule).

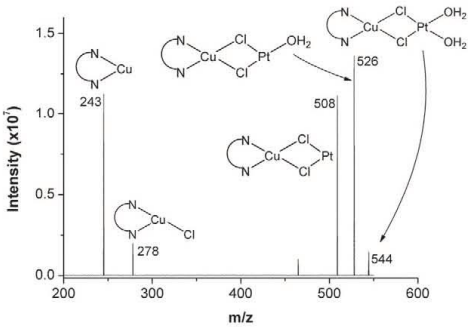

Fig. 7. Tandem MS–MS spectrum of the signals at *m/z* 544. The isotopic pattern was partially lost for the low signal intensity and for the little range of *m/z* isolated (collision energy 20 V, charges are omitted for clarity, the two nitrogen connected by a curved line represent the phen molecule).

complex should have had a +2 charge, while, if the water molecules were linked to the platinum the charge of the complex should have been +1 (note that when copper is tetra-coordinated its oxidation number is +1, if it is penta- or esa-coordinated its oxidation number is +2). The fragment was mono-charged, then only the case *ii* was considered. To define the structure of the parent compound at *m/z* 561, it was convenient to consider it as (*m/z* 544 + *m/z* 17). Ammonia and hydroxide ions have an *m/z* of 17; therefore, the two possibilities were considered as hydroxide or ammonia linked to the copper. If OH^- was linked to the copper, the resulting complex should have had a +1 charge, whereas, if ammonia was present, the charge of the complex should have been +2. The fragment was mono-charged, then only the OH^- ion was considered. Therefore, the structure of the parent ion was proposed as reported in the figure, that is, $[Cu(phen)(OH)\mu\text{-}(Cl)_2Pt(H_2O)_2]^+$.

The study of compound **II** appeared more complicated. As for **I**, the structures of the $[Cu(phen)]^+$, $[Cu(phen)Cl]^+$, and $[CuPt(phen)Cl_2]^+$ were easily proposed, as shown in Fig. 6. As for the fragment at *m/z* 525, it was considered as (*m/z* 508 + *m/z* 17). Then, four possibilities were considered, that is, hydroxide linked to platinum (*i*) or to copper (*ii*) and ammonia linked to platinum (*iii*) or to copper (*iv*). If OH^- or NH_3 were linked to platinum, the resulting complexes (cases *i* and *iii*) should have had 0 or +1 as the charge, respectively. If OH^- or NH_3 were linked to copper, the resulting complexes (cases *ii* and *iv*) should have had a +1 or +2 charge, respectively. As the fragment was mono-charged, only cases *ii* and *iii* were considered. With regards to the fragment at *m/z* 542, as before, it was considered as (*m/z* 525 + *m/z* 17). Then, six possibilities were taken into account, starting from the previous cases *ii* and *iii*, that is, *ii* + OH^- or NH_3 linked to platinum (cases *v* and *vi*), *iii* + OH^- or NH_3 linked to copper (cases *vi* and *ix*), *iii* + OH^- or NH_3 linked to platinum (cases *vii* and *viii*). As the fragments are mono-charged, the only possibilities that were considered were *vi* and *viii*. The last fragment was considered as (*m/z* 525 + *m/z* 18), and a water molecule was added to *vi* and *viii*, to obtain *x* (with +1 charge) and *xi* (with +2 charge). Then, the most probable structure of the parent ion was that of *x*, that is, $[Cu(phen)(OH)\mu\text{-}(Cl)_2Pt(NH_3)(H_2O)]^+$. The entire route is shown in Fig. S7. As far as compound **III** is concerned, similar considerations were made to obtain as the most probable structure, $[Cu(phen)\mu\text{-}(Cl)_2Pt(H_2O)_2]^+$, as shown in the Fig. 7. All of the reported fragmentations were obtained with a CE of 20 V. To fragment the $[Cu(phen)]^+$ complex, a collision energy of 45 V was necessary, but at this energy value, the other fragments were no longer observable.

Compound **III** can be considered as a fragment of **I**, which itself can be considered as a hydrolysis product of **II**. A precursor with the formula $[Cu(phen)(OH)\mu\text{-}(Cl)_2Pt(NH_3)_2)]^+$ can be hypothesised in solution; however, this species was not detected in our experiments. The proposed reaction between copper complexes and cisplatin is finally resumed in Scheme 1. As can be seen, the same complex is formed, regardless of the copper complex (**1**, **2** or **C1**) involved. In the reaction of **2** or **C1** with cisplatin, one phen unit is released; in the case of **C2**, a H_2dit unit is also released. In the formed complex, copper and platinum are linked by two bridging chlorides and the coordination spheres of copper is completed by a phen and a hydroxide ion, and that of platinum is completed by ammonia and water molecules. From the mass spectral evidence, the mixed copper–platinum complex was formed in aqueous solution a few minutes after the mixing of the reagents, and it was stable for at least 1 week. The same reaction carried out in water–acetonitrile required 3 weeks to be completed.

4. Conclusions

Binary combinations of cisplatin and the copper complex $[Cu(phen)_2(OH_2)](ClO_4)_2$ present a synergistic antiproliferative effect against the cisplatin-resistant sublines of leukemic (CCRF-CEM-res) and ovarian (A2780-res) cancer cells *in vitro*. Considering that the synergy may arise from a chemical reaction between the two metal complexes, solutions containing cisplatin and the copper complex $Cu(phen)(OH_2)_2(OClO_3)_2$, $[Cu(phen)_2(OH_2)](ClO_4)_2$ or $[Cu(phen)_2(H_2dit)](ClO_4)_2$ were studied by ESI–MS and tandem MS–MS. A mixed complex containing copper and platinum with a stoichiometry of $[Cu(phen)(OH)\mu\text{-}(Cl)_2Pt(NH_3)(H_2O)]^+$ was detected. This complex was able to hydrolyse to form $[Cu(phen)(OH)\mu\text{-}(Cl)_2Pt(H_2O)_2]^+$ that was actually detected. Both the complexes were formed, regardless of the copper complex used; then, in the reaction of $[Cu(phen)_2(OH_2)](ClO_4)_2$ and $[Cu(phen)_2(H_2dit)](ClO_4)_2$ with cisplatin, one phen and/or one H_2dit was released. Phen presents itself an IC50 value of approximately 2 μM towards the tested cell lines, and it can contribute to the overall cytotoxic activity shown by the mixtures, unlike H_2dit, which is devoid of any biological activity against the tested cells. The formation of the mixed copper–platinum complex could be related to the synergistic effect of the combination of the studied copper complexes with cisplatin shown towards the tested cell line. Given that the synergy was also observed against cisplatin-resistant cells, the formed copper–platinum complex is likely to interfere with one or more of the mechanisms that lead to cisplatin resistance. Furthermore, considerations about the reactivity can be made. In fact, it is accepted that the determining steps in the interaction of cisplatin with DNA are the hydrolysis processes that are slow in saline solutions. Complexes $[Cu(phen)(OH)\mu\text{-}(Cl)_2Pt(NH_3)(H_2O)]^+$ and $[Cu(phen)(OH)\mu\text{-}(Cl)_2Pt(H_2O)_2]^+$ are formed within a few minutes and are already hydrolysed. They can then react with DNA more readily than cisplatin. More experiments

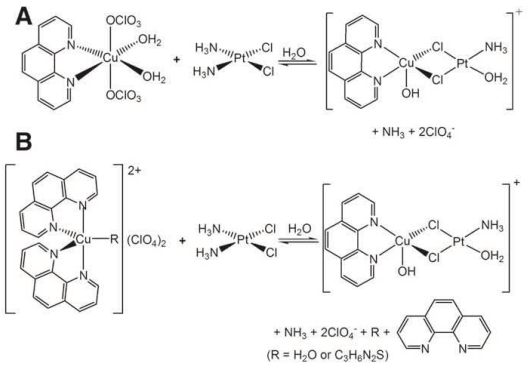

Scheme 1. Reaction mechanism between **1** and cisplatin (A) and **2** or **C1** and cisplatin (B).

have to be carried out in order to obtain more insights and possibly clarify the underlying molecular mechanism(s). In this regards, as a future perspective, we intend to extend these studies to other cisplatin-resistant cell lines.

From the reported results, the ESI–MS and tandem MS–MS appear as suitable tools for the study of the metal complexes formed in solution. Of course, in the transition process from the solution to gas phase, the structure of the complexes may be affected, and this is particularly relevant for large molecules such as metal complexes with biomolecules. In the case of the metal complexes, the electrochemical reactions occurring at the capillary may also modify the valence state of the metal ion inducing a structural change. Also the fragmentation products may recombine to form new species. Then, the species detected in ESI–MS not necessarily correspond to those actually present in the sample solution. Nevertheless, relevant information on the solution stability and reactivity of complexes that are not easily isolable in the solid state can indeed be obtained under several experimental conditions such as different media, pH values and ionic buffers.

Abbreviations

ESI–MS	electrospray ionisation mass spectroscopy
Phen	1,10-phenanthroline
CCRF-CEM	human acute T-lymphoblastic leukaemia
CCRF-CEM-res	cisplatin resistant human acute T-lymphoblastic leukaemia
A2780	ovarian cancer
A2780-res	cisplatin resistant ovarian cancer
MD	multi-drug
MALDI	matrix assisted laser desorption ionisation
LDI	laser desorption ionisation
HTFA	trifluoroacetic acid
TFA	trifluoroacetate
H_2dit	imidazolidone-2-thione
FBS	foetal bovine serum
MTT	3-(4,5-dimethylthiazol-2-yl)-2,5-diphenyl-tetrazolium bromide
IC50	concentration required to inhibit cell proliferation by 50% with respect to untreated cells
MS–MS	tandem mass spectrometry
CE	collision energy

Acknowledgements

Federica Trudu and Daniela Perra gratefully acknowledge the Sardinia Regional Government for the financial support of her PhD scholarship (P.O.R. Sardegna F.S.E. Operational Programme of the Autonomous Region of Sardinia, European Social Fund 2007-2013-Axis IV Human Resources, Objective l.3, Line of Activity l.3.1.).

Appendix A. Supplementary data

Supplementary data to this article can be found online at http://dx.doi.org/10.1016/j.jinorgbio.2015.05.004.

References

[1] S. Ishida, J. Lee, D.J. Thiele, I. Herskowitz, Proc. Natl. Acad. Sci. U. S. A. 99 (2002) 14298–14302.
[2] I. Song, N. Savaraj, Z.H. Siddik, P. Liu, Y. Wei, C.J. Wu, M.T. Kuo, Mol. Cancer Ther. 3 (2005) 1543–1549.
[3] H. Burger, a Zoumaro-Djayoon, a W.M. Boersma, J. Helleman, E.M.J.J. Berns, R.H.J. Mathijssen, W.J. Loos, E. a C. Wiemer, Br. J. Pharmacol. 159 (2010) 898–908.
[4] R.A. Alderden, M.D. Hall, T.W. Hambley, J. Chem. Educ. 83 (2006) 728–734.
[5] S. Trzaska, Chem. Eng. News 83 (2005) 52.
[6] E.R. Jamieson, S.J. Lippard, Chem. Rev. 99 (1999) 2467–2498.
[7] R.C. Todd, S.J. Lippard, Metallomics 1 (2009) 280–291.
[8] N. Eckstein, J. Exp. Clin. Cancer Res. 30 (2011) 91–102.
[9] S. Dhar, F.X. Gu, R. Langer, O.C. Farokhzad, S.J. Lippard, Proc. Natl. Acad. Sci. U. S. A. 105 (2008) 17356–17361.
[10] O. Rixe, W. Ortuzar, M. Alvarez, R. Parker, E. Reed, K. Paull, T. Fojo, Biochem. Pharmacol. 52 (1996) 1855–1865.
[11] J. Michels, I. Vitale, L. Galluzzi, J. Adam, K.A. Olaussen, O. Kepp, L. Senovilla, I. Talhaoui, J. Guegan, D.P. Enot, M. Talbot, A. Robin, P. Girard, C. Oréar, D. Lissa, A.Q. Sukkurwala, P. Garcia, P. Behnam-Motlagh, K. Kohno, G.S. Wu, C. Brenner, P. Dessen, M. Saparbaev, J.-C. Soria, M. Castedo, G. Kroemer, Cancer Res. 73 (2013) 2271–2280.
[12] B. Desoize, Anticancer Res. 24 (2004) 1529–1544.
[13] P.A. Andrews, S.B. Howell, Cancer Cells 2 (1990) 35–43.
[14] K.J. Scanlon, M. Kashani-Sabet, H. Miyachi, L.C. Sowers, J.J. Rossi, Anticancer Res. 9 (1989) 1301–1312.
[15] T. Pivetta, F. Isaia, F. Trudu, A. Pani, M. Manca, Talanta 115 (2013) 84–93.
[16] L. Huang, L.-M. Liao, A.-W. Liu, J.-B. Wu, X.-L. Cheng, J.-X. Lin, M. Zheng, BMC Cancer 14 (2014) 140.
[17] J. Ma, M. Maliepaard, K. Nooter, a W. Boersma, J. Verweij, G. Stoter, J.H. Schellens, Cancer Chemother. Pharmacol. 41 (1998) 307–316.
[18] B. Taylor-Harding, S. Orsulic, B.Y. Karlan, A.J. Li, Gynecol. Oncol. 119 (2010) 549–556.
[19] Y. Lin, M. Tsai, S. Weng, Y. Kuo, Y. Chiu, Mol. Pharmacol. 80 (2011) 136–146.
[20] E.E. Vokes, K.E. Choi, R.L. Schilsky, W.J. Moran, C.M. Guarnieri, R.R. Weichselbaum, W.R. Panje, J. Clin. Oncol. 6 (1988) 618–626.
[21] C. Andreadis, K. Vahtsevanos, T. Sidiras, I. Thomaidis, K. Antoniadis, D. Mouratidou, Oral Oncol. 39 (2003) 380–385.
[22] C. Faivre, P. Rougier, M. Ducreux, E. Mitry, A. Lusinchi, P. Lasser, D. Elias, F. Eschwege, Bull. Cancer 86 (1999) 861–865.
[23] N. Eckstein, J. Exp. Clin. Cancer Res. 30 (2011) 91.
[24] C. Santini, M. Pellei, V. Gandin, M. Porchia, F. Tisato, C. Marzano, Chem. Rev. 114 (2014) 815–862.
[25] L. Tripathi, P. Kumar, A.K. Singhai, Indian J. Cancer 44 (2007) 62–71.
[26] M.M. Cox, D.L. Nelson, Lehninger Principles of Biochemistry, 5th ed., 2008.
[27] D.S. Sigman, D.R. Graham, V.D. Aurora, A.M. Stern, J. Biol. Chem. 254 (1979) 12269–12272.
[28] R.G. Pearson, J. Am. Chem. Soc. 85 (1963) 3533–3539.
[29] V.B. Di Marco, G.G. Bombi, Mass Spectrom. Rev. 25 (2006) 347–379.
[30] R. Sekar, S.K. Kailasa, H.N. Abdelhamid, Y.-C. Chen, H.-F. Wu, Int. J. Mass Spectrom. 338 (2013) 23–29.
[31] P. Sgarbossa, S.M. Sbovata, R. Bertani, M. Mozzon, F. Benetollo, C. Marzano, V. Gandin, R. a Michelin, Inorg. Chem. 52 (2013) 5729–5741.
[32] P. Doležel, V. Kubáň, Chem. Pap. 56 (2002) 0–4.
[33] M.A. Telpoukhovskaia, C. Rodríguez-Rodríguez, L.E. Scott, B.D.G. Page, B.O. Patrick, C. Orvig, J. Inorg. Biochem. 132 (2013) 59–66.
[34] R. Franski, J. Mass Spectrom. 39 (2004) 272–276.
[35] R. Miao, G. Yang, Y. Miao, Y. Mei, J. Hong, C. Zhao, L. Zhu, Rapid Commun. Mass Spectrom. 19 (2005) 1031–1040.
[36] D. Esteban-Fernández, B. Cañas, I. Pizarro, M.a. Palacios, M.M. Gómez-Gómez, J. Anal. At. Spectrom. 22 (2007) 1113–1121.
[37] T.H.J. Niedermeyer, M. Strohalm, PLoS One 7 (2012) e44913.
[38] M. Strohalm, D. Kavan, P. Nova, M. Volny, Anal. Chem. 82 (2010) 4648–4651.
[39] M. Strohalm, M. Hassman, B. Kosata, M. Kodicek, Rapid Commun. Mass Spectrom. 22 (2008) 905–908.
[40] T. Pivetta, F. Isaia, G. Verani, C. Cannas, L. Serra, C. Castellano, F. Demartin, F. Pilla, M. Manca, A. Pani, J. Inorg. Biochem. 114 (2012) 28–37.
[41] T. Pivetta, M.D. Cannas, F. Demartin, C. Castellano, S. Vascellari, G. Verani, F. Isaia, J. Inorg. Biochem. 105 (2011) 329–338.
[42] W. Strober, Curr. Protoc. Immunol.John Wiley & Sons, Inc., 2001
[43] R. Pauwels, J. Balzarini, M. Baba, R. Snoeck, D. Schols, P. Herdewijn, J. Desmyter, E. De Clercq, J. Virol. Methods 20 (1988) 309–321.
[44] C. Hao, R.E. March, J. Mass Spectrom. 36 (2001) 509–521.
[45] M. Cui, Z. Mester, Rapid Commun. Mass Spectrom. 17 (2003) 1517–1527.
[46] W. Henderson, J.S. McIndoe, Mass Spectrometry of Inorganic, Coordination and Organometallic Compounds, John Wiley & Sons, Ltd, Chichester, UK, 2005.

3.5 Analysis of the phospholipid profiles of CDDP-resistant vs. wild type leukemia and carcinoma cell extracts

In neoplastic cells changes in lipid distribution and composition of cellular membranes have been reported In particular, increased levels of glycerophosphoinositol(PI), glycerophosphoserine (PS), glycerophosphoethanolamine (PE) and glycerophosphocholine (PC), as well as of esterified cholesterol have been found. (Kojima, K.. Nagoya J Med Sci 1993,

Lladó *et al.*, Biochim. Biophys. Acta - Biomembr., 2014; Szachowicz-Petelsk, *et al.*, J. Environ. Biol., 2010). Considering that the mechanisms of transport through the plasma membrane depends on its structure, particularly on its rigidity and permeability, and that these characteristics are determined by the composition of the membrane constituents, an alteration of the physiological membrane condition could readily be directly or indirectly related to the undesirable phenomena of drug-resistance, including cisplatin resistance. On the basis of these considerations, the qualitative PL profile in our leukemia and carcinoma cell models were determined.

The results of this study were recently submitted to the journal PLoS One in the manuscript attached below.

PLOS ONE

IDENTIFICATION OF SPECIFIC PHOSPHOLIPIDS TO DIFFERENTIATE CISPLATIN-RESISTANT AND WILD TYPE CELLS IN LEUKEMIC (CCRF CEM) AND OVARIAN CANCER (A2780).

--Manuscript Draft--

Manuscript Number:	
Article Type:	Research Article
Full Title:	IDENTIFICATION OF SPECIFIC PHOSPHOLIPIDS TO DIFFERENTIATE CISPLATIN-RESISTANT AND WILD TYPE CELLS IN LEUKEMIC (CCRF CEM) AND OVARIAN CANCER (A2780).
Short Title:	PHOSPHOLIPIDS IN CISPLATIN-RESISTANT AND WILD TYPE CELLS
Corresponding Author:	Tiziana Pivetta Universita degli Studi Di Cagliari Monserrato, ITALY
Keywords:	CCRF-CEM cells; A2780 cells; cisplatin resistance; phospholipids; ESI-MS; solid phase extraction
Abstract:	Changes in lipid distribution and composition of the cellular membranes have been observed in cancer and several other pathologies. The conformation of the cell membrane could directly or indirectly be related with the cisplatin resistance. With the aim to highlight possible differences between wild type and cisplatin-resistant cells and to identify some specific phospholipids, we studied the phospholipid profile of wild type and cisplatin-resistant cells of two kinds of tumours, acute T-lymphoblastic leukaemia (CCRF-CEM) and ovarian carcinoma (A2780).The analytical procedure proposed in this work, based on solid phase extraction and mass spectroscopy, allowed to identify specific components of the cisplatin-resistant cells. With respect to their wild type counterparts, it was found that some glycerophosphocholines were strongly down represented in the cisplatin-resistant CCRF-CEM cells, while some sphingomyelins were up-represented in the cisplatin-resistant A2780 cells. In both the resistant cell lines, dihydroxyacetone phosphate was found to be more up-represented. The evidenced phospholipid changes play a key role in the detection of the transformation from wild type to cisplatin-resistance cells and can help to clarify the mechanisms underlying the development of the resistance. Moreover, the potential use of some lipids as "markers" for resistant cells could be important for a possible clinical application. In fact, the onset of the resistance during cisplatin treatment could be monitored by detecting those specific lipids. Under this perspective, the obtained findings represent an advancement of knowledge and can be exploited for the design of new strategies in cancer treatment.
Order of Authors:	Elisa Valletta
	Elisabetta Pinna
	Sarah Vascellari
	Graziano Caddeo
	Enzo Cadoni
	Francesco Isaia
	Alessandra Pani
	Tiziana Pivetta
Opposed Reviewers:	
Additional Information:	
Question	**Response**
Financial Disclosure	The author received no specific funding for this work.

IDENTIFICATION OF SPECIFIC PHOSPHOLIPIDS TO DIFFERENTIATE CISPLATIN-RESISTANT AND WILD TYPE CELLS IN LEUKEMIC (CCRF-CEM) AND OVARIAN CANCER (A2780).

*Elisa Valletta[a], Elisabetta Pinna[b], Sarah Vascellari[b], Graziano Caddeo[a], Enzo Cadoni[a], Francesco Isaia[a], Alessandra Pani[b], Tiziana Pivetta[a]**

[a]Dipartimento di Scienze Chimiche e Geologiche, [b]Dipartimento di Scienze Biomediche, University of Cagliari, Cittadella Universitaria, 09042 Monserrato (CA) – Italy

* Corresponding author: Tiziana Pivetta, tpivetta@unica.it, 0039 070 675 44 73, fax 0039 070 584597.

Keywords: CCRF-CEM cells, A2780 cells, cisplatin resistance, phospholipids, ESI-MS, solid phase extraction.

Abstract

Changes in lipid distribution and composition of the cellular membranes have been observed in cancer and several other pathologies. The conformation of the cell membrane could directly or indirectly be related with the cisplatin resistance. With the aim to highlight possible differences between wild type and cisplatin-resistant cells and to identify some specific phospholipids, we studied the phospholipid profile of wild type and cisplatin-resistant cells of two kinds of tumours, acute T-lymphoblastic leukaemia (CCRF-CEM) and ovarian carcinoma (A2780).The analytical procedure proposed in this work, based on solid phase extraction and mass spectrometry, allowed to identify specific components of the cisplatin-resistant cells. With respect to their wild type counterparts, it was found that some glycerophosphocholines were strongly down-represented in the cisplatin-resistant CCRF-CEM cells, while some sphingomyelins were up-represented in the cisplatin-resistant A2780 cells. In both the resistant cell lines, dihydroxyacetone phosphate was found to be more up-represented. The evidenced phospholipid changes play a key role in the detection of the transformation from wild type to cisplatin-resistance cells and can help to clarify the mechanisms underlying the development of the resistance. Moreover, the potential use of some lipids as "markers" for resistant cells could be important for a possible clinical application. In fact, the onset of the resistance during cisplatin treatment could be monitored by detecting those specific lipids. Under this perspective, the obtained findings represent an advancement of knowledge and can be exploited for the design of new strategies in cancer treatment.

Introduction

Cell membranes consist of a lipid bilayer with inserted proteins, whose content depends both on the cell type and on the cell compartment of the membrane itself. In the plasma membrane, for example, lipids and proteins are almost equally distributed, whereas in the inner membrane of mitochondria, a higher proportion of proteins is present (about 75%) [1]. Membranes can be considered as fluids in which lipids and proteins are free to rotate and shift laterally. The fluidity of

the membranes depends principally on the lipid composition. Regions of membrane with long fatty acid residues are more rigid, since the interactions among long acyl chains are stronger than those among short ones, while the degree of unsaturation of the fatty acids increases the membrane fluidity as folds in the chains decrease interactions among them. The asymmetric distribution of lipids between the inner and the outer leaflets defines the characteristics of the cell membranes [1,2]. Three classes of lipids constitute the cell membrane: phospholipids (PLs), glycolipids and sterols. PLs are commonly present in the highest concentration and are considered the fundamental components of all the cell membranes. PLs are amphipathic molecules, consisting of two hydrophobic fatty acid chains linked to a hydrophilic phosphate-containing head group. The principal PLs present in the membranes are glycerophospholipids (GPLs), which contain a glycerol backbone with a fatty acyl or alkyl group at the *sn*-1 position, a fatty acyl group at the *sn*-2 position, and a phosphodiester moiety linked to a polar head-group at the *sn*-3 position [3]. GPLs are classified on the basis of the polar head: glycerophosphocholine (PC), glycerophosphoserine (PS), glycerophosphoethanolamine (PE), and glycerophosphoinositol (PI), in the presence of choline, serine, ethanolamine and inositol, respectively. PC derivatives represent more than 50% of the PLs in most eukaryotic membranes [4]. The second important family of structural polar lipids is represented by the sphingolipids (SLs), which consist of a ceramide unit with phosphocholine or phosphoethanolamine as a head group. In Fig. 1, the most important PLs are depicted.

Changes in lipid distribution and composition of the cellular membranes have been observed in several pathologies and in cancer [5–8]. In neoplastic cells, alterations of the PL's composition, [6] increases in the concentration of PI, PS, PE and PC derivatives, as well as increases in the level of esterified cholesterol were observed [6,9]. Moreover, considering that the mechanisms of transport through the plasma membrane depends on its assembly, particularly on its rigidity and permeability, and that these characteristics are determined by composition and structure of the membrane constituents, an alteration of the physiological membrane condition could readily affect drug influx and efflux across cell membrane. The conformation of the cell membrane could be then directly or

indirectly also be related to the undesirable phenomena of drug resistance, such as cisplatin resistance. Cisplatin (CDDP) is used for the treatment of breast, ovarian [10], prostate [11], testes [12], and non-small cell lung cancer [13]. However, the administration of CDDP is limited by its side effects and the onset of inherited or acquired resistance.

Fig. 1 Principal phospholipids contained in the cell membranes. For a complete description of the nomenclature of the phospholipids see ref. [1] and [14].

Cisplatin resistance is supposed to be related to its mechanism of action. Briefly, cisplatin enters the cells by passive diffusion or by active protein-mediated transport systems, i.e. human organic cation transporter (hOCT2) and copper transport protein (Ctr1). Once in cytoplasm, one of the two chloride ligands of CDDP is displaced by a water molecule to form the complex $[PtCl(H_2O)(NH_3)_2]^+$. This species binds DNA bases, mainly in the N7 position of guanine and adenine, and the N3 of cytosine, to form the monofunctional adduct $[PtCl(DNA)(NH_3)_2]^+$. Also the second chloride ion can be displaced by a water molecule to form $[Pt(H_2O)(DNA)(NH_3)_2]^{2+}$. This last may bind DNA by crosslinking to form a bifunctional adduct that is responsible of the triggering of cell death [15–21]. The influx of the drug inside the cell and/or drug efflux outside the cell represent possible mechanisms for the onset of cisplatin resistance [22]. On the basis of these considerations, we decided to study the qualitative PL profile of two cancer cell lines and of their corresponding cisplatin-resistant sublines, to highlight possible differences and identify some cell-line specific PLs. With this aim, we set up a procedure to analyse the PL content of the cell lysate sample in a fast, routine, accurate, and reproducible method, based on the solid phase extraction (SPE) and electrospray ionisation mass spectrometry (ESI-MS) and tandem mass spectrometry (MS-MS). In particular, the proposed method allows one to obtain mass spectra with high signal to noise ratio, preventing the interference of peptides that act as ionic suppressors and removing the

metabolites that can be recovered for other uses. Moreover, we analysed both the supernatants and pellet of each cell lysate, finding interesting differences between the two lysate fractions. We studied the PL composition of *i*) the acute T-lymphoblastic leukaemia derived CCRF-CEM cell line (CCRF-CEM-wt), *ii*) the ovarian carcinoma derived A2780 cell line (A2780-wt), *iii*) the cisplatin-resistant subline of acute T-lymphoblastic leukaemia cells (CCRF-CEM-res), and *iv*) the cisplatin-resistant subline of ovarian carcinoma cells (A2780-res). The leukemic CCRF-CEM cells were selected since they represent a classical model widely used for studies in biochemistry and biomedicine, while the A2780 cells were selected because ovarian cancer is actually treated with cisplatin.

Experimental

Reagents

Acetonitrile (CH_3CN), ammonium hydroxide (NH_4OH), formic acid (HCOOH), methanol (CH_3OH), and trifluoroacetic acid (HTFA) were purchased from Sigma-Aldrich (Milan, Italy). Cisplatin was purchased from Alfa Aesar (Karlsruhe, Germany). Fetal Bovine Serum, Kanamycin, L-Glutamine medium, and RPMI medium were purchased from Euroclone (Milan, Italy). The commercial reagents were used as received. Ultra-pure water obtained with MilliQ Millipore was used for all the experiments.

Cell culture

The human acute T-lymphoblastic leukaemia cell line (CCRF-CEM-wt) was purchased from the American Type Culture Collection (ATCC, USA), whereas a subline cisplatin-resistant cells (CCRF-CEM-res), was obtained by us via serial passages of the CCRF-CEM cell line in the presence of increasing concentrations of cisplatin. The CCRF-CEM-res subline was stabilized at 5 μM cisplatin (for details see ref. [23]). The human ovarian carcinoma cell line (A2780-wt) and the

cisplatin-resistant subline (A2780-res), were a generous gift by Dr. Eva Fischer (Tumor Biology Laboratory, The Ion Chiricuta Oncology Institute, Cluj-Napoca, Romania). CCRF-CEM cell lines were maintained in culture between 1×10^5 cells/ml and 2×10^6 cells/ml, in RPMI medium with stable L-Glutamine medium supplemented with 10% Fetal Bovine Serum and 1% Kanamycin (growth medium). A2780 cell lines were maintained in culture between 1.5×10^5 cells/ml and 3×10^6 cells/ml (~70% confluency) in the same medium. Mycoplasma contamination was periodically monitored. All cell lines were replaced every 3 months with cells freshly thawed from liquid nitrogen. In addition, CCRF-CEM-res and A2780-res were treated with 5 μM (every passage) and 1 μM (every two or three splits) cisplatin, respectively, in order to maintain the drug resistance. Cisplatin resistance was checked every month. All experiments with cisplatin-resistant sublines were performed using cell populations that were grown for one passage without cisplatin.

Cell lysates

Exponentially growing CCRF-CEM-wt/CCRF-CEM-res (2×10^7 total) and A2780-wt/A2780-res (4×10^6 total) cells were centrifuged at 1500 rpm for 5 minutes. Pellets were resuspended in 1 ml of deionized H_2O. Cell lysates were obtained by using a 2 ml dounce tissue grinder set (Sigma Aldrich) followed by centrifugation at 4600 rpm for 2 minutes. PLs were extracted from supernatants and pellets and analysed by ESI-MS, immediately after the lysis in order to minimize the enzymatic activity. During manipulation, the samples were kept on ice.

Extraction of phospholipids

The SPE of PLs from the crude cell lysate was performed with the Visiprep™ Solid Phase Extraction Vacuum Manifolds 12-Port Model and the SPE HybridSPE-Phospholipid Ultra Cartridge (Supelco). The cartridges were conditioned with 1 ml of CH_3CN containing 1% of HCOOH, followed by 1 ml of water. The lysate pellets or 200 μl of each cell lysate supernatants, was put into a cartridge with 600 μl of CH_3CN containing 1% of HCOOH. To facilitate the protein

precipitation, the mixture was mixed by repeated pipetting with a micropipette. The solution, containing almost metabolites, was extracted under vacuum and stored in freezer for other uses. The cartridge was washed with 1 ml of CH_3CN containing 1% of HCOOH and afterwards the phospholipids were extracted with 1 ml of CH_3OH containing 5% of NH_4OH. The resulting solution was divided in two fractions: one was immediately used for negative ESI-MS spectrometry, the other one was evaporated under vacuum and the solid residue was dissolved in 1 ml of H_2O containing 0.5% HTFA and CH_3OH (1:1) for positive ESI-MS. Five different lysate samples of each cell line were analysed and every extraction was repeated six times from every sample. The error percentage of the repeated measurements was always lower than 1%.

Mass spectrometry

Mass spectra were collected on a triple quadrupole QqQ Varian 310-MS mass spectrometer using the atmospheric-pressure ESI technique.

The sample solutions were infused directly into the ESI source using a programmable syringe pump at a flow rate of 0.70 ml/h. A dwell time of 14 s was used and the spectra were accumulated for at least 10 minutes in order to increase the signal-to-noise ratio. Mass spectra were recorded in the *m/z* 50–1000 range. The experimental conditions for positive- and negative-ion mode were: needle voltage 4500 V and −5500 V, shield voltage 600 V and −600 V, housing temperature 60 °C, drying gas temperature 100 °C and 120 °C, nebuliser gas pressure 40 PSI, drying gas pressure 20 PSI, and detector voltage 1600 V and −1800 V. Tandem MS-MS experiments were performed with argon as the collision gas (1.8 PSI). The collision energy was varied from 2 to 45 V. The isotopic patterns of the measured peaks in the mass spectra were analysed using mMass 5.5.0 software package [24–26]. The assignment of the PLs to the spectral peaks was performed by using the human metabolite database HMDB (www.hmdb.ca) [27–29], on the basis of the MS-MS spectra. In case of ambiguity the human biofluid location of the chosen PL was also considered. Only peaks with intensities higher than 2×10^7a.u. were considered. In some cases, due to the simultaneous presence of PLs with

similar masses, convoluted signals were observed. In these cases, the experimental pattern was attributed to a weighted combination of the isotopic pattern of the different molecules [23]. The weights, that represent the percentage in which each molecule was present, were obtained by multivariate regression analysis of the experimental data.

Results and discussion

Sample preparation for ESI-MS spectrometry

The PLs of the cellular lysate samples were extracted in a fast, routine, accurate, and reproducible method based on the solid phase extraction and analysed by mass spectrometry (Fig. 2).

The mass spectrum of the cell lysate analysed without any pre-treatment is characterised by a high number of overlapped peaks of low intensity and a baseline with poor quality (Fig. 3A). The low intensity of the signals (10^8 a.u.) is mainly due to the presence of proteins that act as ionic suppressors [30]. Following the procedure reported in Fig. 2, a reliable spectrum is instead obtained. Proteins are precipitated inside a cartridge (HybridSPE-Phospholipid Ultra Cartridge, Supelco, HybridSPE is a registered trademark of Sigma-Aldrich Co. LLC.) by addition of CH_3CN and HCOOH. The resulting mixture is passed, under vacuum, through the cartridge to remove the liquid phase containing almost metabolites, while the precipitated proteins are retained in the upper frit of the cartridge. PLs are retained by the cartridge via a selective Lewis acid-base interaction between the proprietary zirconia ions, functionally bonded to the stationary phase, and the phosphate moiety of the PLs [31]. The PLs are then recovered by extraction with NH_4OH in CH_3OH. The resulting solution is divided in two fractions: one is used for negative ESI-MS spectrometry, the other one is evaporated under vacuum and the solid residue is dissolved in a proper amount of 1:1 H_2O (0.5% HTFA) and CH_3OH for positive ESI-MS spectrometry. The proposed procedure was followed for lysate samples of the four cell lines. Sixteen replicates for each cell line were analysed to check the reproducibility of the results and the robustness of the method.

Fig. 2 Experimental procedure followed in this work to extract the phospholipids from the cell lysate. In the picture, the SPE extractor is shown (Visiprep Solid Phase Extraction Manifold - 12 Port Model).

Mass spectrometry

Cell lysates were obtained by a mechanical method using a dounce homogenizer without detergents. The supernatant solutions containing cytoplasmic extracts and the respective pellets having nuclei and cell debris of the cell lysates were analysed by ESI-MS and different results were obtained for the two lysate fractions. The spectra recorded in positive ion mode for supernatant and pellet fractions and untreated lysate of CCRF-CEM-wt cells are reported in Fig. 3. The mass spectra recorded in positive, ESI(+), and negative, ESI(-), ion mode for all the samples are reported in the Supporting Information (Fig. S1-S4).

Fig. 3 ESI(+) mass spectra of the lysate solutions of CCRF-CEM wild type cells without any pretreatment (**A**), after SPE extraction from the supernatant fraction (**B**), and from the pellet fraction (**C**). The intensities are reported in different scales; the intensity of the signals in the *m/z* 500–1000 range was multiplied by a factor of 10 in **B** and **C**.

The spectrum of the untreated lysate (Fig. 3A) is characterised by a very low intensity (10^8 vs 10^9 a.u. of 3B and 3C) and by the presence of many broad peaks due most probably to multi-charged protonated peptides. Comparing the spectrum of the lysate with those of the supernatant and pellet, it appears evident that the SPE treatment produces higher quality spectra. Signals of the PLs fall in the mass/charge ratio (*m/z*) 500–1000 range, while signals falling in the *m/z* 50–400 range are principally due to their fragment products, as confirmed by the MS-MS experiments.

The PL peaks observed in the spectra were identified on the basis of the masses, isotopic distribution patterns and the structural information obtained from tandem MS-MS. PLs were assigned to a given family on the basis of characteristic peaks in the tandem MS-MS spectra and by precursor/product ion scan and neutral loss scan experiments. For example, the *m/z* 184 precursor ion scan gives the possibility to detect all the lipids containing the phosphocholine ion, while the neutral loss of phosphoethanolamine (*m/*z 141) helps in the identification of PEs. The collision-induced fragmentation experiments were carried out varying the collision energy, in order to observe partial and complete fragmentation of the parent peaks. Considering the specific fragments and the common rules of fragmentation, in some cases it is possible to determine precisely the fatty-acyl group and the structure of the long-chain base (number and position of the double bonds). Some MS-MS spectra of PLs with the corresponding assignment are reported in the Supporting Information (Fig. S5-S10).

Phospholipid content

The height of a mass peak is proportional to the concentration of the species that originated that signal but depends also on its ionisation efficacy. Therefore, the intensity of two or more signals originated by different species cannot be directly compared. Instead, providing that the experimental conditions are kept constant, the intensity of signals arising from the same species can be compared each other. The heights of the mass peaks for the studied samples, recorded in ESI(+) and ESI(-), are reported in Fig. 4-7

Fig. 4 Phospholipids identified with ESI(+) in the lysate fractions of supernatant (S) and pellet (P) for the CCRF-CEM wild type (CEM-wt) and cisplatin-resistant (CEM-res) cells (charges of proton and sodium ions are omitted for clarity), the MS-MS spectra of the marked (∗) PLs are presented and discussed in the supporting (Fig. S5-S7). The error percentage in intensity for repeated measurements was always lower than 1%.

Fig.5 Phospholipids identified with ESI(+) in the lysate fractions of supernatant (S) and pellet (P) for A2780 wild type (A2780-wt) and cisplatin-resistant (A2780-res) cells (charges of proton and sodium ions are omitted for clarity), the MS-MS spectra of the marked (*) PLs are presented and discussed in the supporting (Fig. S5 and S7). The error percentage in intensity of the repeated measurements was always lower than 1%.

Fig. 6 Phospholipids identified with ESI(-) in the lysate fractions of supernatant (S) and pellet (P) for the CCRF-CEM wild type (CEM-wt) and cisplatin-resistant (CEM-res) cells (charges of proton, sodium, potassium and formate ions are omitted for clarity), the MS-MS spectra of the marked (*) PLs are presented and discussed in the supporting (Fig. S8-S10). The species $C_{37}H_{72}O_7P$ was not distinguishable between PA(P-34:0) and PA(O-34:1). The error percentage in intensity of the repeated measurements was always lower than 1%.

Fig. 7 Phospholipids identified with ESI(-) in the lysate fractions of supernatant (S) and pellet (P) for the CCRF-CEM wild type (CEM-wt) and cisplatin-resistant (CEM-res) cells (charges of proton, sodium, potassium and formate ions are omitted for clarity), the MS-MS spectra of the marked (*) PLs are presented and discussed in the supporting (Fig. S9 and S10). The species $C_{37}H_{72}O_7P$ was not distinguishable between PA(P-34:0) and PA(O-34:1). The error percentage in intensity of the repeated measurements was always lower than 1%.

The number of PLs detected in supernatant (S) and pellet (P) is different for each studied cell lines, as reported in Table 1.

Table 1. Number of PLs detected in ESI(+) and ESI(-) in supernatant and pellet fractions of lysates of CCRF-CEM and A2780 cell lines in the chosen experimental conditions.

Cell Line	Number of detected phospholipids			
	ESI(+)		ESI(-)	
	supernatant	pellet	supernatant	pellet
CCRF-CEM-wt	21	17	18	15
CCRF-CEM-res	12	7	18	8
A2780-wt	12	23	8	12
A2780-res	14	22	9	15

In ESI(+), the number of PLs detected in the supernatant fraction is higher than that of the pellet fraction in the CCRF-CEM lysate and lower in the A2780 lysate. In ESI(-), the number of PLs detected in the supernatant or pellet fractions is almost identical in the CCRF-CEM lysate, while is higher in the pellet fraction of A2780 lysate compared to the supernatant. Some PLs were detected only in one of the two fractions of the cell lysates.

The intensities of the peaks recorded in ESI(+) are generally higher than those recorded in ESI(-), except for the signals of (DHAP+Na) and (LysoPA(18:2)+K-2H), where the presence of the metal ion increases the ionisation efficacy and originates a very high response. Regards the ESI(+) experiments, the PLs SM(d16:1/24:1), PC(P-34:0), PC(18:0/14:0), LysoPE(22:1), and LysoPE(20:1) are present only in the CCRF-CEM cells, in particular LysoPE(22:1) is present only in the CEM-resS, LysoPE(20:1) only in CEM-wtS, and SM(d16:1/24:1) only in CEM-wtP. The PLs PC(42:10), PE(40:8), PE(28:1), LysoPS(22:5), LysoPS(18:1), LysoPS(15:0), LysoPE(22:5), LysoPE(15:0) and S1P(d20:0) are detected only in A2780 cells. Regards the ESI(-) experiments, the PLs sphinganine 1-phosphate, LysoPC(18:1) and PC(P-34:0) are present only in the CEM cell lysate. PG(40:9) and SM(d18:0/22:2(13Z,16Z)(OH)) are present only in A2780 cell lysate.

From the MS-MS experiments (precursor ion mode and parent ion mode), lysophospholipids were found to be present in the lysate but also formed by collision-induced fragmentation of PLs or by decomposition of precursor ions in ESI phase. LysoPE(15:0), for example, was derived from PE(36:3), PE(34:3) and PE(32:3).

Considering the different results obtained for surpernatant and pellets, it follows that in the study of cell lysates, it is important to analyse both supernatant and pellet fractions and consider the total PL content.

CCRF-CEM wild type and cisplatin-resistant cell lines

The total PL content for CCRF-CEM-wt and CCRF-CEM-res is reported in Fig. 8. Intense changes between cisplatin-resistant and wild type cells are observable in the PL abundances and kinds. In particular, from ESI(+) results, in the resistant cells it appears that i) PC(20:2), PC(34:1), PC(P-34:0), SM(d18:0/18:0), LysoPC(18:1), and LysoPC(16:0) are strongly down-represented, while ii) LysoPE(22:1) and DHAP(18:0e) are moderately up-represented. From ESI(-) results, it appears that i) PC(36:1), PC(18:1/16:0), PC(P-34:0), PC(32:1), LysoPC(18:1), LysoPC(16:0), LysoPA(18:2), DHAP(18:0e) are down-represented, while ii) SM(d18:0/14:1(9Z)(OH)), PA(O-20:4(5Z,8Z,11Z,14Z)/2:0), LysoPE(15:0), LysoPA(P-16:0e/0:0) are up-represented. The PLs S1P(d19:1-P), LysoPE(14:1), LysoPE(O-16:0), PE(31:0), SM(d18:0/16:0), PE(34:3), PE(36:3) are almost retained from wild type to cisplatin-resistant cells.

From the reported results, the principal outcome is that the PC content is strongly reduced in the cisplatin-resistant CCRF-CEM cells, with respect to the wild type ones. This could be due to increased PC catabolism or decreased PC biosynthesis. The biological turnover of PCs produces phosphatidic acid (PA) and choline, by the action of phospholipase D, and arachidonic acid and LysoPC, by the action of phospholipase A2. PA can be then converted in LysoPA, while arachidonic acid can be converted in prostaglandins and leukotriens. LysoPCs play an important role in lipid signaling by acting on the LysoPLs receptors. LysoPA stimulates proliferation,

decreases apoptosis, platelet aggregation, smooth muscle contraction, and tumour cell invasion. PC biosynthesis is regulated by the cytidine 5'-diphosphocholine (CDP-choline), involved in the modulation of choline-phosphate cytidylyltransferase binding to membranes [32]. The CDP-choline reduces phospholipase A2 activity, increases the synthesis of S-Adenosyl methionine and glutathione, stimulates the glutathione reductase activity, and fixes the level of arachidonic acid [33–36]. DHAP(18:0e), moderately up-represented in the resistant cells, is the octadecanoyl derivative of the dihydroxyacetone phosphate (DHAP). DHAP is involved in the glycolysis metabolic pathway and it is produced by dehydrogenation of L-glycerol-3-phosphate (glycolytic pathway). DHAP(18:0e) or 1-octadecyl-glycerone-3-phosphate is converted from 1-octadecanoyl-glycerone-3-phosphate via alkylglycerone phosphate synthase [37]. The alkyl derivatives of DHAPs are intermediates in the synthesis of ether phospholipids, molecules with one or more carbon atoms on a glycerol moiety bonded to the alkyl chain via ether linkage. If a vinyl ether group is present in the first position of the glycerol chain, these lipids are called plasmalogens (1-O-1'-alkenyl-2-acylglycerophospholipids) [38].

Fig. 8 Phospholipids identified with ESI(+) (**A**) and ESI(-) (**B**) in the lysate extract of CCRF-CEM wild type (CEM-wt) and cisplatin-resistant (CEM-res) cells (charges of proton, sodium, potassium and formate ions are omitted for clarity). The species $C_{37}H_{72}O_7P$ was not distinguishable between PA(P-34:0) and PA(O-34:1). The phospholipids that are up-represented (⇧) or down-represented (⇩) in the cisplatin-resistant cells with respect to the wild type ones, are marked.

A2780 wild type and cisplatin-resistant cell lines

As shown in Fig. 9, from ESI(+) measurements, almost all the PLs are present to the same extent in the wild type and cisplatin-resistant cells, except SM(d34:1) which is slightly down-represented, and SM(d18:0/18:0) and PC(20:2(11Z,14Z)/16:0), which are slightly up-represented. On the contrary, the PLs detected in ESI(-) are all up-represented in resistant cells, and some of them are

strongly up-represented. In particular, SM(d18:0/14:1(9Z)(OH)), $C_{37}H_{72}O_7P$, PA(O-20:4(5Z,8Z,11Z,14Z)/2:0), LysoPA(18:2), DHAP(18:0e) and LysoPA(P-16:0e/0:0) are up-represented.

SM(d18:0/14:1(9Z)) is a sphingolipid found in the membranous myelin sheath. The plasma membrane of cells is rich in sphingomyelin, in particular in the exoplasmic leaflet. Sphingomyelins (SMs) are important for signal transduction and are synthesized by the transfer of phosphorylcholine from phosphatidylcholine to a ceramide in a reaction catalyzed by sphingomyelin synthase. Sphingolipids are involved in the formation of rafts and caveolae (lipid raft of 50–100 nm in size), which are cellular domains involved in the regulation of cell function, transporters and proteins, and in the skin barrier permeability. Sphingomyelin turnover alters the structure of membrane domains [39,40].

Fig. 9 Phospholipids identified with ESI(+) (**A**) and ESI(-) (**B**) in the lysate extract of A2780 wild type (A2780-wt) and cisplatin-resistant cells (A2780-res) (charges of proton, sodium, potassium and formate ions are omitted for clarity). The species $C_{37}H_{72}O_7P$ was not distinguishable between PA(P-34:0) and PA(O-34:1). The phospholipids that are up-represented (⇧) or down-represented (⇩) in the cisplatin-resistant cells with respect to the wild type ones, are marked.

Conclusions

We studied the phospholipid profile of wild type and cisplatin-resistant cells of two kinds of tumour, T-lymphoblastic leukaemia (CCRF-CEM) and ovarian carcinoma (A2780), with the aim to highlight possible differences and identify some specific phospholipids between wild type and cisplatin-resistant cells.

The analytical method proposed in this work is based on solid phase extraction and mass spectrometry and allowed us to study the phospholipidic (PL) profile of cell lysates, obtaining reliable and reproducible results and preventing peptide and metabolite interferences. A different

phospholipidic profile was detected in supernatant and pellet fractions of the cell lysates, suggesting that these two fractions have to be taken into account simultaneously for a correct interpretation and a complete characterization of the phospholipidic profile.

Comparing the PL profiles of wild type and cisplatin-resistant cells, the absence of PC(34:1), LysoPC(18:1), PC(20:2(11Z,14Z)/16:0) and PC(P-34:0) was observed as specific for cisplatin-resistant CCRF-CEM cells, whereas the presence of PC(20:2(11Z,14Z)/16:0) and SM(d18:0/18:0) and the absence of SM(d34:1) were observed as specific for cisplatin-resistant A2780 cells. These lipids can be considered, within a specific line, as "markers" to distinguish between wild type and cisplatin-resistant cells.

Considering that the PL composition influences the transport of drugs across the membrane, affects the activity of the drug transporters and the ability of the cells to load and accumulate drugs, it is evident that a change of the PL content is connected with the development of the resistance. However, from the obtained results, it is not possible to define if these changes are the cause or the consequence of the cisplatin-resistance occurrence. Nevertheless, the potential use of some lipids as "markers" for resistant cells could be important for a possible clinical application. In fact, the onset of the resistance during cisplatin treatment could be monitored by detecting those specific lipids. Under this perspective, the obtained findings represent an advancement of knowledge and can be exploited for the design of new strategies in cancer treatment.

Abbreviations used

A2780-res, cisplatin resistant sub-line of ovarian carcinoma cells; A2780-wt, wild type ovarian carcinoma cells; CCRF-CEM-res, cisplatin resistant sub line of acute T-lymphoblastic leukaemia cells; CCRF-CEM-wt, wild type acute T-lymphoblastic leukaemia cells; CDP-choline, cytidine 5'-diphosphocholine; CID, collision-induced decomposition; DHAP, dihydroxyacetone phosphate; ESI(+), electrospray ionisation positive ion mode; ESI(-), electrospray ionisation negative ion

mode; ESI-MS, electrospray ionisation mass spectrometry; FBS, foetal bovine serum; GPLs, glycerophospholipids; HTFA, trifluoroacetic acid; MS-MS, tandem mass spectrometry; P, pellet fraction; PA, phosphatidic acid; PC, glycerophosphocholine; PE, glycerophosphoethanolamine; PI, glycerophosphoinositol; PS, glycerophosphoserine; PLs, phospholipids; RPMI medium, Roswell Park Memorial Institute medium; S, supernatant fraction; SLs, sphingolipids; SMs, sphingomyelins; SPE, solid phase extraction; TFA, trifluoroacetate.

References

1. Cooper GM. The Cell: A Molecular Approach. 2nd ed. Associates S, editor. Sunderland (MA); 2000.
2. van Meer G, de Kroon AIPM. Lipid map of the mammalian cell. J Cell Sci. 2011;124: 5–8. doi:10.1242/jcs.071233
3. Pulfer M, Murphy RC. Electrospray mass spectrometry of phospholipids. Mass Spectrom Rev. 2003;22: 332–364. doi:10.1002/mas.10061
4. van Meer G, R. Voelker D, W. Feigenson G. Membrane lipids - where they are and how they behave.pdf. Nat Rev Mol Cell Biol. 2009;9: 112–124. doi:10.1038/nrm2330.Membrane
5. Riboni L, Campanella R, Bassi R, Villani R, Gaini SM, Martinelli-Boneschi F, et al. Ceramide levels are inversely associated with malignant progression of human glial tumors. Glia. 2002;39: 105–113. doi:10.1002/glia.10087
6. Lladó V, López DJ, Ibarguren M, Alonso M, Soriano JB, Escribá P V., et al. Regulation of the cancer cell membrane lipid composition by NaCHOleate: Effects on cell signaling and therapeutical relevance in glioma. Biochim Biophys Acta - Biomembr. Elsevier B.V.; 2014;1838: 1619–1627. doi:10.1016/j.bbamem.2014.01.027
7. Kojima K. Molecular aspects of the plasma membrane in tumor cells. Nagoya J Med Sci. 1993; 1–18.
8. Naleskina LA, Todor IN, Nosko MM, Lukianova NY, Pivnyuk VM, Chekhun VF. Alteration In Lipid Composition Of Plasma Membranes Of Sensitive And Resistant Guerin Carcinoma Cells Due To The Action Of Free And Liposomal Form Of Cisplatin. 2013;2013: 192–197.
9. Szachowicz-Petelska B, Dobrzynska I, Sulkowski S, Figaszewski Z. Characterization of the cell membrane during cancer transformation. J Environ Biol. 2010;31: 845–850. doi:10.5772/29559
10. Eckstein N. Platinum resistance in breast and ovarian cancer cell lines. J Exp Clin Cancer Res. BioMed Central Ltd; 2011;30: 91–102. doi:10.1186/1756-9966-30-91
11. Dhar S, Gu FX, Langer R, Farokhzad OC, Lippard SJ. Targeted delivery of cisplatin to prostate cancer cells by aptamer functionalized Pt(IV) prodrug-PLGA-PEG nanoparticles. Proc Natl Acad Sci U S A. 2008;105: 17356–17361. doi:10.1073/pnas.0809154105
12. Rixe O, Ortuzar W, Alvarez M, Parker R, Reed E, Paull K, et al. Carboplatin : Spectrum of

Activity in Drug-Resistant Cell Lines and in the Cell Lines of the National Cancer Institute's Anticancer Drug Screen Panel. Biochem Pharmacol. 1996;52: 1855–1865.

13. Michels J, Vitale I, Galluzzi L, Adam J, Olaussen KA, Kepp O, et al. Cisplatin Resistance Associated with PARP Hyperactivation. Cancer Res . 2013;73 : 2271–2280.

14. Cox MM, Nelson DL. Lehninger Principles of Biochemistry. 5th ed. Freeman WH, editor. 2008.

15. Burger H, Zoumaro-Djayoon A, Boersma AWM, Helleman J, Berns EMJJ, Mathijssen RHJ, et al. Differential transport of platinum compounds by the human organic cation transporter hOCT2 (hSLC22A2). Br J Pharmacol. 2010;159: 898–908. doi:10.1111/j.1476-5381.2009.00569.x

16. Ishida S, Lee J, Thiele DJ, Herskowitz I. Uptake of the anticancer drug cisplatin mediated by the copper transporter Ctr1 in yeast and mammals. Proc Natl Acad Sci U S A. 2002;99: 14298–14302. doi:10.1073/pnas.162491399

17. Song I, Savaraj N, Siddik ZH, Liu P, Wei Y, Wu CJ, et al. Role of human copper transporter Ctr1 in the transport of platinum-based antitumor agents in cisplatin-sensitive and cisplatin-resistant cells. Mol Cancer Ther. 2005;3: 1543–1549.

18. Alderden RA, Hall MD, Hambley TW. The Discovery and Development of Cisplatin. J Chem Educ. 2006;83: 728–734.

19. Trzaska S. Cisplatin. Chem Eng News. 2005;83.

20. Jamieson ER, Lippard SJ. Structure, Recognition, and Processing of Cisplatin-DNA Adducts. Chem Rev. 1999;99: 2467–2498.

21. Todd RC, Lippard SJ. Inhibition of transcription by platinum antitumor compounds. Metallomics. 2009;1: 280–291. doi:10.1039/b907567d

22. Trudu F, Amato F, Vaňhara P, Pivetta T, Peña-Méndez EM, Havel J. Coordination compounds in cancer: Past, present and perspectives. J Appl Biomed. 2015; doi:10.1016/j.jab.2015.03.003

23. Pivetta T, Lallai V, Valletta E, Trudu F, Isaia F, Perra D, et al. Mixed copper–platinum complex formation could explain synergistic antiproliferative effect exhibited by binary mixtures of cisplatin and copper-1,10-phenanthroline compounds: An ESI–MS study. J Inorg Biochem. Elsevier Inc.; 2015; doi:10.1016/j.jinorgbio.2015.05.004

24. Niedermeyer THJ, Strohalm M. mMass as a software tool for the annotation of cyclic peptide tandem mass spectra. PLoS One. 2012;7: e44913. doi:10.1371/journal.pone.0044913

25. Strohalm M, Kavan D, Nova P, Volny M. mMass 3 : A Cross-Platform Software Environment for Precise Analysis of Mass Spectrometric Data. Anal Chem. 2010;82: 4648–4651.

26. Strohalm M, Hassman M, Kosata B, Kodicek M. RCM Letter to the Editor. Rapid Commun Mass Spectrom. 2008;22: 905–908. doi:10.1002/rcm

27. Wishart DS, Tzur D, Knox C, Eisner R, Guo AC, Young N, et al. HMDB: the Human Metabolome Database. Nucleic Acids Res. 2007;35: D521–6. doi:10.1093/nar/gkl923

28. Wishart DS, Knox C, Guo AC, Eisner R, Young N, Gautam B, et al. HMDB: a knowledgebase for the human metabolome. Nucleic Acids Res. 2009;37: D603–10. doi:10.1093/nar/gkn810

29. Wishart DS, Jewison T, Guo AC, Wilson M, Knox C, Liu Y, et al. HMDB 3.0--The Human Metabolome Database in 2013. Nucleic Acids Res. 2013;41: D801–7. doi:10.1093/nar/gks1065

30. Henderson W, McIndoe JS. Mass Spectrometry of Inorganic, Coordination and Organometallic Compounds [Internet]. Chichester, UK: John Wiley & Sons, Ltd; 2005. doi:10.1002/0470014318

31. http://www.sigmaaldrich.com/content/dam/sigma-aldrich/docs/Supelco/Product_Information_Sheet/t708008.pdf.

32. Vance DE, Vance JE. Biochemistry of Lipds, Lipoproteins and Membranes. 4th ed. Bernardi G, editor. Elsevier; 2002.

33. Adibhatla RM, Hatcher JF, Dempsey RJ. Citicoline: Neuroprotective mechanisms in cerebral ischemia. J Neurochem. 2002;80: 12–23. doi:10.1046/j.0022-3042.2001.00697.x

34. López-Coviella I, Agut J, Savci V, Ortiz JA, Wurtman RJ. Evidence that 5′-Cytidinediphosphocholine Can Affect Brain Phospholipid Composition by Increasing Choline and Cytidine Plasma Levels. J Neurochem. Blackwell Science Ltd; 1995;65: 889–894. doi:10.1046/j.1471-4159.1995.65020889.x

35. Conant R, Schauss AG. Therapeutic Applications of Citicoline for Stroke and Cognitive Dysfunction in the Elderly: A Review of the Literature. Altern Med Rev. 2004;9: 17–31.

36. Babb S, Wald L, Cohen B, Villafuerte R, Gruber S, Yurgelun-Todd D, et al. Chronic citicoline increases phosphodiesters in the brains of healthy older subjects: an in vivo phosphorus magnetic resonance spectroscopy study. Psychopharmacology (Berl). Springer-Verlag; 2002;161: 248–254. doi:10.1007/s00213-002-1045-y

37. Chanda B, Xia Y, Mandal MK, Yu K, Sekine K-T, Gao Q, et al. Glycerol-3-phosphate is a critical mobile inducer of systemic immunity in plants. Nat Genet. 2011;43: 421–427. doi:10.1038/ng.798

38. Agranoff B, Benjamins J, Hajra A. Basic Neurochemistry: Molecular, Cellular and Medical Aspects. In: Siegel GJ, Agranoff BW, Albers RW et al., editor. 6th editio. Philadelphia: Lippincott-Raven; 1999.

39. Brown D a., London E. Structure and function of sphingolipid- and cholesterol-rich membrane rafts. J Biol Chem. 2000;275: 17221–17224. doi:10.1074/jbc.R000005200

40. Venkataraman K, Futerman AH. Ceramide as a second messenger: Sticky solutions to sticky problems. Trends Cell Biol. 2000;10: 408–412. doi:10.1016/S0962-8924(00)01830-4

41. Voinov VG, Claeys M. Charge-remote fragmentation of fatty acid molecular anions: Examination by using resonance electron capture mass spectrometry. Int J Mass Spectrom. 2000;198: 23–32. doi:10.1016/S1387-3806(99)00267-5

42. Hsu F-F, Turk J. Electrospray ionization/tandem quadrupole mass spectrometric studies on phosphatidylcholines: The fragmentation processes. J Am Soc Mass Spectrom. 2003;14: 352–363. doi:10.1016/S1044-0305(03)00064-3

43. Smith PB, Snyder a P, Harden CS. Characterization of bacterial phospholipids by electrospray ionization tandem mass spectrometry. Anal Chem. 1995;67: 1824–1830.

Figure 1

Click here to download Figure Figure 1.tif

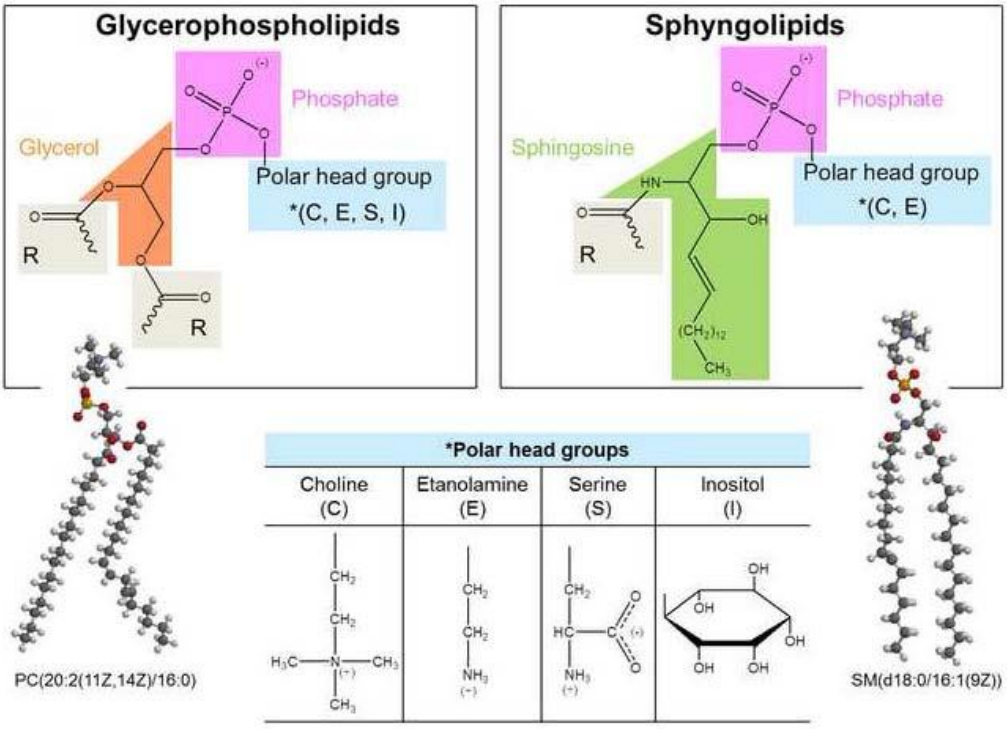

Figure 2

Click here to download Figure Figure 2.tif

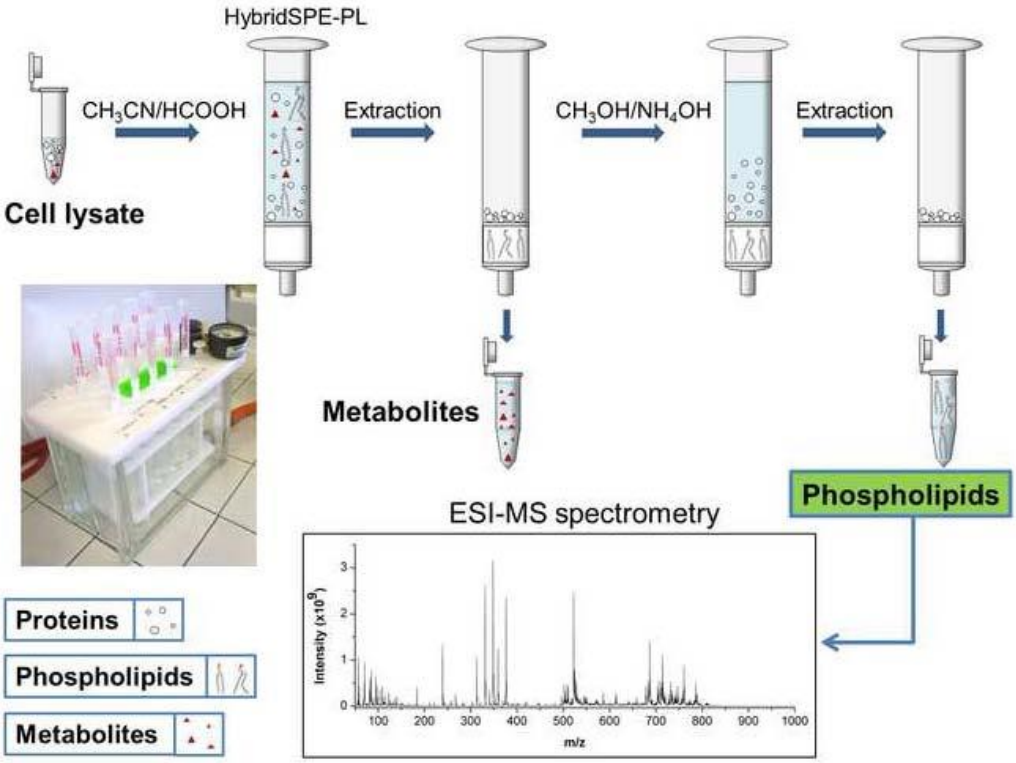

Figure 3

Click here to download Figure Figure 3.tif

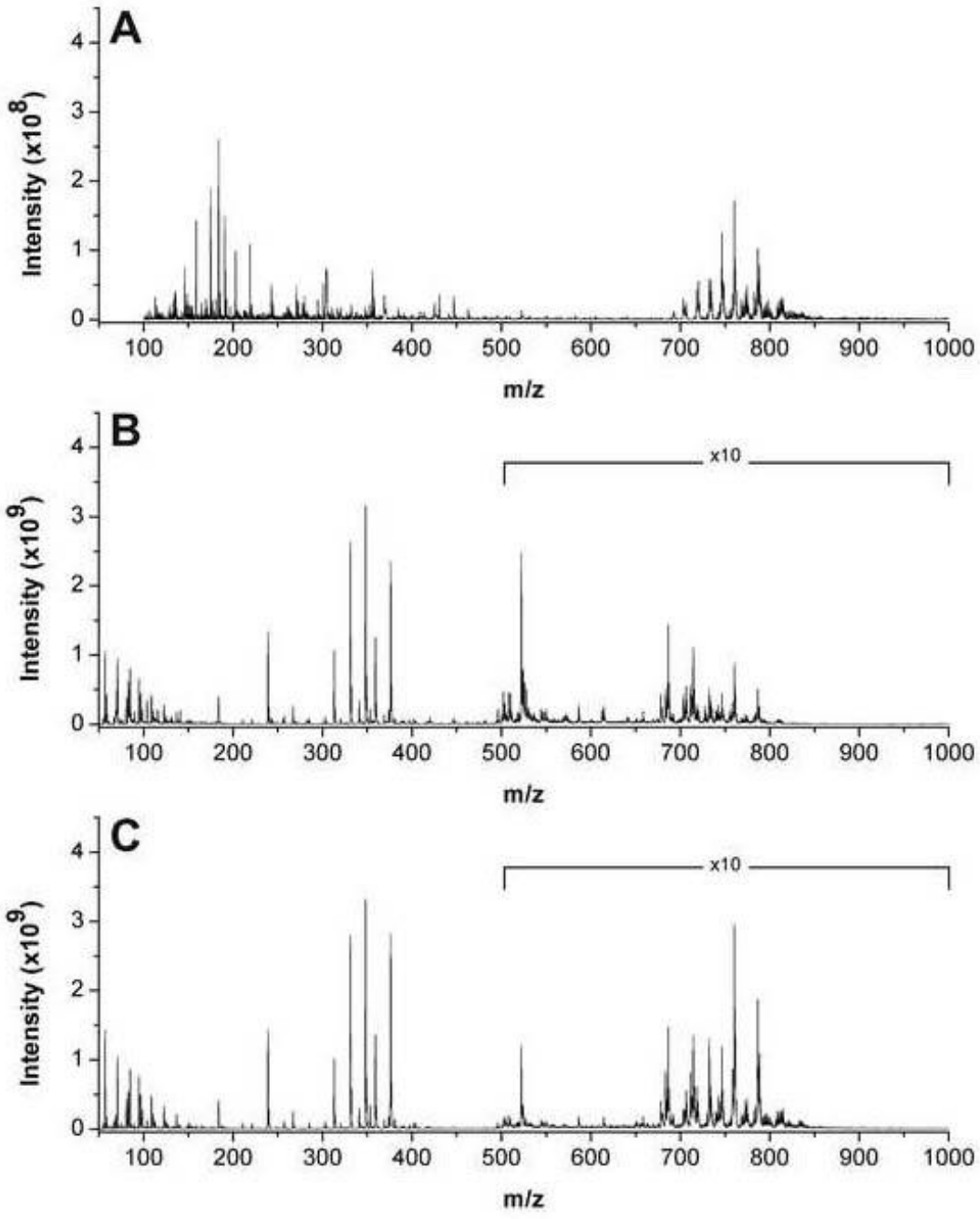

Figure 4

Click here to download Figure Figure 4.tif

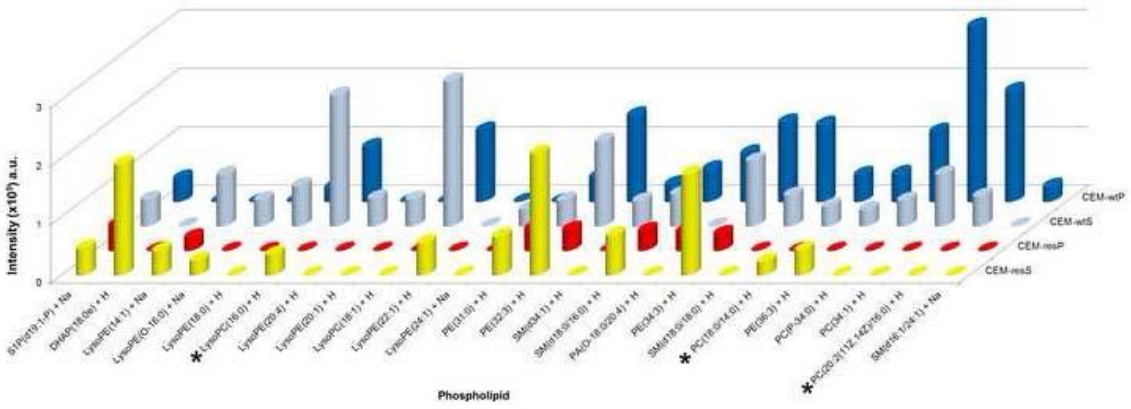

Figure 5

Click here to download Figure Figure 5.tif

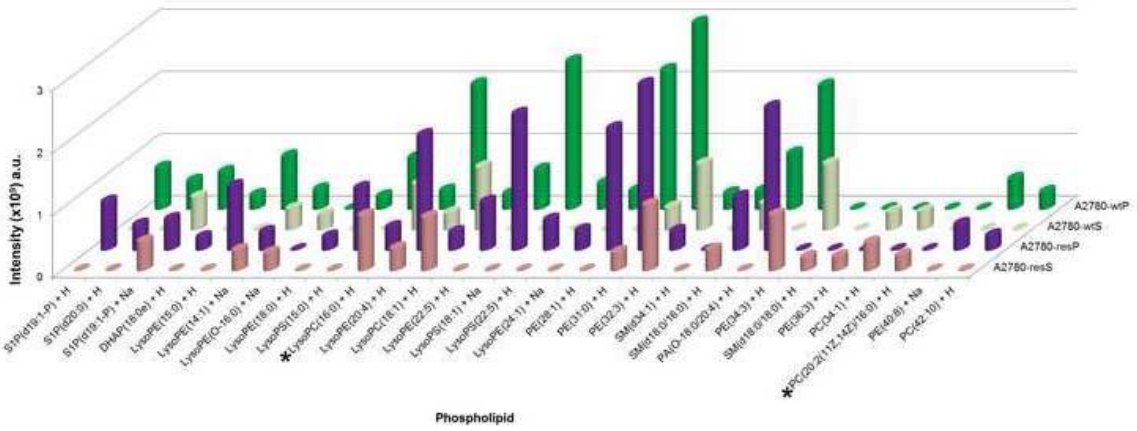

Figure 6

Click here to download Figure Figure 6.tif

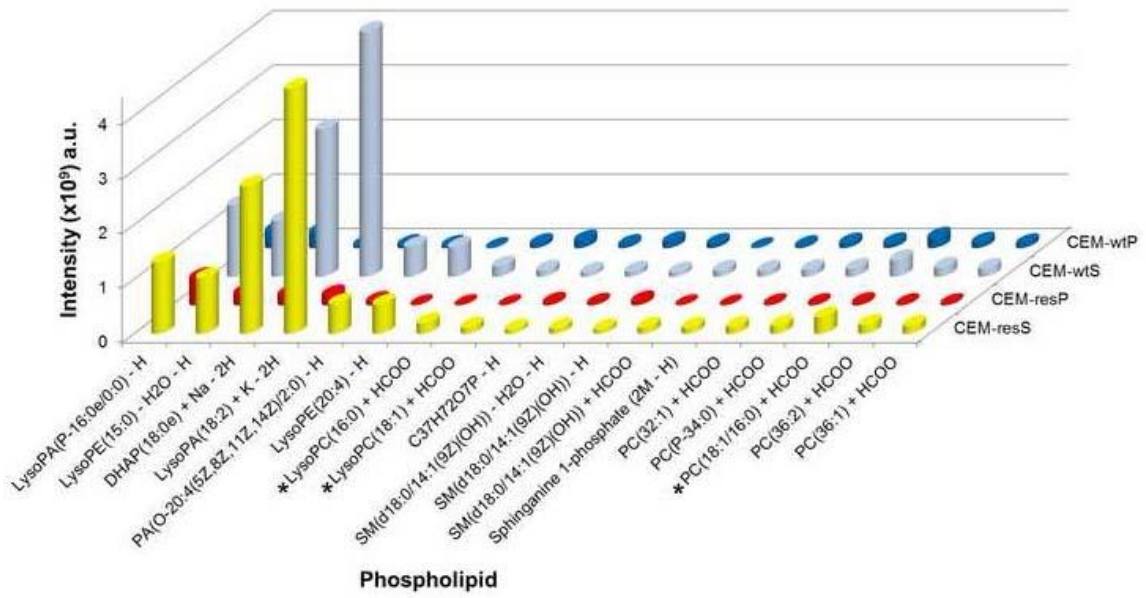

Figure 7

Click here to download Figure Figure 7.tif

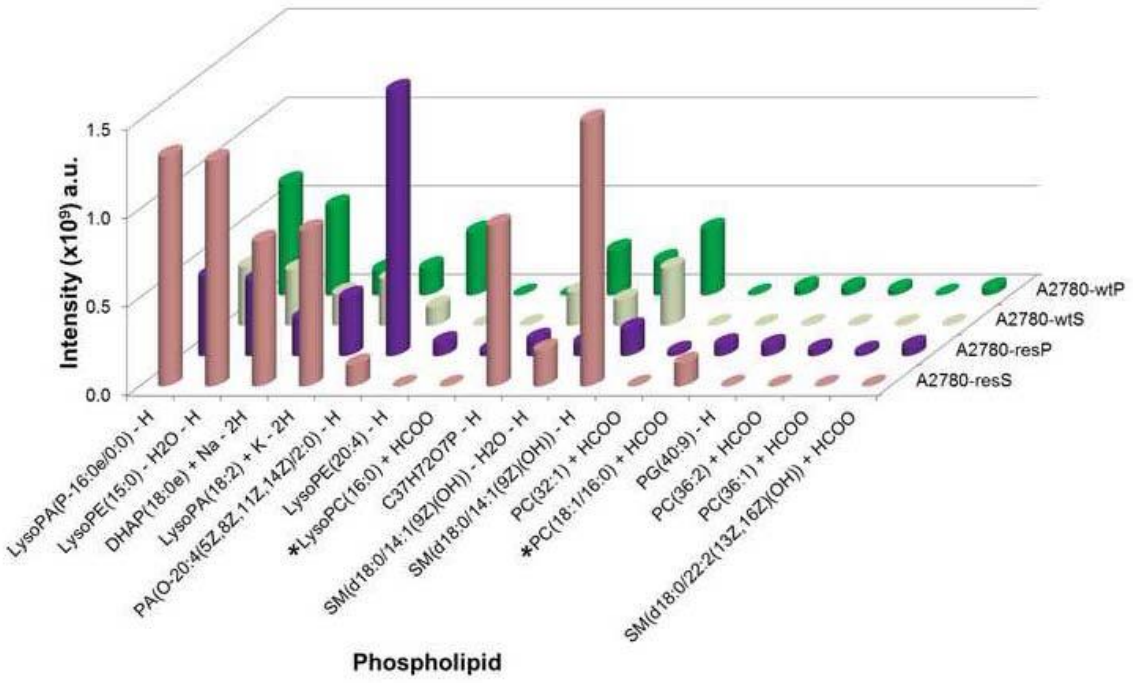

Figure 8

Click here to download Figure Figure 8.tif

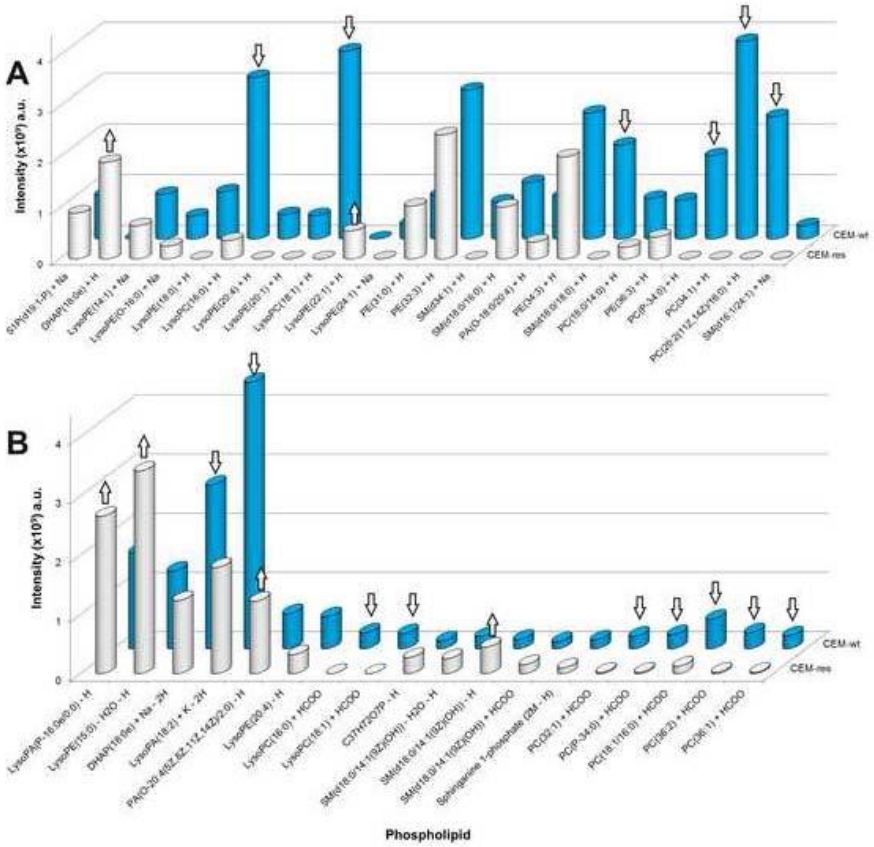

Figure 9

Click here to download Figure Figure 9.tif

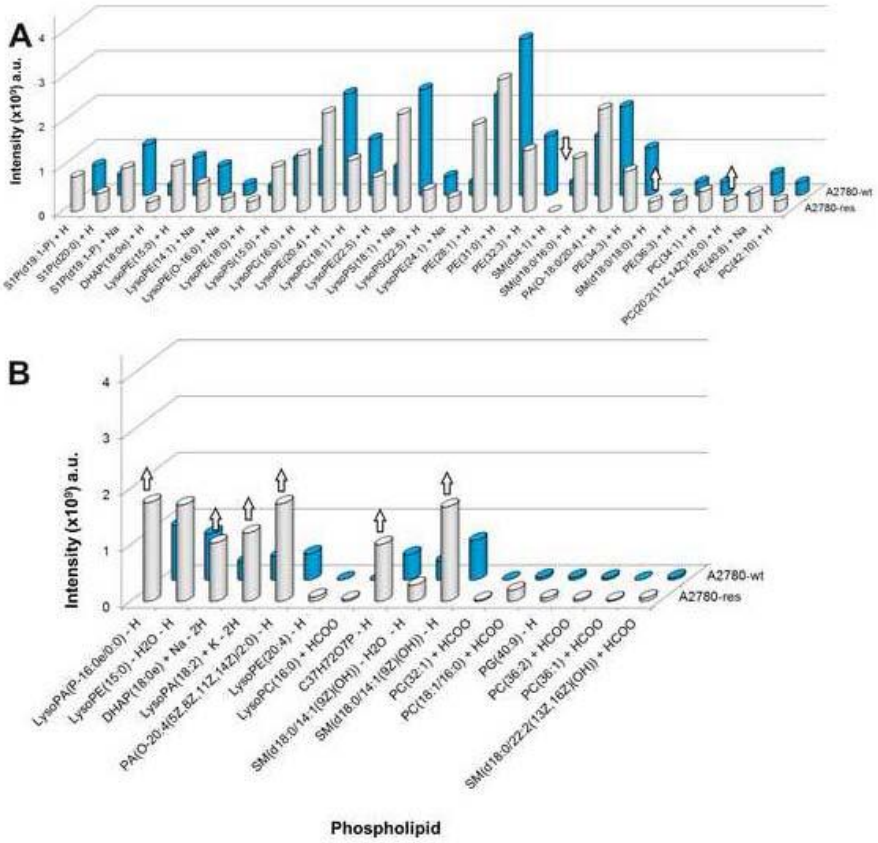

Striking Image

Click here to download Striking Image striking image-Pagina001.tif

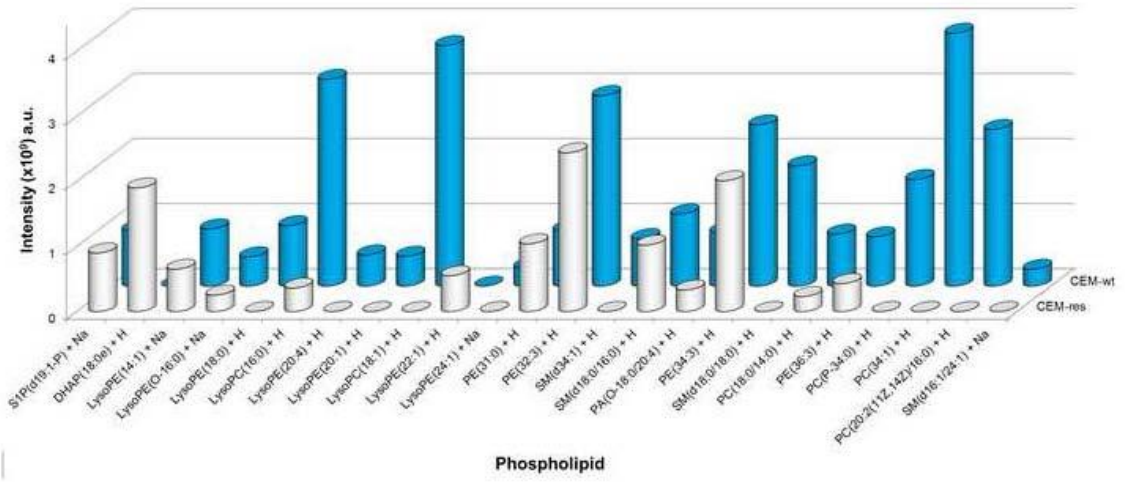

3.6 Study of the selectivity of the ternary drug combination: cytotoxic effect in CEM versus PBLs

On the basis of the strong cytotoxic synergism shown by the CDDP-C0-GSH combination in CEMwt and CEMres tumour cell lines, either drug-sensitive and CDDP-resistant, it was of critical importance to investigate their toxic effect on normal cells so as to have an estimate of the selectivity of action of these cocktails of drugs.

To this end, human peripheral blood lymphocytes (PBLs) freshly isolated from blood samples of healthy donors were seeded at the same cell density as such (i.e. resting PBLs), in the presence of the mitogen PHA (i.e. PHA-activated PBLs), or in the presence of both PHA and the growth factor Interleukin-2 (i.e. PHA/IL2-stimulated PBLs). Each of these cultures were then incubated in the presence of the most synergic three-drug combination in CCRF-CEM-wt cells and in the presence of the single drugs, each of them at the same concentrations present in the combination; i.e. 0.5 μM CDDP, 0.5 μM C0, and 300 μM GSH. The numbers of viable cells were determined by the trypan blue exclusion method and reported as percentage of untreated controls after 24 h (Figure 19A-C), 48 h (Figure 20A-C) and 72 h (Figure 21A-C) of incubation in comparison to those of CEM cells incubated in parallel under the same drug conditions (Figures 19D, 20D, 21D). It has to be mentioned that the PBL values in Figures 19, 20, 21 are the mean data of independent experiments with PBLs isolated from three different donors, whereas in Figure 22 PBL growth curves and viable cell counts of untreated vs. drug combination treated PBLs isolated from one single donor are shown.

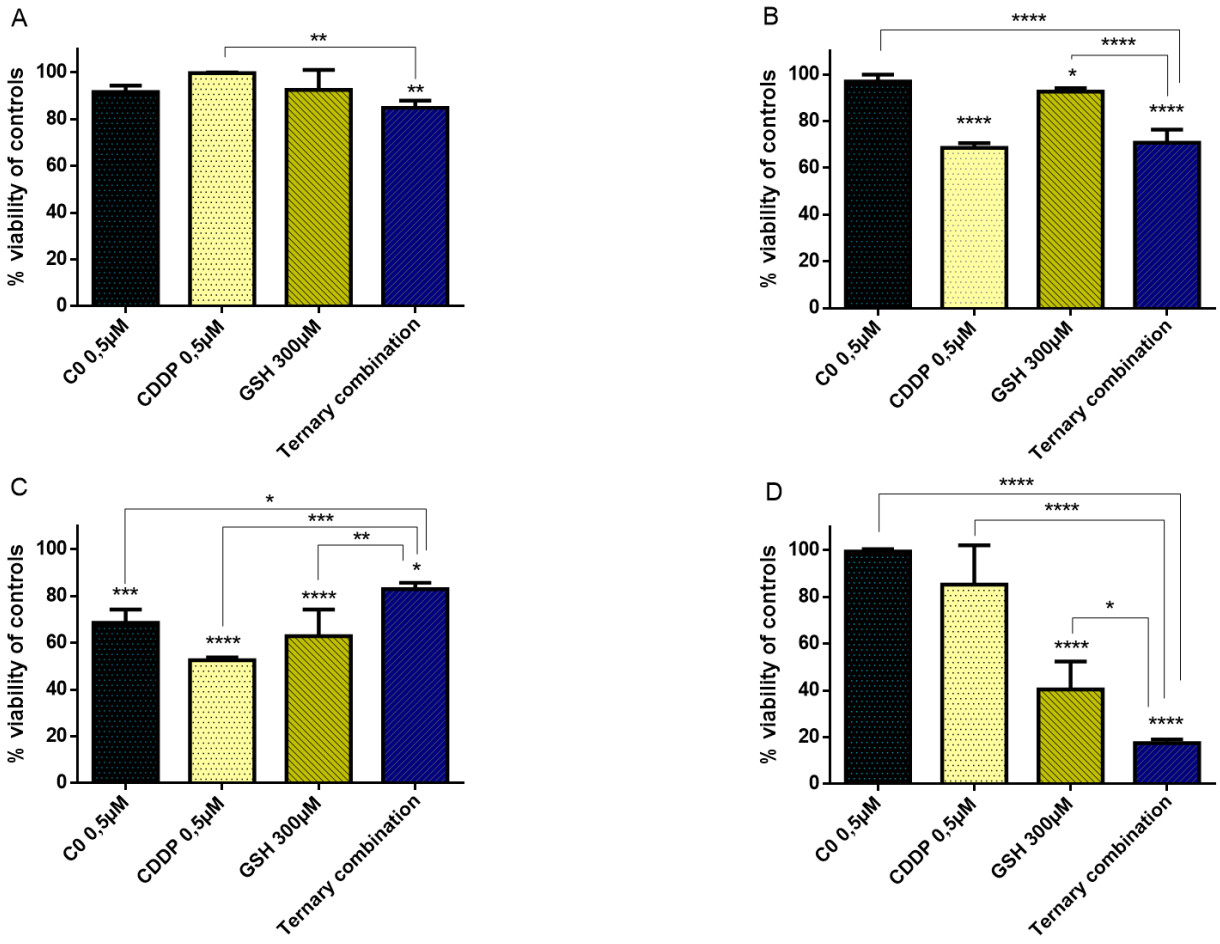

Figure 19. Cytotoxic activity of **C0**, CDDP, and GSH, alone and in ternary combinations, in freshly isolated human PBLs and in CCRF-CEMwt cells after 24 h of treatment. (**A**) resting PBLs, (**B**) PHA-stimulated PBLs, (**C**) PHA+ IL2- stimulated PBLs, (**D**)CEM. Values obtained in drug-treated samples were expressed as percentages of their respective controls.

Results are the mean ± SD from three determinations from three different subjects compared with the corresponding control and . Ternary combination is also compared with each compounds.

*p‹ 0,05; **p‹0,001; ***p‹0,001; ****p‹0,0001 (Anova).

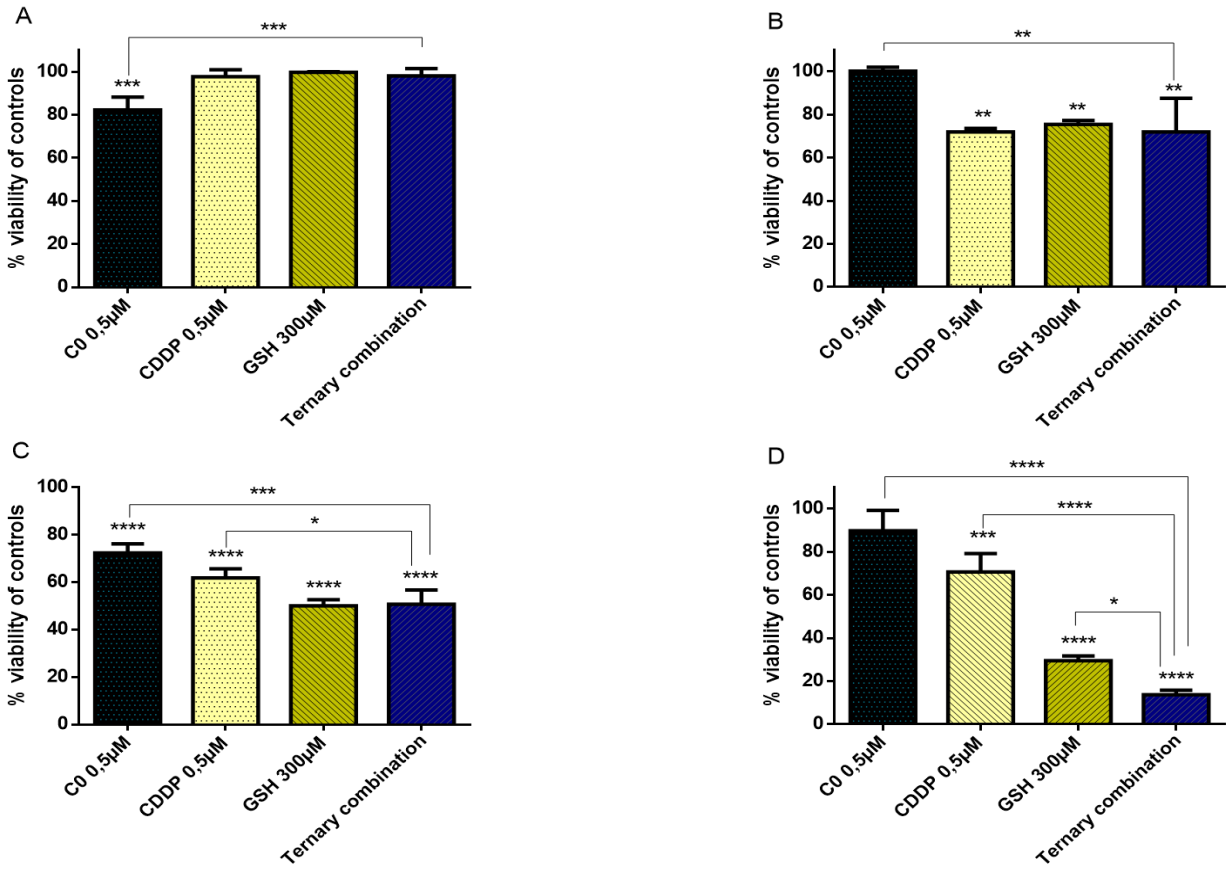

Figure 20. Cytotoxic activity of C0, CDDP and GSH, alone and in ternary combinations, in freshly isolated human PBLs and in CCRF-CEM cells after 48 hours of treatment. (A) resting PBLs, (B) PHA-stimulated PBLs, (C) PHA+ IL2- stimulated PBLs, (D) CCRF-CEM-wt. Values obtained in drug-treated samples were expressed as percentages of their respective controls.

Results are the mean ± SD from three determinations from three different subjects compared with the corresponding control. Ternary combination is also compared with each compounds.

*p‹ 0,05; **p‹0,001; ***p‹0,001; ****p‹0,0001 (Anova).

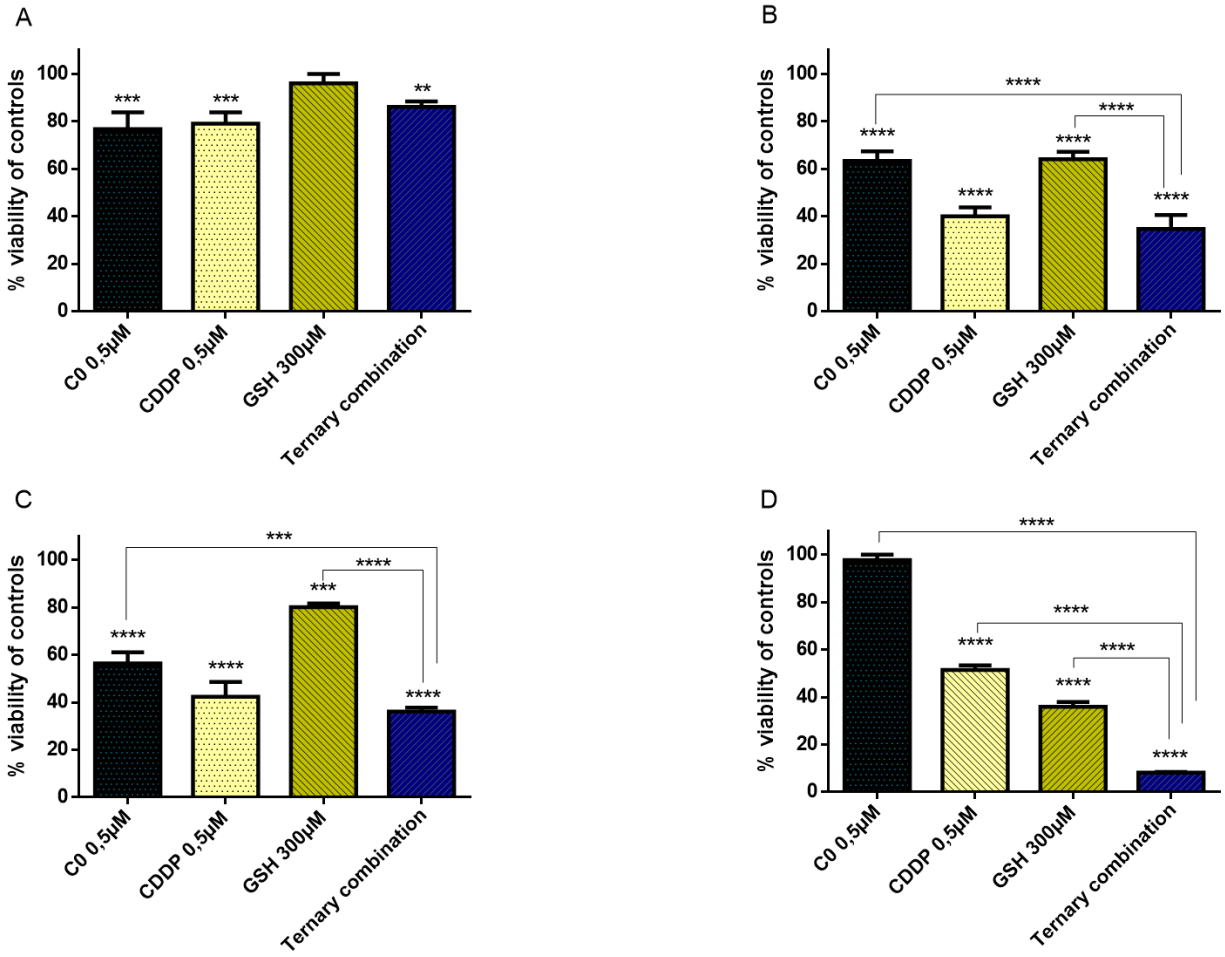

Figure 21. Cytotoxic activity of C0, CDDP and GSH, alone and in ternary combinations, in freshly isolated human PBLs and in CCRF-CEM-wt cells after 72 h of treatment. (A) Resting PBLs, (B) PHA-stimulated PBLs, (C) PHA+ IL2- stimulated PBLs, (D) CCRF-CEM-wt. Values obtained in drug-treated samples were expressed as percentages of their respective controls.

Results are the mean ± SD from three determinations from three different subjects compared with the corresponding control . Ternary combination is also compared with each compounds.

*p‹ 0,05; **p‹0,001; ***p‹0,001; ****p‹0,0001 (Anova).

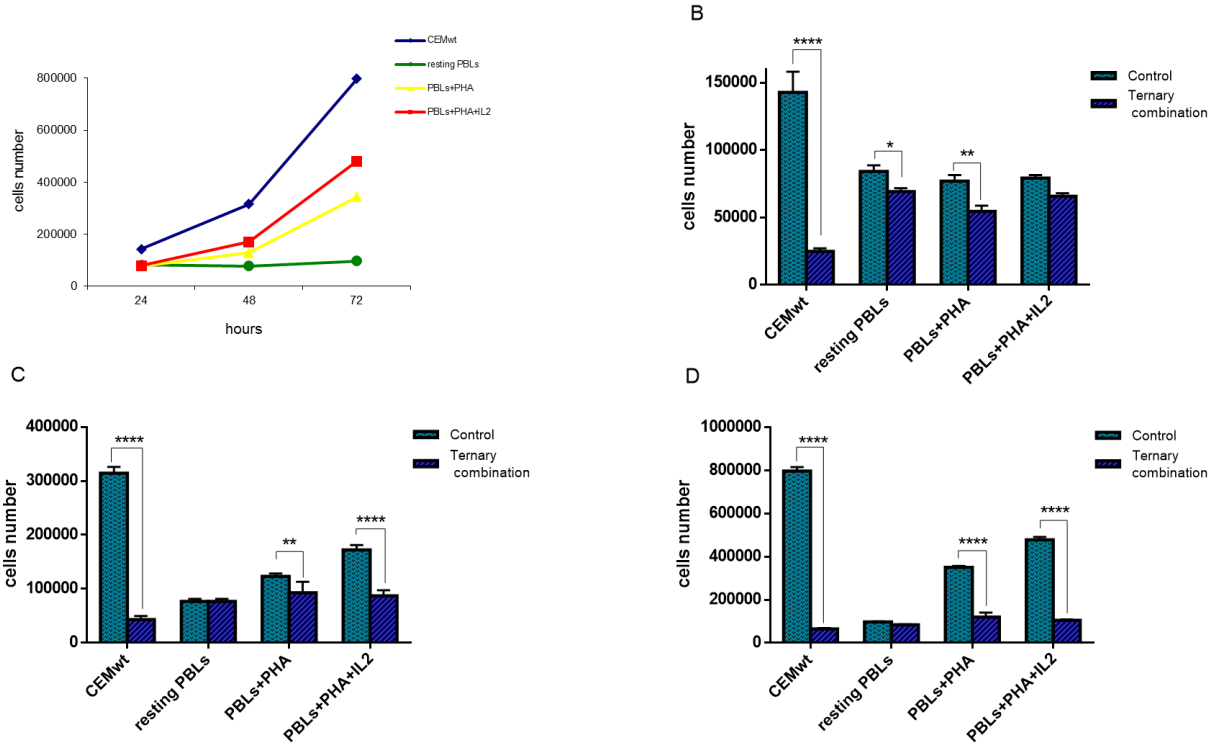

Figure 22. Growth curves and cell numbers of untreated vs. ternary combination-treated CEM and PBL cells. (A) Growth curves of CCRF-CEM-wt and PBLs. Viable cell numbers in untreated vs. ternary combination-treated CCRF-CEM-wt and PBLs after 24 h (B), 48 h (C), 72 h (D).

Results are the mean ± SD from three determinations from three different subjects compared with the corresponding control. Ternary combination is also compared with each compounds.

*p‹ 0,05; **p‹0,001; ***p‹0,001; ****p‹0,0001 (Anova).

Single-drug treatments with 0.5 µM CDDP showed a cytotoxic effect increasing over time only against active/proliferating cell cultures, i.e. against both PHA-activated and PHA/IL2-stimulated PBLs, and against CCRF-CEM cells, while, as expected, it had only negligible effects against non-activated/non-proliferating cells (i.e. resting-PBLs). After 72 h of incubation, the degree of cytotoxicity of CDDP was comparable in PBLs and CEM cells, with an average of 60%-70% cell viability with respect to their respective untreated controls. In the PBL cultures, however, the CDDP effect was more precocious (i.e. in PHA/IL2-stimulated at 24 h; in PHA-activated at 48 h) than in the CCRF-CEM cultures; viable CCRF-CEM cells being still over 80% of controls at 24 h, and over 70% of controls at 48 h.

The cytotoxic effect in PBLs of 0.5 µM C0 appeared to better correlate with the activation stage of the cells; the viability of PHA/IL2-stimolated PBLs was reduced by 30% already after 24 h, while that of the PHA-activated PBLs by 35% only after 72h. Differently from CDDP, C0 seemed to affect the viability also of the resting PBLs as a slight toxic effect, i.e. around 20% mortality was observed in each PBL preparation of the three different donors. In CCRF-CEM cells, the cytotoxicity of C0 appeared to be even lower, if any, than in the resting PBLs: the viability of treated CCRF-CEM cells being over 90% of controls at all time points considered.

Treatments with 300µM GSH were instead more toxic in CEM cells than in PBLs, and among the latter, the PHA/IL2-stimulated were affected the most followed by the PHA-activated, whereas resting PBLs were not affected at all. Although GSH cytotoxicity was greater against the CEM cells (60%-70% mortality) than against PHA/IL2-stimulated PBLs (50% mortality), in both types of cell cultures the maximum effect was reached after 48 h of exposure to GSH.

Compared to the single-drug treatments, in CEM cells the drug cocktail confirmed the synergic effect showing a very strong toxic activity already in the first 24 h (over 80% mortality) which further increased at 48 h and 72 h with a mortality of 87% and 92%, respectively.

For the PBLs, the PHA/IL2-stimulated were the most sensitive of all PBL cultures to the toxic effect of the drug combination that was, however, both less potent and more delayed with respect to that exerted in the CEM cells, i.e. a 50% and 40% mortality after 48 h and 72h respectively, The toxic effect against the PHA-activated PBLs was even slower than that shown in the PHA/IL2-stimulated, 20%- 30% mortality at the first two time points, and comparable only after 72 h. The drug cocktail was totally devoid of cytotoxicity on the resting PBLs at any time points considered (see Figures 23 and 24).

Moreover, if we consider the effects of the ternary combination vs. the single-drug treatments in the PBLs, the drug cocktail always showed a degree of cytotoxicity comparable to that of the CDDP alone, whereas in the CEM cells the toxic effect of the combination was 7 fold greater than that of CDDP alone.

Taken together, these findings are very promising given that the ternary combination showed a selective cytotoxic effect for T-leukemia CEM cells with respect to proliferating normal T-cells. Beside of being more potent against the leukemic CEM cells (8% viability after 72 h) than against PHA/IL2-stimulated PBLs (50% viability at 72 h), the effect of the ternary combination against CEM cells appeared to be also very precocious, i.e. only 17% viability left at 24 h, compared to 80% in the proliferating PBLs at the same time point.

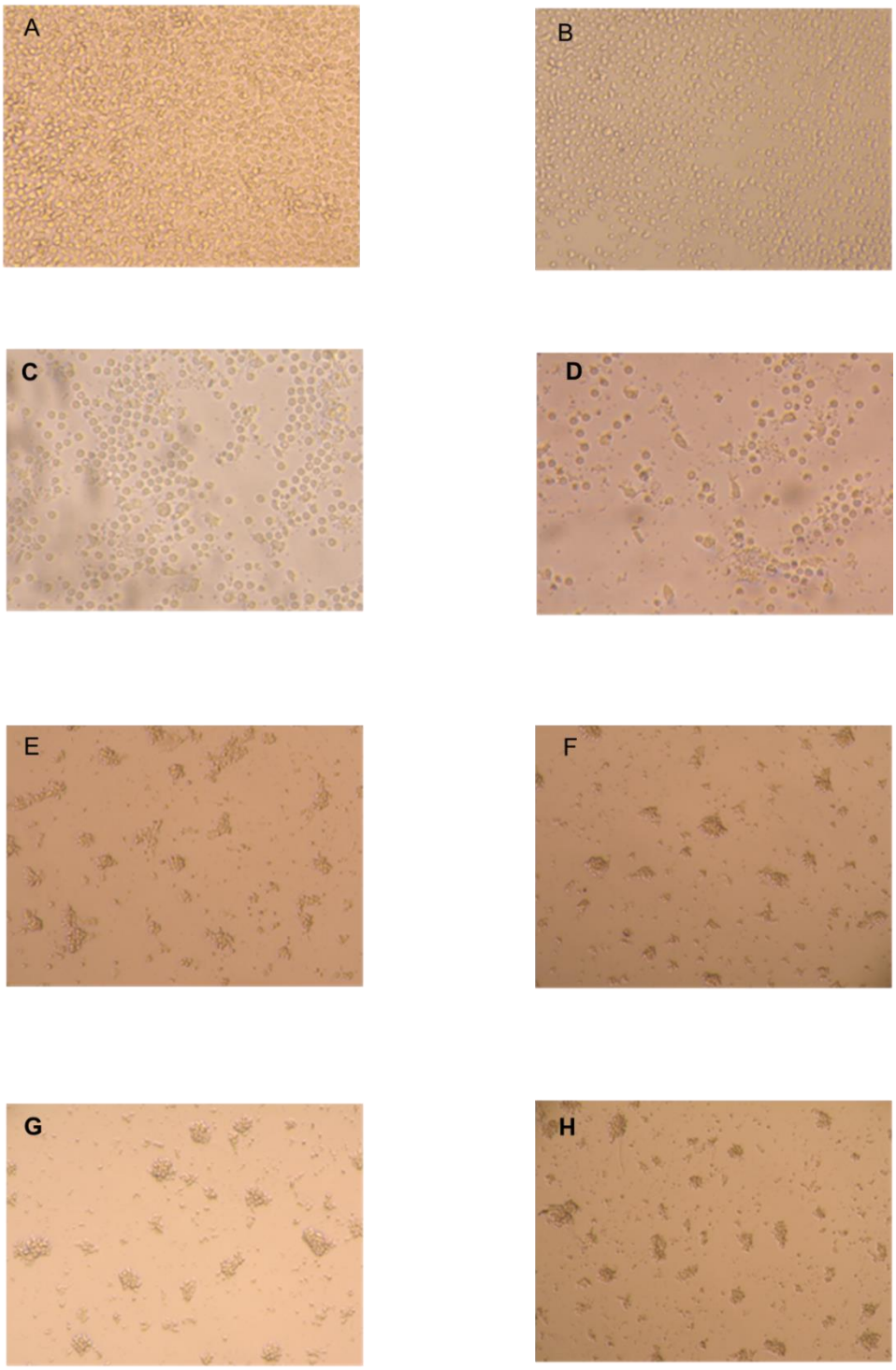

Figure 23. CEM and PBLs after 24 hours of incubation in the absence and in the presence of ternary combination :
A: CEM control, B: CEM + ternary combination, C: resting PBLs control,
D: resting PBLs + ternary combination, E: PBLs +PHA control, F: PBLs + PHA + ternary combination, G: PBLs + PHA+ IL2, PBLs+PHA+IL2+ ternary combination

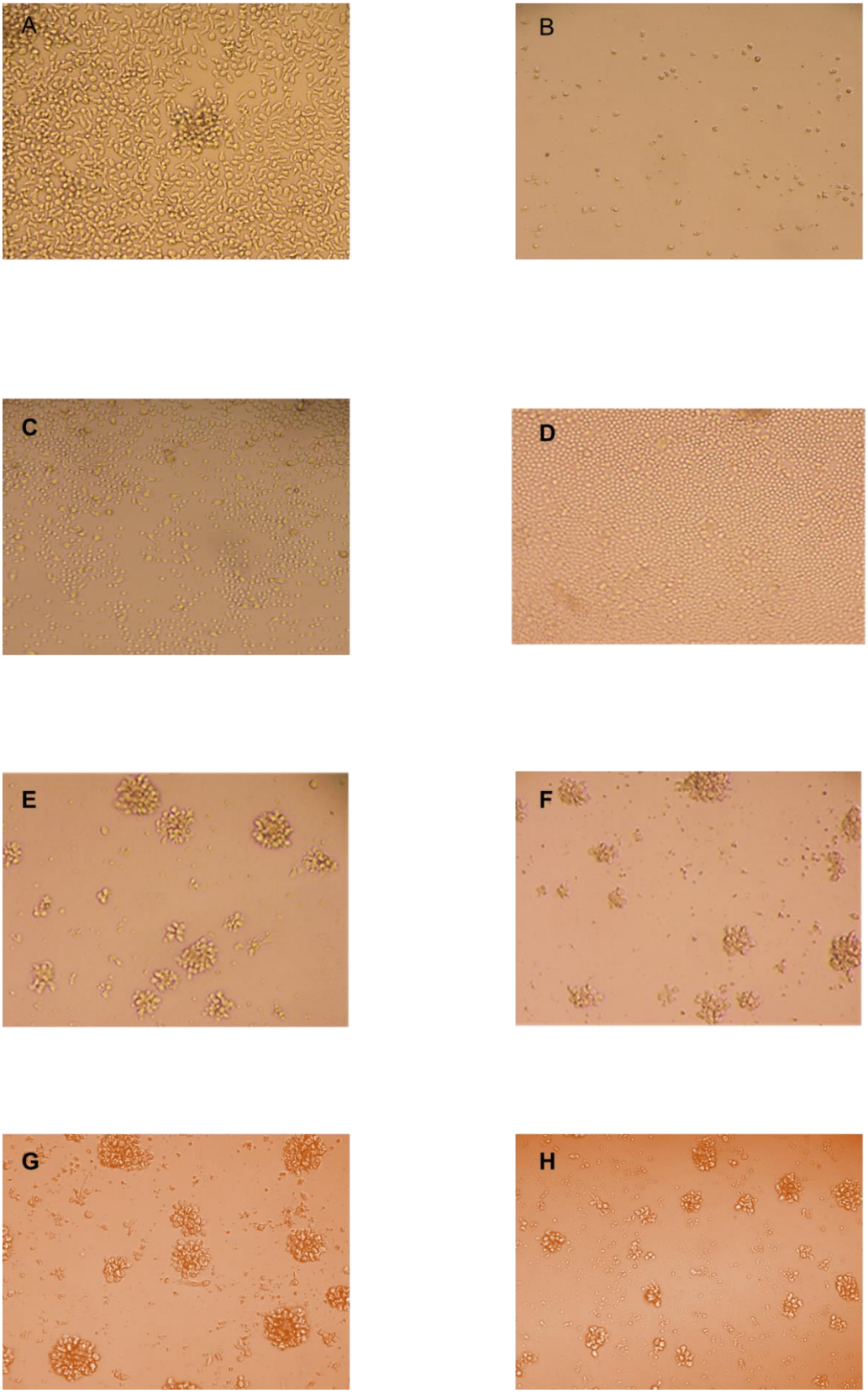

Figure 24. CEM and PBLs after 72hours of incubation in the absence and in the presence of ternary combination : A: CEM control, B: CEM + ternary combination, C: resting PBLs control, D: resting PBLs + ternary combination, E: PBLs +PHA control, F: PBLs + PHA + ternary combination, G: PBLs + PHA+ IL2, H: PBLs+PHA+IL2+ ternary combination

4. GENERAL CONCLUSIONS

The work of my PhD thesis further investigated the *in vitro* anticancer effect against wild type and CDDP-resistant (i.e. CEM and A2780) cancer cells, of binary combinations of CDDP with C0, as well as of a ternary combination that included GSH as a third component of the drug cocktail,.

The data obtained demonstrated that, although the three-drug cocktail was markedly more potent than the two-drug combination, both types of drug associations showed statistically significant synergisms against either the CDDP-sensitive and the CDDP-resistant cancer cells.

Contrarily to most if not all anticancer agents, the cytotoxicity of the most potent cocktail was markedly higher against leukemic lymphocytes (CEM cells) than against normal proliferating lymphocytes (i.e. 90% mortality vs. 50%mortality, respectively). Worth mentioning is that resting PBLs were the least susceptible to the toxic effect of the cocktail (i.e. up to max 15% mortality at 72 hours).

Analyses of the phospholipid profiles in leukemia and carcinoma cell extracts from CDDP-resistant vs. wild type, highlighted specific modifications in the overall cellular lipids, i.e. glycerophosphocholines were strongly lower represented in the CDDP-resistant CEM cells, while some sphingomyelins were up-represented in the CDDP-resistant A2780 cells. Presently, however, we do not know if these changes in membrane lipids are or not related to the drug-resistant status of the cells.

Besides of further studies to unveil the molecular targets of the triple-drug cocktail, and based on the promising selectivity (SI 5) showed against cancer cells *in vitro*, investigations on its effectiveness in a xenograft mice models of human susceptible and CDDP-resistant ovarian carcinoma are on the way.

5. MATERIALS AND METHODS

5.1 Reagents

[Cu(phen)2(OH2)](ClO4)2 (compound C0) was synthesized as previously described (Pivetta J InorgBiochem 2011). Cis-diammineplatinum (II) dichloride (CDDP), dimethyl sulphoxyde (DMSO), Glutathione (GSH), Trypan blue, Doxorubicin were purchased from Sigma-Aldrich, Interleukin-2-human (hIL-2) from Roche; Kanamycin Sulphate, Phytohemagglutinin (PHA) and Foetal bovine serum (FBS) were purchased by Gibco; RPMI 1640 medium with stable L-glutamine was purchased by EuroClone.

Stock solutions of compound C0 and CDDP were prepared in DMSO, at 1000× of the highest concentration to be used on the cell culture and stored at 4 °C in the dark. CDDP stock solution, being stable only for few hours and showing a decreasing of the cytotoxic potency during the time, was prepared fresh each time immediately before the experiments. GSH stock solution was prepared in RPMI medium and filtered before use.

5.2 Cell lines

CCRF-CEM, human acute T-lymphoblastic leukaemia cells, with their respective cisplatin-resistant subline were used in the study. CCRF-CEMwt and CCRF-CEMres cell line was maintained in culture between 1×10^5 cells/ml and 1×10^6 cells/ml in RPMI medium supplemented with10% foetal bovine serum (FBS) and 1% kanamycin (growth medium). To the growth medium for CEMres cell cultures, we also added CDDP (5μM). A2780wt and A2780res cells were grown in RPMI medium with 2 mM glutamine and 10% FBS. Cell monolayers were sub-cultivated when they reached 70% confluency (every 3–4 days) by a 1:3 ratio. A2780res cells were a generous gift by Dr. Eva Fischer (Tumor Biology Laboratory, The Ion Chiricuta Oncology Institute, Cluj-Napoca, Romania) and in order to keep the cisplatin resistance, A2780res were cultured in the presence of 1 μM of cisplatin every two or three passages .The cells were periodically checked for micoplasma contamination. For the experiments, the cell lines were replaced every 3 months with freshly-thawed cells from the cell stores in liquid nitrogen.

5.3 Selection of the cisplatin-resistant CCRF-CEM subline

A CEM subline able to grow at the same extent in the absence and in the presence of 5 μM cisplatin (CCRF-CEM-res) was obtained by serial passages of wild-type cells in the presence of

increasing cisplatin concentrations, starting from a sub-inhibitory concentration (0.5 μM).At each cell passage (every 3–4 days), the number of viable cells of cisplatin-treated cultures was compared to that of duplicate untreated cultures. Initially the CDDP concentration was increased by 0.25 μM at each cell passage up to 1.50 μM; from then on, cisplatin-treated cultures grew poorly and much slower than their untreated counterparts and had to be kept (5 consecutive passages) at the same CDDP concentration until the cell population had regained original growth timing and viability. After that the CDDP concentration was gradually increased. Given that cell cultures never survived at concentrations over 5μM, the cell population was stabilised by 15 further passages at 5 μM CDDP. The number of viable cells was determined at each cell passage by the trypan blue exclusion method. At intervals during the selection process, the level of CDDP resistance was checked by the 3-(4,5-dimethylthiazol-2-yl)-2,5-diphenyl-tetrazoliumbromide (MTT) method in cells that had grown without the drug for one passage; Doxorubicin was used as a reference compound to evaluate the cisplatin-resistance specificity.

5.4 Cytotoxic assays

The biological stability of stocks solutions checked verifying the cytotoxic activity measured by using the same solutions over more than 6 months. The tested compounds maintained the same CC_{50} (concentration of compound that reduce the viable cell by 50% with respect to untreated cells) in all the performed experiments. Dilutions of the drug stocks for biologic investigations were made in RPMI medium at 2x the final concentration for single drug evaluations, or at 4x the final concentration for evaluation of binary and ternary drug combinations. The concentration of DMSO in the cells was never higher than 0.1%. The effects of the drugs and drug combination were evaluated in cultures of exponentially growing cells; for experiments in cisplatin-resistant cell cultures, both CEMres and A2780res cells were allowed to grow in the absence of the drug for one passage. Initially in the experiments with the binary combinations of CDDP and [2], CEMwt and CEMres were seeded at a density of 1×10^5 cells/well of growth medium in flat-bottomed 96-well plates and simultaneously exposed to the drugs or drug combinations. A2780wt and A2780res cells were seeded at a density of 5×10^3 cells/well of flat-bottomed 96-well plates and allowed to adhere overnight before of the addition of the drugs or the drug combinations. Cell growth in the absence and presence of drugs was determined after 96 hrs of incubation at 37 °C and 5% CO_2 (corresponding to three to four duplication rounds of untreated cells), through the MTT method (Pauwels *et al*., Virol. Methods, 1988). Afterwards, for the binary combinations of CDDP+GSH, C0+GSH, CDDP+C0 and for

the ternary combinations, CEMwt and CEMres cells were seeded at a density of 1×10^5 cells/well of grow the medium in flat-bottomed 24-well plates and simultaneously exposed to the drugs or drug combinations. A2780wt and A2780res cells were seeded at a density of 1×10^5 cells/well of flat-bottomed 24-well plates and allowed to adhere overnight before of the addition of the drugs or the drug combinations. Cell growth in the absence and presence of drugs was determined after 96 hrs of incubation at 37 °C and 5% CO_2, through Trypan Blue Exclusion Test of Cell Viability (Strober W., Curr. Protoc. Immunol.John Wiley & Sons, Inc., 2001).This method was used because coloured GSH solution interfered with the MTT method. Values obtained in drug-treated samples were expressed as percentages of those of their respective controls. All experiments were repeated three times. Dose-response curves for each drug were determined and the CC_{50} of single drug and drug combinations were calculated with OriginPro8. To evaluate the cytotoxic effects of CDDP in combination with C0 and GSH the ED-ANNs method was used.

5.5 Peripheral blood Lymphocytes (PBLs) separation and Cytotoxic assays

Peripheral blood Lymphocytes from healthy donors were obtained by method of gradient separation Lympholyte-H (Cedarlane). After extensive washing, cells were resuspended (1 x106/ml) in RPMI-1640 with 10% FBS and incubated overnight. For evalutations in resting PBLs, 1 x 10^5 cells/well were incubated in RPMI-1640 with 10% FBS in the absence or presence of the compounds at the indicate concentration in 24-well plat, at 37° C and 5% CO_2 , for 24h, 48h, 72h.

For experiments with proliferating PBLs, 1 x 10^5 cells/well were incubated in RPMI-1640 with 10% FBS supplemented with PHA (2.5 µg/ml) or with PHA (2.5 µg/ml) and IL-2 (5 U/mL) in the absence or presence of the compounds at the indicate concentration in flat-bottomed 24-well plates, at 37° C and 5% CO_2.

Cell growth in the absence and presence of drugs was determined after 24h, 48h and 72h of incubation at 37 °C and 5% CO_2 as described above. All experiments were repeated three times using PBLs from three different healthy donors.

6. REFERENCES (*Alphabetical order*)

1. Ahamad A, Jhingran A. **New radiation techniques in gynecological cancer**, 2004 Jul-Aug;14(4):569-79.
2. **AIRTUM Associazione italiana dei registri tumori**
3. Albrechtsen N. , Dornreiter I., Grosse F., Kim E., Wiesmuller L- and Deppert W., **Maintenance of genomic integrity by p53: complementary roles for activated and non-activated p53,** *Oncogene* (1999) 18, 7706–7717.
4. Alderden, R.A., Hall, M.D., and Hambley, T.W. (2006) **The discovery and development of cisplatin**. *J. Chem. Educ.*, 83, 728–734.
5. Andrews P.A,. Howell S.B, **Cellular pharmacology of cisplatin: perspectives on mechanisms of acquired resistance**. *Cancer Cells* 1990 Feb;2(2):35-43 (1990).
6. Blanc E., Goldschneider D., Ferrandis E., Barrois M., Le Roux G., Leonce S., Douc-Rasy S., Bénard J., Raguénez G**. MYCN enhances P-gp/MDR1 gene expression in the human metastatic neuroblastoma IGR-N-91 model** *American Journal of Pathology*, Vol. 163, No. 1, July 2003.
7. Brozovic A.; Ambriović-Ristov A.; Osmak M. **The relationship between cisplatin-induced reactive oxygen species, glutathione, and BCL-2 and resistance to cisplatin**. *Crit. Rev. Toxicol*. 2010, 40, 347–359.
8. BurgerH., Zoumaro-Djayoon **A.**,. Boersma **A.** W.M, HellemanJ.,. BernsE.M.J.J, MathijssenR.H.J., LoosW.J., WiemerE. **A.** C., **Differential transport of platinum compounds by the human organic cation transporter hOCT2 (*hSLC22A2*)** *Br J Pharmacol*. 2010 Feb; 159(4): 898–908.
9. Carvallo-Chaigneau F., Trejo-Solis C., Gomez-Ruiz C., Rodriguez-Aguilera E., Macias-Rosales L., Cortes-Barberena E., Cedillo-Pelaez C., Gracia-Mora I., Ruiz- Azuara L., Madrid-Marina V., Constantino-Casas F., **Casiopeina III-ia induces apoptosis in HCT-15 cells in vitro through caspase-dependent mechanisms and has antitumor effect in vivo**. *Biometals* 21 (2008) 17–28.
10. Chakravarty A.R., Reddy P.A.N., Santra B.K., Thomas A.M.. **Copper Complexes as chemical nucleases**. *Proc. Indian Acad. Sci.* 2002, Vol. 114, pp. 391-401.
11. Chen H.H., Song I.S., Hossain A., Choi M.K., Yamane Y., Liang Z.D., Lu J., Wu L. Y., Siddik Z.H., Klomp L.W., Savaraj N., Kuo M. T**. Elevated glutathione levels confer**

cellular sensitization to cisplatin toxicity by up-regulation of copper transporter hCTR1. *Molecular Pharmacology.* 2008, Vol. 74, pp. 697-704.

12. Desoize, B.; Madoulet, C. **Particular aspects of platinum compounds used at present in cancer treatment.** *Crit. Rev. Oncol. Hematol.* 2002, 42, 317–325.
13. DeVita V.T., R.C. Young, G.P. Canellos.**Combination versus single agent chemotherapy: a review of the basis for selection of drug treatment of cancer.** *Cancer.* 1975, Vol. 35, pp. 98-110.
14. Drottar, M.; Liberman, M.C.; Ratan, R.R.; Roberson, D.W. **The histone deacetylase inhibitor sodium butyrate protects against cisplatin-induced hearing loss in guinea pigs.** *Laryngoscope* 2006, 116, 292–296.
15. Duhem C., Ries F., Dicato M., **What does Multidrug Resistance (MDR) Expression Mean in the Clinic?** The Oncologist,1996;1:151-158.
16. Eckstein N.,**Platinum resistance in breast and ovarian cancer cell lines**, *Journal of Experimental and Clinical Cancer Research* 2011, 30:91.
17. Ferreira A.M.D.C., Ciriolo M.R., Marcocci L., Rotilio G. **Copper(I) transfer into metallothionein mediated by glutathione**.1993, *Biochem. J.*, Vol. 292(3), pp. 673-676.
18. Florea A.M., Busselberg D. Cisplatin as an Anti-Tumor Drug: **Cellular Mechanism of Activity, Drug Resistance and Induced Side Effects**. *Cancers.* 2011, Vol. 3, pp. 1351-1371.
19. Freedman J.H., Ciriolo M.R., Peisach J.. **The role of glutathione in copper metabolism and toxicity.** 1989, *J. Biol. Chem.*, Vol. 264(10), pp. 5598-5605.
20. Fuertes M.A., Alonso C., Perez M.J. **Biochemical modulation of Cisplatin mechanisms of action: enhancement of antitumor activity and circumvention of drug resistance**. *Chemical Review* 2003 Mar;103(3):645-62.
21. Godwin A. K., Meister A., O'Dwyer P. J., Huang C. S., Hamilton T. C., and Anderson M. E., **High resistance to cisplatin in human ovarian cancer cell lines is associated with marked increase of glutathione synthesis**, *Proceedings of the National Academy of Sciences of the United States of America*, vol. 89, no.7, pp. 3070–3074, 1992.
22. Goodsell D., **The Molecular Perspective:Cisplatin**., *Stem Cells*, 2006 Mar; 24(3):514-5
23. Gottesman M.M. **Mechanisms of cancer drug resistance,** *Annu. Rev. Med*. 2002. 53:615–27.

24. Haber M., Bordow S.B., Haber P.S., Marshall G.M., Stewart B.W. and Norris M.D., **The Prognostic Value of MDR1 Gene Expression in Primary Untreated Neuroblastoma** *European Journal of Cancer*, Vol. 33, No. 12, pp. 2031±2036, 1997.
25. Halliwell B., Gutteridge J.M**.. Role of free radicals and catalytic metal ions in human disease: An overview** *Methods Enzymol*. 1990 Vol. 186, pp. 1-85.
26. Heinrichs S. and Deppert W. **Apoptosis or growth arrest: modulation of the cellular response to p53 by proliferative signals**, *Oncogene* ,2003, 22, 555–571.
27. Huang G.C., Liu S.Y., Lin M.H., Kuo Y.Y., Liu Y.C..**The synergistic cytotoxicity of Cisplatin and Taxol in killing oral squamous cell carcinoma**. *Jpn J. Clin. Oncol*. 2004, Vol. 9, pp. 499-504.
28. Ishida S., Lee J., Thiele D.J.,. Herskowitz I, **Uptake of the anticancer drug cisplatin mediated by the copper transporter Ctr1 in yeast and mammals.** *Proc. Natl. Acad. Sci.* U. S. A. 99 (2002) 14298–14302.
29. Ishikawa T., Ali-OsmanF**. Glutathione-associed cis-diamminedichloroplatinum (II) metabolism and ATP-dependent efflux from leukemia cells. Molecular characterization of glutathione-platinum complex and its biological significance**. *Journal of Biological Chemistry*, 1993, Vol. 38, pp. 327-345.
30. Jamieson E.R., Lippard S.J., **Structure, Recognition, and Processing of Cisplatin−DNA Adducts** *Chem. Rev*. 99 (1999) 2467–2498.
31. Kasherman Y., Strurup S., Gibson D.**Is glutathione the major cellular target of cisplatin? A study of the interactions of cisplatin with cancer cell extracts.** *Journal of Medicinal Chemistry* 2009, Vol. 52, pp. 4319-4328.
32. Kartalo, M.; Essigmann, J.M. **Mechanisms of resistance to cisplatin**. *Mutat. Res.* 2001, *478*, 23–43.
33. Kelland L**, The resurgence of platinum-based cancer chemotherapy**. *Nat. Rev. Cancer* 2007, 573-584.
34. Kojima, K**. Molecular Aspects of the Plasma Membrane in Tumor Cells.** *Nagoya J Med. Sci.* 1993, 1–18.
35. Lladó, V.; López, D. J.; Ibarguren, M.; Alonso, M.; Soriano, J. B.; Escribá, P. V.; Busquets, X. **Regulation of the Cancer Cell Membrane Lipid Composition by NaCHOleate: Effects on Cell Signaling and Therapeutical Relevance in Glioma.** *Biochim. Biophys. Acta - Biomembr.* 2014, *1838* (6), 1619–1627.

36. Lane DP **Cancer**: **p53, guardian of the genome**. *Nature* 1992 Jul 2;358(6381):15-6.

37. Laussac J.P. and Sarker B. **Characterization of the copper(II)- and nickel(II)-transport site of human serum albumin. Studies of copper(II) and nickel(II) binding to peptide 1-24 of human serum albumin by 13C and 1H NMR spectroscopy.** *Biochemistry* 1984 Jun 5;23(12):2832-8.

38. Lebwohl, D., Canetta, R. **Clinical development of platinum complexes in cancer therapy: An historical perspective and an update**. *Eur. J. Cancer* 1998, 34, 1522–1534.

39. Lee Y.Y., Choi C.H., Do I.G., Song S.Y., Lee W., Park H.S., Kim M.K., Kim T.J., Lee J.W, Bae D.S., Kim B.G. **Prognostic value of the copper transporters, CTR1 and CTR2, in patients with ovarian carcinoma receiving platinum-based chemotherapy** *Gynecol. Oncol.* 122 (2011) 361-365.

40. Lin X.J., Okuda T., Holzer A., Howell S.B., **The copper transporter CTR1 regulates cisplatin uptake in Saccharomyces cerevisiae** *Mol. Pharmacol.* 62 (2002) 1154–1159.

41. Lladó V. , López David J. , Ibarguren M., Alonso M., Soriano J. B., Escribá P.V. , Busquets X., **Regulation of the cancer cell membrane lipid composition by NaCHOleate. Effects on cell signaling and therapeutical relevance in glioma** *Review Biochimica et Biophysica Acta* 1838 (2014) 1619–1627.

42. Luqmani YA1. **Mechanisms of drug resistance in cancer chemotherapy**. *Med Princ. Pract.* 2005;14 Suppl 1:35-48.

43. Marchini S, D'Incalci M, Broggini M. **New molecules and strategies in the field of anticancer agents**. *Curr Med Chem - Anticancer Agents* 2004 May;4(3):247-62.

44. Marzano C., Pellei M., Tisato F., Santini C. **Copper Complexes as Anticancer Agents**. *Anti-Cancer Agents in Medicinal Chemistry* 2011, Vol. 9, pp. 185-211.

45. Munoz M., Henderson M., Haber H. and Norris M. **Role of theMRP1/ABCC1 Multidrug Transporter Proteinin Cancer** *IUBMB Life*,59(12):752–757, December 2007.

46. Nelson D.L., Cox M.M., Lehninger **Principles of Biochemistry**, 5th ed., 2008.

47. Norris D.A., Guo A., Makhey V.D. and Sinko P.J. (1997). **Functional expression and immunoquantitation of multidrug resistance (MDR) e,uxpumps, Pgp and MRP, in Caco-2 cells as a function of passage number.** *Pharm. Res*., 14, S669 -S670.

48. Pauwels R., Balzarini J., Baba M.,. Snoeck R, Schols D., Herdewijn P., Desmyter J., De Clercq E**., Rapid and automated tetrazolium-based colorimetric assay for the detection of anti-HIV compounds.** *J. Virol. Methods* 20 309–321.1988.
49. Payet D., Gaucheron F., Sip M., Leng M. **Instability of the monofunctional adducts in cis-[Pt(NH3)2(N7-N-methyl-2-diazapyrenium)Cl](2+)-modified DNA: rates of cross-linking reactions in cis-platinum-modified DNA.** *Nucleic Acids Res.* 1993 Dec 25; 21(25): 5846–5851.
50. Perez R.P.,**Cellular and molecular determinants of cisplatin resistance.** *Eur. J. Cancer* 1998, 34:1535-1542.
51. Pivetta T., Demartin F., Castellano C., Vascellari S., Verani G., Isaia F. **Synthesis, structural characterization, formation constants and in vitro cytotoxicity of phenanthroline and imidazolidine-2-thione copper(II) complexes**. *J. Inorg. Biochem.* 2011 Mar;105(3):329-38.
52. Pivetta T, Isaia F, Verani G, Cannas C, Serra L, Castellano C, Demartin F, Pilla F, Manca M, Pani A**. Mixed-1,10-phenanthroline-Cu(II) complexes: synthesis, cytotoxic activity versus hematological and solid tumor cells and complex formation equilibria with glutathione**. *J. Inorg. Biochem.* 2012 Sep;114:28-37.
53. Pivetta T, Isaia F, Trudu F, Pani A, Manca M, Perra D, Amato F, Havel J. **Development and validation of a general approach to predict and quantify the synergism of anti-cancer drugs using experimental design and artificial neural networks**. *Talanta* 2013 Oct 15;115:84-93.
54. Rademaker-Lakhai, J.M.; Crul, M.; Zuur, L.; Baas, P.; Beijnen, J.H.; Simis, Y.J.; van Zandwijk,N.; Schellens, J.H., **Relationship between Cisplatin administration and the development of ototoxicity.** *J. Clin. Oncol.* 2006, *24*, 918–924).
55. Riboni L., Campanella R., Bassi R., Villani R., Gaini S.M., Martinelli-Boneschi F., Viani P., Tettamanti G., **Ceramide levels are inversely associated with malignant progression of human glial tumors.** *Glia* 2002 Aug;39(2):105-13.
56. Rodriguez-Enriquez S., Marin-Hernandez A., Gallardo-Pérez J.C., Carreño-Fuentes L., Moreno-Sànchez R..**Targeting of cancer energy metabolism**. *Mol. Nutr. Food Res.* 2009, Vol. 53, pp. 29-48.
57. Rosenberg, B. **In *Nucleic Acid-Metal Ion Interactions***; Spiro, T.G., Ed. John Wiley & Sons, Inc.: New York, NY, USA, 1980; Volume 1, pp. 1–29.

58. Safaei R., Holzer A.K., Katano K., Samimi G., Howell S.B..**The role of copper transporters in the development of resistance to Pt drugs** 98(10), 2004, *J. Inorg. Biochem.*, pp. 1607-1613.
59. Santini C., Pellei M., Gandin V., Porchia M., Tisato F., Marzano C**., Advances in copper complexes as anticancer agents.** *Chem. Rev.* 114 (2014) 815–862.
60. Scanlon K.J, Kashani-Sabet M., Miyachi H., Sowers L.C., Rossi J.J., **Molecular basis of cisplatin resistance in human carcinomas: model systems and patients** *Anticancer Res.* 9 (1989) 1301–1312.
61. Siddik, Z.H.**Cisplatin: mode of cytotoxic action and molecular basis for resistance**. Oncogene. 2003, Vol. 22, pp. 7265-7279.
62. Sigman D.S., Graham D.R., Aurora V.D., Stern A.M., **Oxygen-dependent cleavage of DNA by the 1,10-phenanthroline . cuprous complex. Inhibition of Escherichia coli DNA polymerase I.** *J. Biol. Chem.* 1979 Dec 25;254(24):12269-72.
63. SionovRonit Vogt and HauptYgal, **The cellular response to p53: the decision between life and death** *Oncogene* (1999) 18, 6145 – 6157.
64. Song, N. Savaraj, Z.H. Siddik, P. Liu, Y. Wei, C.J. Wu, M.T. Kuo, **Role of human copper transporter Ctr1 in the transport of platinum-based antitumor agents in cisplatin-sensitive and cisplatin-resistant cells.** *Mol. Cancer Ther.* 2004 Dec;3(12):1543-9.
65. Strober W., *Curr. Protoc. Immunol*. John Wiley & Sons, Inc., 2001.
66. Szachowicz-Petelska B., Dobrzynska I., Sulkowski S. and Figaszewski Z., **Characterization of the cell membrane during cancer transformation** *Journal of Environmental Biology* September 2010, 31(5) 845-850 (2010).
67. Talmadge J.E and Fidler I.J: **The Biology of Cancer Metastasis: Historical Perspective** *Cancer Res*. 2010 July 15; 70(14): 5649–5669).
68. Tang W.X., Cheng P.Y., Luo Y.P., Wang R.X**. Interaction between cisplatin, 5-fluorouracil and vincristine on human hepatoma cell line (7721)**. *World Journal of Gastroenterology*. 1998, Vol. 5, pp. 418-420.
69. Taylor-Harding B., Orsulic S., Karlan B.Y., Li A.J.**Fluvastatin and cisplatin demonstrate synergistic cytotoxicity in epithelial ovarian cancer cells.** *Gynecologic Oncology* 2012, Vol. 119, pp. 549-556.
70. Todd R.C., Lippard S.J, **Inhibition of transcription by platinum antitumor compounds** *Metallomics* 1 (2009) 280–291).

71. Tripathi L., Kumar P., Singhai A.K., **Role of chelates in treatment of cancer.** *Indian J. Cancer* 2007 Apr-Jun;44(2):62-71.
72. Tsang, R.Y.; Al-Fayea, T.; Au, H.J. **Cisplatin overdose: Toxicities and management.** *Drug Saf*. 2009, 32, 1109–1122.
73. Trzaska S., **Cisplatin,** *Chem. Eng. News* 83 (2005) 52.
74. Vogelstein B., Lane D. & Levine A.J. **p53 network** *Nature* 408, 307-10, 16 November 2000.
75. Yang X.L., Wang A.H.**Structural studies of atom-specific anticancer drugs acting on DNA,** *Pharmacology & Therapeutics* 83 (1999) 181–215.
76. Zamble DB, Lippard SJ: **Cisplatin and DNA repair in cancer chemotherapy**. *Trends Biochem. Sci*. 1995; 20: 435–439.